Functional multimodality and cellular heterogeneity in peripheral somatosensory nervous system

Behrang Sharif

Department of Physiology
&
Montreal Neurological Institute (Neuro)

McGill University

Montreal, Quebec, Canada

December 2021

A thesis submitted to McGill University in partial fulfilment of the requirements of the degree of Doctor of Philosophy

© Behrang Sharif 2021

TO

Maman and Baba,

Behzad, Behnam, Solmaz, and Roja,

Adrian, Aram, Nava, and Shaya,

and My Friends…

Table of contents

Abstract

How is it possible to feel different sensations from the same area on the skin? Although very basic, there are still fundamental questions like this, that remain to be answered on the topic of sensory perception. One of the more prominent theories on how the nervous system solves the sensory discrimination dilemma is the “labeled line” or “specificity” theory which claims dedicated compartments of the system, e.g. marked peripheral afferent subpopulations, are responsible for specific sensory modalities. If proven accurate, this model inspires “compartmentalized therapy” which aims to alleviate sensory diseases through targeting specific elements responsible for individual modalities, like pain or itch. In contrast, if multiple modalities share similar elements of the sensory system, compartmentally targeting such flexible system can lead to compensatory modulation of other compartments leading to inefficacy of the therapeutic approach. Although the debate on specificity versus multimodality is ongoing in the field of sensory biology, in the recent years, absence of evidence for multimodality in certain specific genetic and behavioral studies has been interpreted as evidence of absence. Here, I will propose that the failure to detect evidence of multiple compartments’ contribution to diverse modalities is due to overlooked technical limitations. Limitation of common approaches such as animal sensory behavioral assays, optogenetics, chemogenetics, and single time point snapshot transcriptomic tools such as single cell RNA sequencing may have led us to believe that compartments not tuned for a specific modality are dispensable for that sensation.

In this dissertation, with the aim to iterate the need for wholesome approaches in sensory biology, I will bring convincing evidence for functional dynamism and genetic heterogeneity in the peripheral primary sensory system. In the first data chapter (Chapter 2) I will focus on multimodal capacity of a subset of primary afferents to prove a single population of neurons can contribute to transmission of different senses, itch and pain. I will also introduce molecular players that are involved in modulation of the signals in a modality specific manner, i.e. engagement of TRP channels in itch but not pain transmission through MRGPRA3 expressing afferents. In the second data chapter (Chapter 3), with multimodality in mind, I will provide elements of a single-cell transcriptomic atlas of human primary sensory ganglia. Taking advantage of single-nucleus RNA and ATAC sequencing, I lay down how multiple functional pathways are expressed in single neuronal populations of human dorsal root ganglia. As important contributors to sensory coding in health and disease, information of the transcriptomic and genomic repertoire of non-neuronal ganglia resident cells will also be included in this chapter.

I trust that this dissertation will highlight the necessity of recognizing technical pitfalls in sensory research, particularly pain related studies. I also hope to assert the importance of multimodality and to build a solid base for more wholesome research that can lead to a better understanding of sensory discrimination mechanisms.

Résumé

Multimodalité fonctionnelle et hétérogénéité cellulaire dans le système nerveux somatosensoriel périphérique

Comment est-il possible d'éprouver différentes sensations sur une zone déterminée de la peau ? Dans le domaine de la perception sensorielle, un très grand nombre de questions fondamentales comme celle-ci, même élémentaires, restent toujours sans réponse. Afin d'expliquer de quelle façon le système nerveux est capable de discriminer les différentes perceptions sensorielles, la théorie prédominante est celle des "lignes étiquetées" ou de la "spécificité". Selon cette théorie, des compartiments dédiés du système nerveux, par exemple des sous-populations afférentes périphériques génétiquement définies, seraient responsables de modalités sensorielles spécifiques. Si ce modèle s'avère exact, il encouragerait la "thérapie compartimentée" dont le but est de soulager les troubles sensoriels en ciblant spécifiquement les éléments responsables de modalités individuelles, telle que la douleur ou le prurit par exemple. A l'inverse, si plusieurs modalités ont en commun des éléments du système sensoriel, les cibler de façon compartimentée pourrait entraîner l'apparition de phénomènes compensatoires, ce qui conduirait à un échec de l'approche thérapeutique. Récemment, et alors que le débat entre spécificité et multimodalité est en cours dans le domaine de la recherche sensorielle, l'absence de preuve de multimodalité dans certaines études génétiques et comportementales a été interprétée comme une preuve de son absence. Je propose ici de

montrer que si la contribution de multiples compartiments à des modalités différentes n'a pu être mise en évidence, c'est en raison de l'existence de certaines limitations techniques qui ont été négligées. En effet, ces limitations dans les approches fréquemment utilisées que sont les tests de comportement sensoriels chez les animaux, l'optogénétique, la chimiogénétique ou les outils transcriptomiques comme le séquençage d'ARN de cellule unique, ont pu nous conduire à penser que des compartiments non adaptés à une modalité spécifique sont superflus pour une sensation donnée

Dans ce travail, avec l'objectif de renforcer la nécessité d'utiliser une approche neuroscientifique plus globale, j'apporterai des preuves concrètes de l'existence d'un dynamisme fonctionnel et d'une hétérogénéité génétique au sein du système sensoriel primaire périphérique. Le premier chapitre de données (Chapitre 2) abordera la capacité multimodale d'un sous-ensemble d'afférents primaires, avec la démonstration qu'une sous-population de neurones peut contribuer à la transmission de différentes sensations telles que douleur et démangeaison. Je présenterai également les acteurs moléculaires contribuant à la modulation des signaux d'une modalité donnée, avec l'implication des canaux TRP dans la transmission de la sensation de démangeaison, mais pas dans celle de la douleur, via les afférences exprimant MRGPRA3. Dans le second chapitre de données (Chapitre 3), et dans le contexte de multimodalité, je partagerai des éléments d'un atlas transcriptomique en cellule unique des ganglions sensoriels primaires humains. Bénéficiant des techniques de séquençage d'ARN à noyau unique et d'analyse de l'accessibilité de la chromatine (ATAC-seq), j'apporterai la preuve de la co-expression de plusieurs voies fonctionnelles dans une population neuronale unique des ganglions spinaux humains. Du fait de leur contribution essentielle au codage

sensoriel chez les individus en santé et chez les individus malades, le répertoire génomique des cellules non neuronales résidentes des ganglions sera également inclus dans ce chapitre.

J'espère que ce travail fera ressortir la nécessité de reconnaître l'existence d'écueils techniques dans la recherche sur les systèmes sensoriels, plus particulièrement dans les études sur la douleur. J'espère également souligner l'importance de la multimodalité et jeter une base solide pour l'utilisation d'une recherche plus globale afin de mieux comprendre les mécanismes de la discrimination sensorielle.

Acknowledgements

This dissertation is the fruit of a very long journey that started with my move to Canada. This could not be done without the help and support of many who tagged along with me for various portions of this journey. I am grateful to each and every one of my fellows during these years and here I will name few as a simple token of appreciation.

Professor **Philippe Séguéla**, my PhD supervisor, supported me throughout my graduate studies. I am wholeheartedly grateful for his trust in me and for empowering me to be truly autonomous. Throughout these years he initiated many collaboration opportunities for me and let me learn all aspects of academic career whether it be project development, grant writing, or supervising younger trainees. Acceptingly, he allowed me to explore my interests and ideas, many of which winding up at dead-ends, and advised me how to navigate around hardships. I will hold the lessons I learned from Philippe and my years at his lab at the Neuro dearly forever.

Professor **Alfredo Ribeiro da Silva**, helped me throughout my years at McGill. He paved my way to land in Philippe's lab, truly supported me when I needed it, and promoted me through his recommendations. I will be forever indebted to his kindness and mentorship.

My PhD advisory committee, professors **Ellis Cooper**, **Jeffrey Mogil**, and **Alfredo Ribeiro da Silva** provided much appreciated scientific input and helped me think critically about all aspects of my research while keeping my horizons open. I truly appreciate their time and support as it helped shape my projects.

It is a true honor for me to have professors **Jeffrey Mogil** and **Yves De Koninck**, two of my academic role models, as my PhD thesis examiners. I appreciate their scientific aptitude and admire them both at personal and professional levels. I also thank my thesis defence committee professors **Laura Stone**, **Steve Lomber**, and **Massimo Avoli** for their valuable input and instructive discussions.

Ms. **Van Nguyen** and Dr. **Ariel Ase**, my colleagues at the Neuro made the Séguéla lab my "home" laboratory and supported me throughout these years. Our daily chats and discussions helped me maintain a healthy level of motivation to keep at my work even during the hard days of the pandemic. Their presence was essential for my journey and I sincerely thank them.

Dr. **Mathilde Chaineau** helped me with the French translation of my abstract and Dr. **Noosha Yousefpour** helped with editing parts of the introduction. I would like to thank them both, not only for their help with these sections but also as their friendship and collaborations meant a lot through my years at McGill. It has always been an honor to have scientific and non-scientific discussions with them and I owe them very much for accompanying me in this journey.

In different parts of these years I received very much appreciated technical support from Ms. **Albena Davidova**, Ms. **Manon St. Louis**, and Ms. **Dominique Blais**. I would like to hereby thank them as they significantly contributed to my academic experience at McGill.

Many members of the Séguéla team supported me over the years. I would like to particularly thank Dr. **Julien Gibon**, Ms. **Maria Zamfir**, Dr. **Ihab Daou,** Dr. **Shannon Buckley** and Mr. **Thomas Deluc** as the scientific exchanges and friendly chats that we engaged in were essential for my success and livelihood.

I am very appreciative of the support I received from McGill department of Physiology over these years. Our great program coordinator Ms. **Rosetta Vasile** walked me through every step of this program and supported me in many routine and extraordinary assignments. The graduate program directors, professors **John White** and **Alvin Shrier** also helped me significantly through my lab switching and time limitation confusions. I sincerely thank them for their continued support.

I worked in multiple centers and were part of various scientific circles over the years at McGill. Here, I would like to thank the co-workers and friends that significantly contributed in my scientific advancement.

From the department of Physiology, my dear friends Dr. **Ashkan Golzar**, Dr. **Navid Khosravi**, Dr. **Tushare Jinadasa**, Dr. **William (Corey) Valinsky**, Dr. **Natasha Saviuk** and Dr. **Kimberley Young** made my initial years at McGill the most productive and enjoyable years. I would not have been able to adapt to my new environment and develop a social network without their help and for this I am forever indebted to these great people.

My first lab environment at McGill was at the Bellini Life Sciences complex and I cannot imagine my scientific career without the interactions with the researchers and trainees in that center. I truly owe much of my scientific understanding to the weekly discussions that took place in the student room of Prof. Derek Bowie's team. From those days, I want to thank Prof. **Derek Bowie**, Dr. **Jay Penney**, Dr. **Bryan Daniels**, Dr. **Mark Aurousseau**, Dr. **Patricia Brown**, Dr. **Mario Calderon**, Dr. **George (Brent) Dawe**, Dr. **Erik Larsson**, Dr. **Ryan Alexander**, Dr. **Mark Jacunski**, and Ms. **Brittany Williamson**. My electrophysiology basics was built with these friends and at

the molecular neuroscience group (MNG) meetings where I met and had the chance to discuss with people such as professors **Edward Ruthazer**, and **David Stellwagen**.

I also had the opportunity to participate in meetings with the pain research community of McGill and Quebec pain research network (QPRN). Discussions at these meetings also contributed significantly to my understanding of pain and somatosensory biology. I should thank Dr. **Claire Magnussen,** Dr. **Robert Bonin**, Dr. **Elora Midavaine**, and Dr. **Farin Bourojeni** as they helped me with discussions and techniques at several points. Also Dr. **Arkady Khoutorski** for our collaborations and discussions.

At the Montreal Neurological Institute (MNI), over the years I overlapped with many great researchers and learned significantly from them. I would like to specifically thank Dr. **Matthew Krause**, Dr. **Pariya Salami**, and Mr. **Pooya Laamerad** as they have helped me significantly with my coding issues and general science inquiries in various instances. I very much appreciate their friendship and am honored to have them as great supports.

At the Neuro, I had the opportunity to collaborate and interact with many people from different labs. I would like to thank Dr. **Vincent Soubanier,** Dr. **Valerio Piscobo**, Dr. **Mathilde Chaineau**, Dr. **Cornelia Zorca**, and Ms. **Frederique Larrocquette** from Prof. **Edward Fon** and Dr. **Thomas Durcan**'s teams for their collaborations and the discussions that taught me a lot about human pluripotent stem cells. Also Mr. **Marius Tuznik** from Dr. **David Rudko**'s team and Dr. **Emmanuel Darcq** and Dr. **Taufiq Nasseef** from Dr. **Brigitte Kieffer**'s team for our fMRI project collaboration.

I am sincerely grateful to my collaborators outside my PhD institute, the Neuro. Great colleagues like Dr. **Corina Nagy** from Douglas research center, Dr. **Spyros Oikonomopoulos**, Mr. **Yu (David) Chang Wang**, and Dr. **Ashot Harutyunyan** from McGill genome center for training me for single-cell sequencing experiments. Likewise, I thank Dr**. Ulrich Zeilhofer**, Dr. **Hendrik Wildner** and their team, particularly Dr. **Martina Pagani**, Dr. **Elena Neumann**, Dr. **Gioele Albisetti**, Dr. **Robert Ganley** for supporting me during our spinal cord electrophysiology collaboration at the University of Zurich. I also learned a lot from working with Dr. **Reza Sharif-Naeini** at the Bellini life sciences complex and his team, particularly Ms. **Albena Davidova** in the early years of my studies at McGill.

Last but not least, I would like to acknowledge those who have always been my motivators and support. Without my friends, some mentioned above and some below, I would not be who I am, and I could not achieve what I have. I am wholeheartedly grateful for the privilege of being acquainted with these incredible individuals and am humbled by the great eminence of each and every one of them. In Montreal, I was blessed by the friendship of Nassim and Yasi, Pegah, Amir Pourti, Rahi, Hanieh, Nasim, Sepide, Mariana, Rob Nahas, Joe Makkerh, Marjan, Cecil, Fary, Saba, Maria La Calle, Maryse, Kate, Rochelle, Pauline, Andrew, Golia, Andrea, Devin, Danielle, Ken Hastings, Mina, Jeanne, Daryan, Bruno, Fernanda, Rozzy, Samira, Ebi, Saeed, Daniel, Kasia, Alex, Ryan, Ryan, Khady, Karissa, Pirooz, Ania, Mo, Kelly, Ronan, Raquel, Robina, Alice, Dastan, and Sina Aslani who enriched the last decade of my life significantly. Also, I am truly happy to continually have the unconditional support of Amirhossein, Niusha, Mahdiyar, Negar, Omid, Mehrnoosh, Faraz, Hessam, Alborz, Pooyan, Yasser, Bahar, Setareh, Tara, Elmira, Parham, Fariborz, Nazanin, Mona, Azar, Loghman, Aram, Rita, Ali Sharif, Fariba, Farhad,

Soroosh, Arash, Laila, Vida, Milad, Ali Khatibi, Mohsen, Nazanin, Ayda, Ali, Behrooz, Ana, Sina, Mehrnoosh, Samaneh, Naghmeh, Dordane, Mazdak, Solmaz, and Arian with who I have taken, and know I can take refuge when life gets difficult.

Contribution to original knowledge

This dissertation represents a coherent body of work regarding the functional multimodality and structural heterogeneities of primary somatosensory system. Notwithstanding, the data chapter of this dissertation (Chapters 2 and 3) are original research articles:

Chapter 2:

Sharif, B., Ase, A.R., Ribeiro-da-Silva, A., and Séguéla, P. (2020). Differential coding of itch and pain by a subpopulation of primary afferent neurons. *Neuron* 106, 940-951.e4.

This chapter shows, for the first time, possibility of a single subpopulation of afferents transmitting multiple sensations, pain and itch, in behaving naïve animals. It is also shown that divergent behaviors can be evoked through optogenetic versus chemogenetic activation of the same population of neurons, pointing at distinct mechanisms of action. Differential engagement of TRP channels for transmitting one, but not all modalities is demonstrated.

Chapter 3:

Sharif, B., Oikonomopoulos, S., Ragoussis, J., and Séguéla, P. (2022). Comprehensive cellular atlas of human dorsal root ganglia using single-nucleus RNA and ATAC sequencing. *In preparation*.

This chapter is about developing the first comprehensive transcriptomic and epigenomic atlas of human dorsal root ganglia including neuronal and non-neuronal cells.

Authors Contributions

Below is the detailed contribution of authors for different parts of this dissertation:

Dissertation

(All sections but the chapters 2 and 3, including Introduction and Discussion):

B.S. conceived and authored the sections, P.S. reviewed and edited the text.

Chapter 2:

Sharif, B., Ase, A.R., Ribeiro-da-Silva, A., and Séguéla, P. (2020). Differential coding of itch and pain by a subpopulation of primary afferent neurons. *Neuron* 106, 940-951.e4.

B.S. and P.S. designed the experiments and all authors contributed to data analysis.

B.S. performed the histology, calcium imaging, and behavioral experiments.

B.S. and A.R.A. performed the electrophysiological experiments.

B.S. and P.S. wrote the paper with contributions from all authors.

P.S. supervised all aspects of the work.

Chapter 3:

Sharif, B., Oikonomopoulos, S., Ragoussis, J., and Séguéla, P. (2022). Comprehensive cellular atlas of human dorsal root ganglia using single-nucleus RNA and ATAC sequencing. *In preparation*.

B.S. performed the experiments, ran the data analyses, and prepared the manuscript.

S.O. assisted with the experiments and analyses.

P.S. and J.R. supervised the study.

All authors contributed to the design, troubleshooting, interpretation of experiments, and to the editing of the manuscript.

Chapter 1:

General Introduction

In this chapter I will provide the rationale for the current thesis, state the main objectives, and outline the background upon which the general hypotheses were built. Further introduction and more detailed literature review are provided within each data chapter.

Rationale

Senses were called "the windows of the soul" by ancient philosophers. Some also believed senses are essential for distinguishing "animals" from "plants". In 350 BC as part of his "Short Treatises on Nature" in "Sense and the Sensible"[1], Aristotle wrote:

> *"The most important attributes of animals, whether common to all or peculiar to some, are, manifestly, attributes of soul and body in conjunction, e.g. sensation, memory, passion, appetite and desire in general, and, in addition pleasure and pain. … Now it is clear, alike by reasoning and observation, that sensation is generated in the soul through the medium of the body."*

Senses are the inputs to the nervous system, whether they are from within the body or from the external world. Arguably, these inputs are what shape and mature the function of the nervous system in order to maintain one's normal functions in health and to signal menace during disease. Therefore, understanding how various sensory modalities are transmitted and differentiated by the nervous system is crucial for understanding the physiological basis of health and disease.

Current beliefs that dedicated cellular subpopulations are involved in exclusive transmission of specific sensory modalities have justified efforts for developing therapeutic strategies that target isolated classes of cells defined by genetic markers. Evidence for multimodal capacity of neuronal subpopulations, i.e. contribution of cells to transmission of multiple sensory modalities, can underline the need for revisiting specificity or partly redefining how these cell

[1] Parva Naturalia, De Sensu et Sensibilibus, translated by J.I. Beare and G.R.T. Ross (Oxford 1931)

types are distinguished. This can also highlight the importance of molecular modulations that can contribute to sensory discrimination in an overarching manner, which is irrespective of which cluster the transmitting fibers belong to. To this end, dissecting the genetic material of the primary sensory cells at single-cell levels can provide the basis for required redefinitions and also formulate the molecular maps for finding the overarching modulators. Furthermore, inclusion of non-neuronal cells of the primary sensory ganglia in such single-cell genomic surveys can shine light on extra-neuronal modulations of sensory coding as new areas of research and novel therapeutic targets.

Objectives

The general rationale described in the previous section pertains to different modalities, organs, and levels of the sensory system, yet the research included in this dissertation is targeted to primary sensory ganglia. More specifically, this research is focused on the dorsal root ganglia (DRGs) which are the forefronts of the nervous system receiving first-hand information from multiple sensory organs including the skin. As the largest organ in our body, skin is responsible for detection of various sensory modalities. Among the most primitive of such modalities are pain and itch. These distinct yet very similar aversive sensations can be detected from the same location on the skin, i.e. receptive fields, and are also transmitted through similar DRGs. This, among other reasons described later, makes these two modalities ideal for investigating multimodality. Furthermore, the first order somatosensory neurons are among the most studied in the context of "labeled line theory" with different cells claimed as "pain-specific", "itch-specific", "proprioceptive-specific", etc. Hence, DRGs are important sites for transcriptomic studies with extensive clustering efforts towards identifying compartmentalized therapy targets.

In order to prove multimodality in first order neurons, and to push somatosensory research advancement in new directions, I will have two main objectives in this dissertation: 1) to provide solid evidence that a single population of primary afferents are capable of transmitting multiple sensory modalities and introduce possible molecular contributors to this multimodality. 2) to provide a comprehensive and reliable genomic resource for understanding the molecular repertoire and functional capacities of individual cells in the human DRGs as prototypical human primary sensory ganglia.

1) Prove multimodality in the peripheral sensory system

In contemporary somatosensory research, the question of peripheral sensory coding has been streamlined to specificity versus polymodality. Surprisingly, despite a large body of contrary evidence from old (Beitel and Dubner, 1976; Solís-Cámara and Negrete-Martínez, 1968) and modern (Prescott and Ratté, 2012; Prescott et al., 2014; Wang et al., 2018) literature, it seems that specificity theories have gained more support in the recent years. This may be owing to several transgenic ablation/silencing studies that demonstrated single modality reductions while other sensory modalities tested are spared (i.e. absence of statistically significant reduction) (Han et al., 2013; Roberson et al., 2013; Stantcheva et al., 2016). It can also be due to easier conceivability of such theories and their appeal for conceptualization of compartmentalized therapies. On the other hand, the complexity of experimental design, analysis, and interpretation for polymodal sensory afferents, and the difficulty to theorize how they contribute to sensory coding in health and disease may have caused setbacks. Notwithstanding, there are several key arguments for supporting specificity that are utilized for dismissing the multimodal nature of primary afferents. Among these are dispensability, experimental effects, and definition issues. Here I will briefly discuss these arguments and describe how I address these issues in the experiments performed for objective 1 (Chapter 2) of this dissertation.

As briefly mentioned, many studies promoting somatosensory labeled lines and claiming specificity in the recent years have relied on dispensability. In other words, upon ablation, or silencing, of population X, sensation A is reduced but sensation B is not significantly changed,

hence population X is a labeled line for sensation A. This is regardless of the fact that recording studies might have shown sensitivity of population X to stimuli with modality B; the argument being that behavioral outcomes are more important than cellular responses as redundant signals can be filtered further in the sensory pathway. As mentioned in the introduction in chapter 2, for itch alone, there are multiple studies identifying "itch-specificity" in distinct neuronal populations (Han et al., 2013; Liu et al., 2012; Roberson et al., 2013; Solinski et al., 2019; Stantcheva et al., 2016). These populations, when combined can sum up to 40% of the DRG neuronal population and almost half of the C nociceptors known to be mechanically activated. Therefore, we designed novel behavioral assays, trying to show the possibility of transduction of sensory modalities other than itch by activating one of these "itch-specific" populations. As argued in chapter 2 discussion, we believe precision of the behavioral tests used and detection sensitivity of previous experiments might be the main source of discrepancy.

Another source of discrepancy in the studies debating specificity vs. multimodality, is the experimental effects and the changes that research techniques impose on the afferents. For instance, Emery and colleagues (Emery et al., 2016) discuss that *in vivo* recording of calcium responses in dorsal root ganglia shows that more than 85% of these cells are activated solely by single stimulus modalities, unlike previous *in vitro* studies showing up to 80% being polymodal (Lawson et al., 2019) and further studies re-confirming widespread multimodality (Chisholm et al., 2018; Wang et al., 2018). They also argue that the high rate of multimodality observed in electrophysiological recordings of cultured primary afferents is likely a side effect of experimental conditions and the fact that these neurons are not intact and in their natural

milieu. Moreover, they discussed that by inducing chemical inflammation at the peripheral terminal site of primary afferents in hindpaws, they observed a slight increase in multimodal afferents. Although there are more detailed studies published since, that show greater percentages of multimodal cells in DRGs *in vivo* (Wang et al., 2018), it is still important to keep in mind the general concern about experimental manipulations and their effects on multimodality. Therefore, in order to reduce the possible alteration by experimental effects, in experiments described in objective 1 of this dissertation (chapter 2), we included behavioral assays performed on naïve wild-type animals that were not genetically or surgically manipulated in any forms as well.

Finally, incongruity of definition, the fallacy of an overly broad definition for subpopulations, is another commonly referred to argument when multimodality is demonstrated. In other words, if there is evidence that population X can contribute to modalities A and B, this might be due to the fact that a subpopulation of afferents, Xa, is responsible for A and another subpopulation, Xb, is responsible for B. Although likely to fall into circular debates and truly hard to refute, I will try to address this argument by elimination. Strictly speaking, if population X is shown to be involved in both sensory modalities A and B, and if population Xa is shown to transmit modality A, if we remove A-inducing Xa subset from X and as a result perception of sense B is reduced, at least part of Xa is multimodal and contributes to both A and B. In chapter 2, after activity-dependent silencing of target afferents, I will measure pain modality to verify these “itch” fibers’ contribution to pain.

As a proof of concept, chapter 2 will be dedicated to proving multimodal coding of itch and pain through the chloroquine receptor MrgprA3-expressing population of primary sensory afferents

previously described as “specifically linked to itch” (Han et al., 2013). Other than their significant clinical importance (St Sauver et al., 2013; Vos et al., 2016), itch and pain were chosen as they are similarly aversive sensations induced in the same receptor fields but they evoke distinct behavioral responses (withdrawal vs removal) (refer to literature review for further details about these modalities).

2) Provide a cellular atlas of primary sensory ganglia

Beyond theoretical models of specificity and multimodality in sensory systems, there is no doubt on the physiological and clinical importance of primary sensory ganglia. As gateways for somatosensory signals, the primary sensory ganglia (DRG and trigeminal ganglia), are already the sites of therapeutic interventions for sensory disorders such as chronic pain (Liem et al., 2016). These ganglia are composed of highly heterogeneous cells and unique anatomical structures that support the cell bodies of primary afferents, the longest cells in vertebrates (Devor, 1999). It is becoming more and more evident that key information for improving therapeutic interventions, e.g. analgesic or anti-pruritic treatments, is ingrained in understanding these cellular heterogeneities in sensory ganglia; not only among the neurons but also among their non-neuronal counterparts. Depending on the sensory coding models in mind, the elements defining diversities among ganglionic cells can be used as markers for categorization (e.g. for labeled lines), or for better understanding common molecular pathways that can modulate sensory signal transmissions (e.g. in multimodal signaling).

For this objective, as shown in chapter 3, I will take advantage of single-nucleus RNA and ATAC sequencing of whole human DRGs. The single-cell resolution of transcriptomic data has been used for providing new ways of grouping and categorizing primary afferents in rodents and humans (Nguyen et al., 2017, 2019, 2021; Ray et al., 2018; Sharma et al., 2020; Usoskin et al., 2015; Wangzhou et al.; Zeisel et al., 2018). As mRNA molecules are relatively short-lived, with half-lives of up to hours (Chen et al., 2008), complementing transcriptomic data with information on longer-lasting epigenomic modifications, which can persist in neurons for

months to years (Maze et al., 2015), at the single-cell level, can generate a one-of-a-kind resource. Furthermore, inclusion of non-neuronal cells in this resource can bring additional value and contribute to sensory research in ways never explored before.

Literature Review

Sensations

Historically, five modalities of sensation were described by philosophers such as Aristotle: touch, taste, smelling, hearing, and seeing. It is known now that several types of sensory modalities can be perceived by human sensory systems generating awareness for external (exteroception) or internal (interoception) stimuli: e.g. thermosensation, proprioception, equilibrioception, nociception, pruriception. While by representing attractive and aversive stimuli and providing feedbacks, these sensations help mature and maintain the nervous system throughout development and health, if the representation mechanisms become faulty, they can undergo malignant states and cause disabilities of their own. Therefore, it is of essential importance to understand sensory biology both in health and disease.

Sensory signals are primarily transduced by first-order afferents bearing specialized receptors from sensory organs with specialized receptive fields. These receptors and receptive fields are defined individually, depending on the sensory modality, e.g. colors in different parts of the visual field, frequencies and amplitudes of audible acoustic waves, or the temperature of an object on finger tips. Abnormal signals from these afferents can result in abnormal perceptions which can be categorized based on their sensory outcome. Hypoesthesia is when sensations are lowered in intensity (or complete insensitivity). Hyperesthesia happens when there is oversensitivity to stimuli (e.g. hyperalgesia). Paresthesia happens when an unusual sensation

(e.g. a mixture of burning, tingling or prickling) is perceived. And dysesthesia is the condition where sensations are confused with one another (e.g. allodynia or alloknesis).

Arguably the goal of sensory research is to provide options for treating sensory disorders. Yet, the first step is to understand how senses are detected and transmitted by the primary afferents so we can then figure how their messages can be altered in order to signal altered intensities or sensory cross talks. Before introducing some of the models for sensory coding and how intensities and modalities are transmitted, in the next section I will introduce the sensations that I selected as model modalities to investigate some of these questions. I will use pain and itch to describe in more details some of the interactions sensory modalities may have with one another and further in this chapter will use them to introduce the theories on how sensory discrimination can be achieved.

Pain and itch

After years of international debate, in year 2011 through the "Declaration of Montreal", access to pain management was declared a fundamental human right (International Pain Summit Of The International Association For The Study Of Pain, 2011). Not only this speaks to the importance of pain and the burden it is imposing on individuals and societies, but also it highlights the shortcomings and limitations that exist in understanding, treating, and managing pain. As a common symptom of many clinical conditions, and now accepted as its own disease, pain is the single top reason for visits to medical professionals, closely followed by other sensory complications such as itch (Fishman, 2007; St Sauver et al., 2013; Vos et al., 2016).

In the last decade, pain researchers have shown an increasing interest in understanding itch. Itch, or pruritus, is defined as an unpleasant sensation which leads to scratching behavior (or the desire to scratch). Similarly, pain can be defined as an unpleasant sensation associated with actual or potential damage (Merskey, 1979), with the difference being that it leads to withdrawal behavior rather than scratching. This similarity might be the reasons why Max von Frey, a prominent pain physiologist, in the early twentieth century, called itch "pain's little brother" and why scientists who study nociception (mechanisms for encoding and processing pain) are also interested in pruriception (mechanisms for encoding and processing itch). Here, I will highlight some similarities between these two sensations.

In the following paragraphs I will describe how nociception and pruriception, more than any other sensory modality, share anatomical pathways, influence one another, exhibit similar traits

and can transform interchangeably into one another (Akiyama et al., 2012; Bautista et al., 2014; Green and Dong, 2016; Han and Dong, 2014; Schmelz, 2015; Wilson and Bautista, 2013).

Anatomically, pain and itch share peripheral and central pathways. In the periphery, there is no evidence of purely itch-sensitive afferent fibers; all proposed pruriceptors (primary afferent fibers which convey itch sensation) are also responsive to painful stimuli, i.e. are nociceptors (LaMotte et al., 2014). This pathway overlap continues into the central nervous system (CNS) as well; itch information is projected to the same loci in the brain as pain is relayed to (Mochizuki et al., 2013), through the same spinal column (anterolateral system, or spinothalamic tracts) (Warren et al., 2018).

Pain and itch sensations can interact with each other. An example of the main influences of these two unpleasant sensations on one another is the occurrence of itch suppression by high-threshold noxious stimuli such as scratching. Decreased responsiveness to itch, or hypoknesis, can also be observed after painful electrical stimuli (Nilsson et al., 1997) or in the allodynic area surrounding an injection of capsaicin, the pungent compound in hot chili pepper (Brull et al., 1999). On the other hand, increased responsiveness to peripheral stimuli has been shown in itch-relaying projection neurons of the spinothalamic tract after capsaicin injection (Simone et al., 2004).

Similar characteristics of nociception and pruriception have been demonstrated in analogous conditions. One remarkable example of these similarities is agonist-evoked dysesthesia. While injection of an algogen (i.e. a pain-producing substance such as capsaicin) can induce allodynia (Sang et al., 1996), injection of a pruritogen (i.e. an itch-inducing substance such as histamine)

can result in alloknesis (Heyer et al., 1995) in a similar fashion. Furthermore, there are circumstances in which pain can be perceived as itch and vice-versa. These misperceptions can occur in specific disease states. For instance, patients with atopic dermatitis might sense itch when exposed to painful stimuli (Ikoma et al., 2004) while some patients suffering from neuropathic pain experience pain following application of pruritogens, such as histamine (Baron et al., 2001). Such sensory transformation can also be induced in experimental settings. For example, ablation of neurons which express the vesicular glutamate transporter 2 (VGluT2) (Liu et al., 2010) or silencing the neurons which express transient receptor potential cation channel V1 and A1 (TRPV1 and TRPA1) concurrently (Roberson et al., 2013) turned pain into itch. On the other hand, itch can be transformed into pain when bradykinin injection preceded histamine (Koppert et al., 1993).

These similarities, which are extended from cellular and anatomical levels to behavioral and cognitive levels, indicate that within the interconnected realm of somatosensation, itch and pain modalities share an even closer relationship. This close relationship, added to the existence of animal behavioral assays designed for discriminating their perception (Akiyama et al., 2014; LaMotte et al., 2011; Shimada and LaMotte, 2008; Yuan et al., 2016), makes the study of these two sensory modalities the ideal experimental paradigm for addressing the sensory discrimination dilemma.

Sensory coding theories

Regarding how multiple sensory modalities can be sensed from the same body area, e.g. skin, the cellular mechanisms are still debated. It is accepted that the initial sensory signals are carried through the primary sensory afferents, i.e. the focus of this dissertation, but whether these signals hold the modality information or they only carry intensity information, is a point of contention. Here I would try to introduce some of the theories that have been debated over the years. These theories can be reviewed based on two distinct parameters: "information contents" and "informative units". In other words, what type of information is carried by sensory neurons when activated by a stimulus, and what the minimum information units of sensory system are that can sufficiently signal a stimulus.

In terms of information contents, sensory coding theories can primarily be categorized based on how they conceive neurons and neural coding mechanisms. Many current models of sensory coding reduce neurons to ON/OFF switches that can message start, end, and possibly intensity of stimuli by their firing (Azarfar et al., 2018; Gjorgjieva et al., 2019). These models suggest that other information, for instance the modality and location of stimuli, is inherent to the "messenger", i.e. which neurons or pathways are activated. Other models propose that neurons can transmit further information through mechanisms such as time-to-first spike (Johansson and Birznieks, 2004), phase-of-firing (Montemurro et al., 2008), and firing patterns (Shoemaker et al., 2018).

Whether exclusively carrying intensity, or carrying multimodal information, neuronal coding of sensation can alternatively be classified based on their perspective on minimum information

units. At this level, sensory coding theories can be divided into models relying on single neurons vs populations of neurons for reliably transmitting stimuli information. Depending on how to perceive information contents of the signals transmitted through single neurons, the recruitment of neuronal populations can either be proposed for modulation of modalities (Ma, 2012), improved subthreshold signal and error detection (e.g. through stochastic resonance) (McDonnell and Abbott, 2009), disambiguation of signals (e.g. through population voting (Georgopoulos et al., 1988)), or for quality and modality coding (Panzeri et al., 2015).

Somatosensory modalities, such as pain, itch, touch, and thermosensation, have been used for development of models for sensory discrimination. As mentioned above, I have opted to focus on two of these modalities, itch and pain. Historically, the cognitive, anatomical, and physiological similarities of pruriception and nociception have contributed to proposals of various models for the neurophysiological basis of sensory discrimination. In the following paragraphs a brief review of common sensory coding models, specifically focused around itch and pain, is presented.

One of the first and most intuitive models proposed for somatosensory discrimination is "intensity theory" which is based on rate/frequency coding. This model suggests that transition from itch to pain is made through peripheral afferents increasing their discharge frequency. In the case of itch and pain, there is evidence that increased amounts of purely pruritogenic compounds, such as histamine, or reduced concentrations of pure algogens such as capsaicin, do not lead to modality shifts (or behavioral switches in animal models) (LaMotte et al., 2014). Yet as there are recent evidence for increased activity of higher-order neurons resulting in

differential behavior generation, e.g. mating versus fighting (Lee et al., 2014), revisiting such intensity based theories, particularly at population levels, may be necessary.

Pattern theory is the basis to another model of itch/pain discrimination. This model, proposes that itch and pain are differentiated by the firing patterns of the nociceptors. Entertaining ideas such as differential release of neuro-modulators based on firing patterns generated by distinct stimuli, there are recent studies showing itch transmission upon burst stimulation of primary afferents while their single pulse activation did not generate increased behavioral outcomes (Pagani et al., 2019).

As mentioned before, specificity models of somatosensory discrimination, i.e. “labeled line” model, suggest that there are certain types of afferents allocated to itch sensation. Several populations of pruriceptive neurons have been proposed in the periphery (Han et al., 2013; Liu et al., 2012; Roberson et al., 2013; Solinski et al., 2019; Stantcheva et al., 2016) and the CNS (Sun and Chen, 2007). While there is clear evidence that activation of these neurons can induce itch, activation of these fibers by painful stimuli and their contribution to nociception remains a highly debated matter.

Another proposed model for modality discrimination based on population coding of peripheral afferents is the “spatial contrast theory” (Namer and Reeh, 2013). This model claims that itch sensation can be perceived if a single or very few activated nociceptor receptive fields are surrounded by inactive ones. One specific piece of evidence for the relevance of spatial pattern of stimuli on the skin was shown by induction of itch, and not pain, when capsaicin was delivered in a punctate manner by inactivated cowhage spicules (Sikand et al., 2009, 2011). As

combinatorial models, that suggest single-cell and population coding strategies being used concurrently by the peripheral nervous system, are gaining more support (Fardo et al., 2020; Follmann et al., 2018; Panzeri et al., 2017), the spatial contrast theory is expected to receive more attention in the coming years.

Cellular diversity in primary ganglia

Regardless of how sensations are coded, cellular diversity among primary afferents is clearly a contributor to their function (Koerber and Mendell, 1988; Lallemend and Ernfors, 2012; Marmigère and Ernfors, 2007; Meltzer et al., 2021; Mense, 1990). Studying the peripheral sensory afferents has always been linked to categorizations based on these diversities, whether they are stemming from morphological, cytochemical, or extracellular interaction characteristics. Here, I will briefly introduce some of these classification approaches and their contribution to understanding sensory biology.

Many of the original studies on sensory afferents, identified different clusters based on anatomical characteristics. Depending on the site of investigation, these characteristics could be based on cell bodies (Campbell, 1946; Clark, 1926; Hatai, 1901; Yoshida and Matsuda, 1979), size of fibers (i.e. diameters) (Hursh, 1939; Rexed and Sourander, 1949), structures they innervate (Koerber et al., 1988), or myelination states (Gasser, 1950). In some of these early studies, theoretical modeling, combined with electrical stimulation and recording techniques, unraveled correlations between these anatomical characteristics and the information contents of the fibers (Dawson, 1956; Goldman and Albus, 1968). These studies also built the foundation of our understanding on sensory receptive fields (Eccles, 1964; Johansson, 1976; Johansson and Vallbo, 1980), sensory sensitization (Torebjörk and Ochoa, 1980), and differences in conduction velocity among major classes of fibers (Dawson, 1956; Gasser and Erlanger, 1927; Hursh, 1939). This in turn was expanded to classifications based on myelination states with Aβ fibers being fast-conductive highly myelinated cells, Aδ slow conducting lightly myelinated cells, and small-

diameter unmyelinated C fiber cells (Harper and Lawson, 1985a, 1985b). This classification also correlated with previous morphological clusterings as highly myelinated cells also tend to have larger cell bodies and higher diameter axons (Bishop, 1959; Lawson and Waddell, 1991). As stimulation thresholds, conduction velocities, and signal patterns were shown to be different among primary sensory neurons with different myelination states, cells belonging to different categories of such classification were easily correlated with different sensory modalities (Torebjörk and Ochoa, 1980). Based on such deductions, it has become a common belief that nociceptive afferents are mainly of C types and most A afferents are low threshold mechanoreceptors (Todd and Koerber, 2006). Although there is evidence for myelinated fibers contributing to pain (Burgess and Perl, 1967; Djouhri and Lawson, 2004) and unmyelinated fibers' contribution to touch (Johansson et al., 1988; Vallbo et al., 1993), this classification is still commonly referred to in the field of somatosensory research as they also tend to correlate well with cytochemical classifications (Lawson and Waddell, 1991).

With the advancement of cytochemical techniques and establishment of proteins as functional units in the cells, expression of sensory-related proteins in primary afferents was presented as a classification method (Senba and Kashiba, 1996). Over the years, the use of functionally relevant cytochemical elements as clustering parameters (Carr and Nagy, 1993; Le Pichon and Chesler, 2014) evolved into efforts to find markers that are differentially expressed in subpopulations of afferents (Gatto et al., 2019). With this new approach, taking advantage of large scale "omics" techniques, there are many published and ongoing projects that aim to "unbiasedly" cluster primary afferents based on their cytochemistry (Kupari et al., 2021; Nguyen et al., 2021; Ray et al., 2018; Usoskin et al., 2015; Wangzhou et al.; Zeisel et al., 2018).

Another source of diversity is unmasked when sensory neurons are considered in their natural environment and not in isolation. The networks these cells belong to, the chemical milieu around their cellular compartments, and the other cells they interact with can fundamentally change their function. In terms of networks in the spinal cord, different subpopulations of peripheral afferents tend to have distinct innervation densities into various layers of the dorsal horn (Yousefpour, 2021). Although there are no modality-specific nuclei or regions known in the spinal cord, it is generally accepted that various circuits in the dorsal horn contribute to sensory modality processing in health and disease by involving different interneuron populations (Bourojeni, 2020). In terms of chemical milieu, there is evidence that subsets of primary sensory neuronal subtypes express different immune and cytokine receptors (Cevikbas et al., 2014; Jakob et al., 2021; Solinski et al., 2019). It has also been shown that the excitability of sensory afferents and their signaling properties can be influenced by local chemical changes such as inflammation (Miller et al., 2009; Momin and McNaughton, 2009). Nevertheless, there are not many studies that attempted the clustering of peripheral afferents based on their capability to respond to local environmental changes (for instance immune interactions such as those discussed by (Solinski et al., 2019)), nor are there detailed studies on differential capacities of neuronal subtypes to react to physiological changes (Nguyen et al., 2019). Finally, when aiming to understand the functional diversity of peripheral afferents, it is important to consider the other cell types they interact with. Other than evidence for close connections between neurons in sensory ganglia (Amir and Devor, 1996; Kim et al., 2016; Rozanski et al., 2012), there are multiple non-neuronal cell types that are shown to closely interact and influence primary afferents (Esposito et al., 2019; Feldman-Goriachnik and Hanani, 2021;

Haberberger et al., 2019; Kung et al., 2013). These non-neuronal cells and their - possibly differential - contribution to sensory coding are gaining attention in the recent years as important sensory players in health and disease (Hanani and Spray, 2020; Iwai et al., 2021).

Chapter 2:

Differential coding of itch and pain by a subpopulation of primary afferent neurons

Behrang Sharif[1,2,3], Ariel R. Ase[1,2], Alfredo Ribeiro-da-Silva[2,4], and Philippe Séguéla[1,2,*]

[1] Montreal Neurological Institute, Department of Neurology & Neurosurgery, McGill University, Montreal H3A 2B4, Quebec, Canada

[2] Alan Edwards Centre for Research on Pain, Montreal H3A 0G1, Quebec, Canada

[3] Department of Physiology, McGill University, Montreal H3G 1Y6, Quebec, Canada

[4] Department of Pharmacology & Therapeutics, McGill University, Montreal H3G1 Y6, Quebec, Canada

* Lead contact. Correspondence: philippe.seguela@mcgill.ca

PUBLISHED: APRIL 15, 2020,

NEURON, VOLUME 106, ISSUE 6, 17 JUNE 2020, PAGES 940-951.E4

https://doi.org/10.1016/j.neuron.2020.03.021

Summary

Itch and pain are distinct unpleasant sensations which can be triggered from the same receptive fields in the skin, raising the question of how pruriception and nociception are coded and discriminated. Here we tested the multimodal capacity of peripheral first-order neurons, focusing on the genetically-defined subpopulation of mouse C-fibers that express the chloroquine receptor MrgprA3. Using optogenetics, chemogenetics and pharmacology, we assessed the behavioral effects of their selective stimulation in a wide variety of conditions. We show that metabotropic Gq-linked stimulation of these C-afferents, through activation of native MrgprA3 receptors or DREADDs, evokes stereotypical pruriceptive rather than nocifensive behaviors. In contrast, fast ionotropic stimulation of these same neurons through light-gated cation channels or native ATP-gated P2X3 channels predominantly evokes nocifensive rather than pruriceptive responses. We conclude that C-afferents display intrinsic multimodality and we provide evidence that optogenetic and chemogenetic interventions on the same neuronal populations can drive distinct behavioral outputs.

Keywords

pruritus, nociception, somatosensation, optogenetics, chemogenetics, C-fibers, MrgprA3, P2X3

Introduction

Itch and pain are the primary presenting symptoms in most clinical visits (St Sauver et al., 2013) and the causes of disability in many burdensome diseases (Vos et al., 2016). Basic understanding of how distinct somatosensory modalities are transduced and perceived in healthy and disease states has significantly improved with the identification of neuronal subcategories and spinal pathways. In particular, primary afferents have been categorized and characterized extensively (Le Pichon and Chesler, 2014; Usoskin et al., 2015; Zeisel et al., 2018). Despite advancements in understanding somatosensory transduction, the basic principles of sensory modality discrimination, especially for overlapping modalities such as itch and pain, remain unclear.

Itch is defined as an unpleasant sensation which leads to scratching or the desire to scratch, a behavior aimed at removal of chemical or mechanical irritants. Similarly, pain can also be described as an unpleasant sensation, with the difference being that it leads to withdrawal or mitigating behavior rather than scratching. Pruriception and nociception share anatomical pathways (Davidson and Giesler, 2010; Klein et al., 2011) and influence one another (Brull et al., 1999; Nilsson et al., 1997; Simone et al., 2004). However, this close relationship, contrasted by distinct behavioral outcomes, poses a conundrum: how does the somatosensory system differentiate itch from pain to trigger the appropriate response i.e. fight (removal) versus flight (withdrawal)?

Historically, various models for somatosensory discrimination have been proposed, based on intensity of stimuli, firing pattern of the afferents, subcategories of modality-specific neuronal

populations, or spatial pattern of the stimuli (LaMotte et al., 2014; McMahon and Koltzenburg, 1992; Schmelz, 2015). The most studied model for itch is the “labeled line” or “specificity” theory: dedicated cellular components, from the periphery to the brain, are specialized for pruriceptive transduction, transmission and perception (McMahon and Koltzenburg, 1992). The Mas1-related G protein-coupled receptor A3 (MrgprA3)-expressing subpopulation of unmyelinated (C) afferents has been proposed as one “labeled line” for itch (Han et al., 2013). Mrgprs constitute a family of G protein-coupled receptors enriched in non-peptidergic primary somatosensory neurons (Dong et al., 2001; Lembo et al., 2002; Liu et al., 2009; Zylka et al., 2003). MrgprA3, or its human ortholog MrgprX1, is the main receptor of the pruritogenic compound chloroquine (CQ) and multiple converging evidence indicate that the MrgprA3-expressing primary sensory neurons specifically mediate CQ-induced itch responses (Han et al., 2013; Liu et al., 2009; Ru et al., 2017). As no significant reduction in pain behavior was observed following ablation of MrgprA3 C-afferents in adult mice, their dispensability for nociception was inferred. Essentiality and sufficiency of these neurons for pruriception were also demonstrated as their ablation leads to a reduction in itch behavior while their activation by capsaicin in $Trpv1^{-/-}$;$MrgprA3^{Cre\text{-}GFP}$;$ROSA26^{Trpv1}$ mice resulted predominantly in scratching behaviors (Han et al., 2013).

Other peripheral “labeled lines” have been characterized as pruriceptive primary afferents, including somatostatin-expressing neurons responsible for itch induced by Il-31 and 5HT (Stantcheva et al., 2016), MrgprA3-negative histamine-sensitive pruriceptors (Roberson et al., 2013), and MrgprD afferents mediating β-alanine-induced itch (Liu et al., 2012). Tallying the “labeled lines” for itch results in a large proportion of primary somatosensory neurons including

most non-peptidergic C-fibers reported as mechano-nociceptors (Scherrer et al., 2009). The simple fact that these pruriceptors can also respond to noxious stimuli calls for alternative models as the “specificity” theory requires the existence of a subset of primary sensory neurons that respond to pruritogenic stimuli and no other (McMahon and Koltzenburg, 1992).

Attesting to intrinsic multimodality of primary sensory neurons, we report here that metabotropic stimulation of MrgprA3 C-afferents predominantly triggers itch while fast ionotropic stimulation of the same neuronal population predominantly drives pain. We further confirm distinct sensory perceptions by pharmacological interference with gastrin releasing peptide (GRP) signaling for itch or opioid signaling for pain. We also show that, downstream of MrgprA3 C-afferent stimulation, pruriception depends on the recruitment of calcium-permeable TRP channels, whereas these channels do not contribute to nociception, providing a molecular basis for somatosensory discrimination at the peripheral level. Finally, we demonstrate for the first time that the MrgprA3 C-afferents indeed contribute to acute pain coding as their conditional silencing significantly reduces ATP-induced nocifensive responses.

Results

Metabotropic activation of MrgprA3 C-afferents induces itch

Chloroquine (CQ) induces itch through activation of the G protein-coupled MrgprA3 receptor. The dependence of CQ-induced pruriception on MrgprA3 has been established by knock-out and rescue experiments (Liu et al., 2009). To test the sufficiency of metabotropic receptor activation for the induction of itch, we expressed the excitatory Gq-coupled DREADD hM3Dq-mCherry (Urban and Roth, 2015) in MrgprA3^{+} neurons through AAV-mediated delivery in hemizygote MrgprA3$^{Cre\text{-}eGFP}$ mice. Viral transduction efficiency and expression of heterologous hM3Dq were validated by immunofluorescence of mCherry (Figure 1a). The GFP fused to Cre recombinase in MrgprA3$^{Cre\text{-}eGFP}$ mice allowed visualization and counting of MrgprA3^{+} cells. We observed a relatively small population of MrgprA3^{+} C-afferents in the primary sensory ganglia (8.6 ± 1.3% SEM, 18 DRG sections, 6 animals). A viral transduction efficiency of 44.4 ± 5.1% (SEM) was observed in Cre-eGFP-expressing neurons with almost perfect specificity (i.e. complete overlap of hM3Dq-mCherry and Cre-eGFP reporter). Functionally, hM3Dq-evoked excitation of virally transduced MrgprA3 neurons was validated by ratiometric calcium imaging using the DREADD agonist clozapine N-oxide (CNO) *in vitro* (Figure 1b). From the 12 recordings performed on primary DRG cultures from 3 animals, 61 EYFP^{+} cells were analyzed as they responded to the positive control high KCl. Out of the 61 cells, 50 cells (82%) were responsive to CQ and 12 cells (20%) showed calcium transients in response to CNO. To study the behavioral consequences of *in vivo* activation of MrgprA3 C-afferents through heterologous Gq-coupled receptors, scratching responses to 3 mM CNO injection in the nape of the neck of AAV hM3Dq-

mCherry-transduced mice were compared to responses of their MrgprA3$^{Cre\text{-}eGFP\text{-}/\text{-}}$ cage/littermates who also received postnatal AAVs (Figure 1c-f). Animals were videotaped from three angles (Suppl. Figure 1a) for 60 minutes after injection. Accurate and unbiased measurement of each scratching bout was performed offline by a blinded experimenter identifying all start and end points. The number of scratching bouts and sum of durations spent scratching for each individual mouse in every 30 second bin after injection is visualized in separate heatmaps (Figure 1c). To qualitatively study the behaviors, we documented the distribution of durations of individual scratching bouts for every single scratching behavior observed (Figure 1d). This measurement indicates how effective the scratching is and the similarity of the distribution histograms suggests a similar perceptive state. Our scoring approach also enables us to detect changes in behavior over time (Figure 1e) as well as overall differences over the one-hour period (Figure 1f). CNO injection in the nape of the neck of AAV-injected Cre-negative mice did not induce scratching (Figure 1c), whereas in their Cre^{+} cagemate littermates a robust itch developed soon after injection (Figure 1e) resulting in significantly higher total number of bouts (Figure 1f). When the same Cre^{+} animals received 10 mM CQ (Green et al., 2006), pruritus built up for longer time (Figure 1e) with higher intensity (Figure 1e, f) compared to the itch induced by CNO. Comparable bout durations resulted in similar, and statistically akin, time-course and total time of scratching (Suppl. Figure 1b and c)

In agreement with previous reports (Han et al., 2013), our results indicate that selective chemical stimulation of MrgprA3 C-afferents induces pruriception. The intensity of itch responses caused by the activation of endogenous MrgprA3 receptors by CQ was significantly higher than the intensity of itch responses evoked by selective stimulation of the DREADD-

expressing subset. The weaker response may be attributed to viral transduction (i.e. smaller afferent population activated), different levels of expression of hM3Dq and MrgprA3 receptors at the surface of the afferents, suboptimal coupling of the DREADD to intracellular signaling pathways, or the different pharmacokinetic properties of the agonists CNO and CQ.

Selective light-gated ionotropic activation of MrgprA3 C-afferents induces aversive responses distinct from scratching

To test a different mode of stimulation on the same genetically-defined primary afferents, we expressed the excitatory light-gated actuator channelrhodopsin-2 (ChR2) in MrgprA3^{+} neurons by crossing transgenic lines to produce MrgprA3$^{Cre\text{-}eGFP+/-}$:Rosa26$^{ChR2\text{-}eYFP+/-}$ animals. Selective Cre-dependent expression of ChR2 in MrgprA3^{+} neurons was validated by the localization of their respective conjugated fluorophores, membrane-bound eYFP for ChR2 and nuclear eGFP for Cre (Supplementary figure 2a), in primary sensory ganglia (Figure 2a). Trafficking of ChR2 to peripheral terminals was validated by the eYFP signal observed in the epidermis of the nape of the neck counterstained with the peripheral neural marker PGP9.5 (Figure 2b), confirming the feasibility of transdermal illumination for activation of cutaneous MrgprA3^{+} nerve endings. In order to check the functionality of the excitatory opsins in MrgprA3^{+} neurons, *in vitro* electrophysiology experiments were performed. Recordings on ChR2^{+} cells confirmed inward photocurrents (7.54 ± 1.24 pA/pF, 20 cells, 3 animals) (Figure 2c), optically-induced action potentials, and firing frequencies of up to 10 Hz driven by blue (470 nm) laser pulses (Figure 2d). Blue laser illumination of the nape of the neck evoked behavioral responses distinct from stereotypical scratching behavior. Other aversive behaviors such as vocalization, escaping, and

attempts to bite the light source, rather than scratching, constituted the vast majority of responses evoked by transdermal optical stimulation (Figure 2e and Suppl. Video 1). We did not observe a correlation between the frequency or intensity of the laser pulses and the type of elicited behavior despite screening multiple protocols of frequency-intensity combinations. Similar illumination of control MrgprA3$^{Cre\text{-}eGFP\text{-}/\text{-}}$:Rosa26$^{ChR2\text{-}eYFP+/\text{-}}$ cagemate littermates did not elicit any behavioral responses above background (Suppl. Video 2), neither did yellow (589 nm) laser pulses with same or higher intensity in the same animals, indicating that the responses are generated through ChR2 channels rather than through thermal or visual effects of light pulses.

These results demonstrate that, similar to other subsets of primary somatosensory neurons (Daou et al., 2013), MrgprA3 C-afferents can be controlled *in vitro* and *in vivo* by optogenetic actuators. They also suggest that nocifensive responses are evoked by optical stimulations of MrgprA3 C-afferents, although in rare occasions stereotypical pruriceptive behaviors can be observed.

MrgprA3 C-afferents trigger distinct somatosensory perceptions based on their activation mode

In order to clarify the sensory modalities evoked by differential activation of MrgprA3-expressing fibers, we used the cheek behavioral discrimination assay (Shimada and LaMotte, 2008). Although the nape assay represents a common behavioral assay for studying itch in mice, it cannot definitively discriminate between itch and pain. In the cheek assay however, pruritogenic stimuli evoke hindpaw scratching while algesic stimuli evoke unilateral forepaw wiping (Shimada and LaMotte, 2008). Therefore, to confirm the sensory modality perceived

following excitatory DREADD activation, AAV-injected MrgprA3$^{Cre\text{-}eGFP+/-}$ animals were videotaped from different angles for one hour after injection of CNO in the cheek. Accurate frame-by-frame timings of scratching bouts and unilateral wipes targeted to the site of administration, i.e. ipsilateral to the injection, were recorded offline by a blinded experimenter (Supplementary Video 3). The timeline of both behaviors in each individual mouse is shown in Figure 3a. Similarly, behavioral responses evoked by activation of MrgprA3 by CQ in the cheek of wildtype mice were analysed (Figure 3b). In both conditions, animals exhibited significantly higher counts of scratching bouts than wipings (Figure 3c), indicating pruriception. Similar to our results in the neck (Figure 2), the scratching induced by CQ is stronger than that of CNO (Suppl. Figure 2b). To be able to unambiguously assess the sensory modality associated with optical activation of MrgprA3-expressing fibers, we designed an optogenetic version of the cheek assay. In order to keep constant both location and light power for transdermal optical stimulation of the cheek with a blue laser, and also to avoid movement hindering, custom 3D-printed headposts were designed as optical fiber holders (Figure 3d). Headposts were chronically implanted on the skull of adult MrgprA3$^{Cre\text{-}eGFP+/-}$:Rosa26$^{ChR2\text{-}eYFP+/-}$ mice several weeks before the experiments (Figure 3d) after confirmation of ChR2 expression in trigeminal ganglia and trafficking to the cheek hairy skin (Suppl. figure 2c & d). Acclimated animals then received 470 nm blue laser pulses on their cheek and the behavioral responses, i.e. forepaw wiping or hindpaw scratching, were recorded. Restricting the illumination site to the same single spot on the skin increased the probability of desensitization after few stimulations. To minimize desensitization, each animal received a maximum of 8 trains of light pulses (trials), in each experiment session and the sessions were at least 48 hours apart. With such approach,

light-evoked behavioral responses were observed in 36.2 ± 3.9% (SEM) of the trials (5 animals, 15 sessions total, with 8 trials per session). Stereotypical pain-associated cheek wipings were observed in most responses (77.6 ± 7.0% SEM) to blue light pulses (Figure 3d and Supplementary video 4). The same animals did not respond to yellow light pulses with similar or higher laser power in control experiments (Supplementary video 5), confirming that the behavioral responses are induced by ionotropic excitation of MrgprA3 C-afferents through ChR2 activation. Furthermore, the control MrgprA3$^{Cre\text{-}eGFP\text{-}/\text{-}}$:Rosa26$^{ChR2\text{-}eYFP+/\text{-}}$ cagemate littermates showed no response to similar illumination ruling out the effect of bright light causing aversion and/or visual distraction (Supplementary video 6). The perception evoked by fast ionotropic activation of these MrgprA3 C-afferents is dictinct from the perception evoked by their metabotropic activation, and this multimodality is supported by distinct wiping/scratching ratios in the cheek assay (Figure 3f).

Our results demonstrate that the MrgprA3 C-afferents are intrinsically capable of multimodal sensory coding based on their activation mode. For the first time we provide evidence that a single population of primary afferents can be sufficient to induce more than one modality of somatosensation, itch and pain in this case.

Itch and pain mediated by MrgprA3 C-afferents engage distinct pathways

To verify whether the distinct behavioral responses evoked by different activation modes have unique tractable properties and network consequences, we investigated higher-order pathways recruited at the spinal cord level. To confirm the spinal pathways engaged downstream of

peripheral activation of MrgprA3 C-afferents *in vivo*, we checked the involvement of the gastrin-releasing peptide (GRP) and its receptor GRPR, as several studies have indicated that itch depends on the GRP-GRPR pathway in the spinal cord (Albisetti et al., 2019; Sun and Chen, 2007; Sun et al., 2009). Verifying MrgprA3 afferents' innervations to the dorsal horn of spinal cord (Suppl. Figure 3a & b), we blocked GRPR by intra-cisternal (i.c.) administration of the GRPR antagonist, RC-3095. Dye injection tests confirm that compounds administered i.c. can diffuse to the lumbar enlargement as soon as 5 minutes post injection. CQ was injected intra-dermally (i.d.) 15 minutes after i.c. administration of RC-3095 or vehicle (saline). Animals were videotaped from multiple angles for one hour. Accurate time points for all scratching bouts were analyzed offline for generation of bout count and scratching duration heatmaps (Figure 4a). Overall similarity of the heatmaps and comparable bout duration histograms indicate qualitative similarity in the scratching behaviors in drug or vehicle conditions (Figure 4a, b). Analysis of the scratching time course following GRPR inhibition reveals a decreased intensity in early time points after CQ injection (Figure 4c and Supplementary Figure 3c). Efficiency of GRPR blockade is also demonstrated by the significant decrease in total scratching bout counts and total time spent scratching during the 1-hour period following CQ injection (Figure 4d and Supplementary Figure 3d).

These data confirm that a spinal GRP/GRPR-dependent pruriceptive pathway is engaged when MrgprA3 C-afferents are stimulated metabotropically through activation of native Gq protein-coupled receptors. Injection of the selective μ-opioid receptor agonist DAMGO i.c. did not cause a significant change in the number of scratching bouts.

To study the recruitment of similar or distinct central pathways downstream of optical activation of MrgprA3 C-afferents *in vivo*, we designed experiments for quantitative analysis of nociception based on well-established models of pain scoring in mouse hindpaws. Trafficking of ChR2 in the peripheral MrgprA3 fibers in the glabrous skin of hindpaw was confirmed by the presence of eYFP (Figure 5a) in addition to its expression validation in the lumbar DRGs and the trafficking to the central terminals in dorsal horn of the spinal cord (Supplementary Figure 4). Transdermal illumination of the hindpaw induces nocifencive behaviors in the MrgprA3$^{Cre\text{-}eGFP+/-}$:Rosa26$^{ChR2\text{-}eYFP+/-}$ mice (Supplementary video 7). These responses range between withdrawal and flinches, to licking, shaking, and, rarely, vocalization. No evoked behavioral response was observed in Cre-negative cagemate littermates after illumination of the hindpaw, eliminating concerns about possible thermal or visual effects of the laser light (Supplementary video 8). When treated with RC-3095, similarly to when they received vehicle, animals showed behavioral responses to nearly all optical stimulations (Figure 5c). On the contrary, when the animals received DAMGO, they were found to be insensitive to the majority of stimulations (Figure 5c). This difference was also evident by comparison of the probability of single behavior types such as shaking which is linked to higher pain intensities. The lack of RC-3095 effect on shaking behavior is in contrast with the powerful suppressing effect of the opioid DAMGO (Figure 5d).

These results indicate that unlike pruriception caused by metabotropic excitation of MrgprA3 C-afferents, nociception induced by optical stimulation of these primary sensory neurons is not GRP/GRPR-dependent. Furthermore, we provide evidence that, like most nocifensive responses, optically induced MrgrA3 neuron-dependent pain behavior is sensitive to opioids.

Calcium-permeable TRP channels contribute exclusively to the pruriception but not to the nociception mediated by MrgprA3 C-afferents

Next we investigated what molecular pathways in the MrgprA3 C-fiber neurons may be differentially involved downstream of their metabotropic (i.e. GPCRs) or ionotropic (i.e. ChR2) stimulation. As TRP channels have been proposed as key components of CQ-evoked pruriception (Hill et al., 2018; Moore et al., 2018; Than et al., 2013; Wilson et al., 2011), we tested the effects of blocking sensory TRPC3, TRPA1, and TRPV1 channels with selective antagonists (Figure 6).

For the pruriception arm of this experiment, acclimated animals were injected subcutaneously with pyrazole 10, HC030031, AMG9810 (selective blockers of TRPC3, TRPA1, and TRPV1, respectively), or their vehicle, in the nape of the neck 10 minutes before i.d. injection of chloroquine. They were then videotaped for 1 hour from multiple angles and behaviors were scored offline by a blinded experimenter (Figure 6a-d). Overlapping bout duration distribution and general similarity of bout counts and time spent scratching heatmaps suggest similar perceptual quality evoked in all groups (Figure 6a and b). Behavioral analysis of bout counts as well as time spent scratching indicates that all three blockers significantly decrease pruriception intensity in early time points after CQ injection (Figure 6c and Suppl. Figure 5). Notwithstanding, total counts and times of scratching for the 1-hour period after CQ injection were significantly reduced only following TRPA1 and TRPV1 blockade (Figure 6d). This can be attributed to the different pharmacokinetics of the blockers or differences in the contributions of specific TRP

channels to the pruriceptive signal. In agreement with previous studies, we show that the pruriception caused by chemical activation of MrgprA3 primary afferents engages calcium-permeable TRP channels.

Reciprocally, for the nociception arm of this experiment, we asked if the TRP channels are specifically linked to the itch modality or are activated regardless of stimulation mode. Habituated animals received selective TRP blocker or vehicle in both hindpaws 10 minutes before intermittent pulses of 470 nm (blue) laser were applied to their glabrous skin. Unlike the opioidergic intervention on the central terminals with DAMGO described previously (Figure 5), there were no significant changes observed after peripheral blockade of the TRP channels TRPC3, TRPV1, or TRPA1. In all instances of optical stimulation the animals manifested nocifensive responses, and expression of higher-intensity behaviors such as shaking did not show any significant decrease (Figure 6e). We conclude from these observations that calcium-permeable TRPC3, TRPA1 and TRPV1 channels do not contribute significantly to the pain signaling pathway downstream of optical activation of MrgprA3 C-afferents.

Collectively, these results indicate that TRP channels expressed in MrgprA3 C-afferents are engaged in itch transduction but are not recruited in optically induced nociceptive transduction.

MrgprA3 C-afferents contribute to acute pain responses in wildtype mice

To assess the contribution of MrgprA3 C-afferents to pain in more naturalistic conditions and in non-transgenic wildtype mice, we studied the behavioral effect of their fast ionotropic stimulation through the activation of native cation channels. We took advantage of the fact that

most nonpeptidergic C-afferents, including the MrgprA3 subset, express P2X3 ATP-gated channels (Usoskin et al., 2015). It has been shown that application of the P2X3 agonist α,β-methylene ATP (αβmeATP) in rats and mice induces pain (Bland-Ward and Humphrey, 1997; Kakimoto et al., 2008; Kato et al., 2002; Tsuda et al., 2002). We confirmed that the nocifensive behavioral responses evoked by selective P2X agonists consists of lifting and licking, manifested chiefly in the first 5 minutes after injection in the hindpaw. These responses are similar to that of nocifensive ChR2-evoked responses in MrgprA3$^{Cre\text{-}eGFP+/-}$:Rosa26$^{ChR2\text{-}eYFP+/-}$ mice (Figure 5). To study the contribution of MrgprA3-expressing afferents to αβmeATP-induced pain, we used the approach of conditional activity-dependent silencing with QX-314. It has previously shown that CQ effectively induces the influx of QX-314 in MrgprA3 neurons, resulting in their silencing (Roberson et al., 2013). Acclimated wildtype C57Bl6 mice were placed on the testing platform for at least 30 minutes before receiving a conditioning intraplantar coinjection of 5 mM CQ and 1% QX-314, or a control solution of saline and 1% QX-314. Thirty minutes after conditioning 10 µL of 20 mM αβmeATP was administered to the same hindpaw. Total counts and time spent licking or lifting the injected hindpaw in every 10 second bin post-injection is visualized in separate heatmaps (Figure 7a). Temporal progression of the total time spent behaving shows significantly higher intensities of nociceptive behavior in controls compared to the QX-314 + CQ group (Figure 7b). The total duration of time spent manifesting nocifensive responses over the 5 minutes post-αβmeATP injection also indicates a significant decrease when the MrgprA3 C-afferents were silenced with QX-314 + CQ (Figure 7c). Separate analysis of lifting and licking responses show similar reduction in the QX-314 + CQ group compared to that of the QX-314 + saline group (Supplementary Figure 6).

We conclude that MrgprA3 C-afferents significantly contribute to the acute pain behavior caused by αβmeATP injection as their silencing results in decreased nociceptive responses in this model. These data support our hypothesis that, in specific conditions such as optogenetic or naturally-occuring fast purinergic ionotropic stimulations, these C-fibers can convey pain signals.

Discussion

Taking advantage of cell type-selective stimulation techniques, we provide evidence that a single genetically-determined population of peripheral afferents, the MrgprA3 subset previously proposed as a "labeled line" for itch, is sufficient for coding both itch and pain signals. Regardless of their genetic labeling, we also show that CQ-responsive afferents can signal both acute pruriceptive and nociceptive stimuli in natural conditions. We further demonstrate that these neurons exhibit their multimodal properties by recruiting specific ion channels and by engaging divergent pathways in the spinal cord. Challenging the "labeled line" theory, our data support the concept that somatosensory discrimination can be initiated at the peripheral level in primary afferents through cell-autonomous mechanisms.

In order to dissect functional contribution of primary sensory afferentsto somatosensation, various methods of genetic and morphological categorization have been implemented (Le Pichon and Chesler, 2014; Usoskin et al., 2015; Zeisel et al., 2018). Basic molecular and functional characterization of MrgprA3 C-afferents provides hints of their multimodality as this neuronal subset does not fit in any single conventional category of primary afferents, e.g. peptidergic vs. non-peptidergic, mechano- vs. heat-sensitive, or nociceptors vs. pruriceptors. Indeed approximately 85% of MrgprA3 neurons express the peptidergic marker CGRP while ~80% express the non-peptidergic marker IB4, and ~85% express P2X3 ATP receptors. They display electrophysiological properties of C-mechanoheat (CMH) nociceptors and respond to histamine, capsaicin, chloroquine and cowhage (Han et al., 2013). Thus, in addition to cellular categorizations, we propose recognizing their mode of stimulation. For controlled comparisons, we chose to engage MrgprA3^{+} cells through either the native metabotropic actuator MrgprA3

or the heterologous ionotropic actuator ChR2. We ensured access to the same population of neurons and co-expression of ChR2 and MrgprA3, by crossing the MrgprA3-Cre driver with Cre-dependent actuator lines as almost perfect co-expression of reporters (over 96%) has been previously established (Han et al., 2013; Tang et al., 2016). Furthermore, independently from any genetic targeting intervention, we present evidence that CQ-responsive afferents convey itch (Figures 1 & 3) while the same pharmacologically-identified afferents contribute to pain coding (Figure 7). Therefore, different modes of stimulation induce distinct behaviors reflecting different sensory modalities with distinct pharmacological characteristics consistent with the perception of pain and itch. We also report that coding itch modality is independent of the size of the MrgprA3 afferent population recruited, since stimulation of only a fraction of these cells through virally-transduced DREADDs generates stereotypical itch responses qualitatively identical to behaviors evoked by their global activation through endogenous MrgprA3 receptors, yet with lower intensity.

Quantitative animal behavioral assays have significantly improved our understanding of itch as a sensory modality (Dong and Dong, 2018; LaMotte et al., 2011). Using a detailed quantitative method we confirm the “waxing and waning” of itch (Forster and Handwerker, 2014). In addition to measuring itch intensity with scratching bout counts or time spent scratching, individual scratching bout durations can also be used to describe itch perception. Considering the complex nature of pruritus, with multiple initiation mechanisms (Green and Dong, 2016; Han and Simon, 2011; Luo et al., 2015), cellular/molecular diversity (Bautista et al., 2014; Song et al., 2018), behavioral itch-scratch cycles (Mack and Kim, 2018), we believe analyzing and presenting scratching data over time improves detection and comparison between

interventions. We also used a quantitative approach towards behavioral analysis of nociception because animals present various responses to painful stimuli at various locations on their body. Therefore, we measured all nocifensive responses as well as intense-pain behaviors like shaking for pain quantification (Figures 5 and 6). A lack of sensitivity may be the main cause for not observing significant pain reduction following ablation or inactivation of small subsets of C-afferents such as MrgprA3^{+} cells representing less than 10% of DRG neurons (Han et al., 2013; Liu et al., 2009). Proving that with appropriate readouts the MrgprA3 afferents' contribution to acute nociception is detectable, our results further show that in specific conditions their stimulation can be sufficient to evoke nocifensive behaviors.

Although pruriceptive and nocifensive behaviors have been characterized in mice in different assays, not all behavioral manifestations are associated with either itch or pain, like grooming in the cheek assay (Shimada and LaMotte, 2008). An unbiased characterization of behavioral responses is particularly important when it comes to testing the effects of unnatural stimuli such as optical stimulations in optogenetic experiments. This could be one main cause of discrepancy between our results and data by Sun et al. (2017) showing induction of itch and no pain upon transdermal photostimulation of MrgprA3 fibers. We quantified all responses that were elicited by laser illumination on the neck, including but not limited to scratching, and measured uncategorized aversive behaviors separately. It is also important to consider that itch responses directed to different areas of the body can differ, e.g. hindpaw scratching of the cheek but rapid biting of the calf in response to pruriception (LaMotte et al., 2011). This is partly due to anatomical constraints, e.g. not reaching the nape with the forepaw and precluding wiping behavior upon neck illumination as mentioned by Sun et al. (2017). We

believe that in experiments without stabilized optical sources, uncontrolled illumination site and power, due to moving targets, is a source of discrepancy in interpreting results. That is why we chose to use the cheek assay (Shimada and LaMotte, 2008) with constant stimulation field. Our unambiguous results with the cheek assay, and the fact that on three different body areas (neck, cheek and hindpaw), we did not observe predominant stereotypical itch behaviors (hindpaw scratching or biting), support our conclusion that optical stimulation of MrgprA3 C-afferents triggers pain and not itch. We further validated the distinct perception of itch or pain based on their specific sensitivity to known pharmacological anti-pruritic or analgesic interventions.

TRP channels have been identified as transducers downstream of metabotropic receptors for pruritogens (Dong and Dong, 2018; Feng et al., 2017; Moore et al., 2018; Xie and Hu, 2018). TRPA1 and TRPC3 have been shown to play a significant role in the activation of primary afferents by CQ (Than et al., 2013; Wilson et al., 2011), while action potential generation induced by CQ did not seem to be altered in a constitutive double knock-out of TRPV1 and TRPA1 in an ex vivo preparation (Ru et al., 2017). *In vivo*, however, constitutive TRPA1 knockout animals exhibit shorter total scratching time following CQ injection, while constitutive TRPV1 knockout animals show similar duration of scratching (Wilson et al., 2011). On the other hand, it has been shown that CQ sensitizes TRPV1 channels in MrgprA3 neurons (Than et al., 2013). Our data on the exclusive involvement of TRP channels in pruriception also confirms the capability of MrgprA3 C-afferents to respond distinctively to different stimuli in a cell-autonomous manner. The differential coding of algesic and pruritic stimuli mediated by these afferents may be carried by distinct firing patterns or secondary messengers, resulting in

distinct neurochemical or temporal outputs in their central terminals (Hong et al., 2012; Ratté et al., 2013; Wang et al., 2017; Zeldenrust et al., 2018). These biased responses engage separate pathways in the spinal cord, as shown here by the differential sensitivity of MrgprA3 neuron-mediated itch and pain responses to the GRPR antagonist RC-3095 and the μ-opioid receptor agonist DAMGO, respectively. Differential spinal integration of signals transmitted by a single peripheral neuronal population likely depends on spatiotemporal properties of its outputs, where short synchronous ionotropic signals can carry different messages than longer asynchronous metabotropic signals. Whereas slow sporadic asynchronous signals evoked by chemical activation of MrgprA3 C-afferents favors pruriception (Han et al., 2013), our results suggest that fast synchronous signals evoked by optogenetic or purinergic stimulation of these same C-fibers favors nociception. Another contributing factor to the spatiotemporal signature of central outputs is the afferents firing patterns. Indeed, spinal GRP interneurons can engage both pain and itch pathways (Sun et al., 2017) and they require burst-like activity in order to relay pruriceptive signals to higher-order neurons (Pagani et al., 2019). Our data indicate that primary afferents can also transmit distinct modality-specific signals to the spinal cord. For instance, single action potentials versus burst-like firing pattern generated by MrgprA3 afferents could differentially code for pain versus itch modalities.

Similar principles of multimodal coding based on stimulation conditions will likely be observed in other sensory circuits. Furthermore, beyond the field of sensory neurobiology and in view of the widespread use of heterologous actuators in modern neuroscience, this study provides evidence that fast ionotropic and slower metabotropic stimulation of the same genetically-defined populations of neurons can lead to different outcomes at cellular and behavioral levels.

Acknowledgments

We thank our McGill colleagues Jeffrey Mogil and Stuart Trenholm for their input, Xinzhong Dong (Johns Hopkins, HHMI) for the MrgprA3-Cre-EGFP mouse line, as well as Van N'Guyen for her technical support. B.S. received scholarships from the Fonds de Recherche du Québec-Santé and the Louise and Alan Edwards Foundation. This work was funded by the Canadian Institutes of Health Research (A.RdS., P.S.), the Natural Sciences and Engineering Research Council (P.S.), the Quebec Pain Research Network (A.RdS., P.S.) and the Louise and Alan Edwards Foundation (A.RdS., P.S.).

Author Contributions

B.S. and P.S. designed the experiments and all authors contributed to data analysis. B.S. performed the histology, calcium imaging, and behavioral experiments. A.R.A. and B.S. performed the electrophysiological experiments. B.S. and P.S. wrote the paper with contributions from all authors. P.S. supervised all aspects of the work.

Declaration of Interests

The authors declare no competing interests.

Figures & Legends

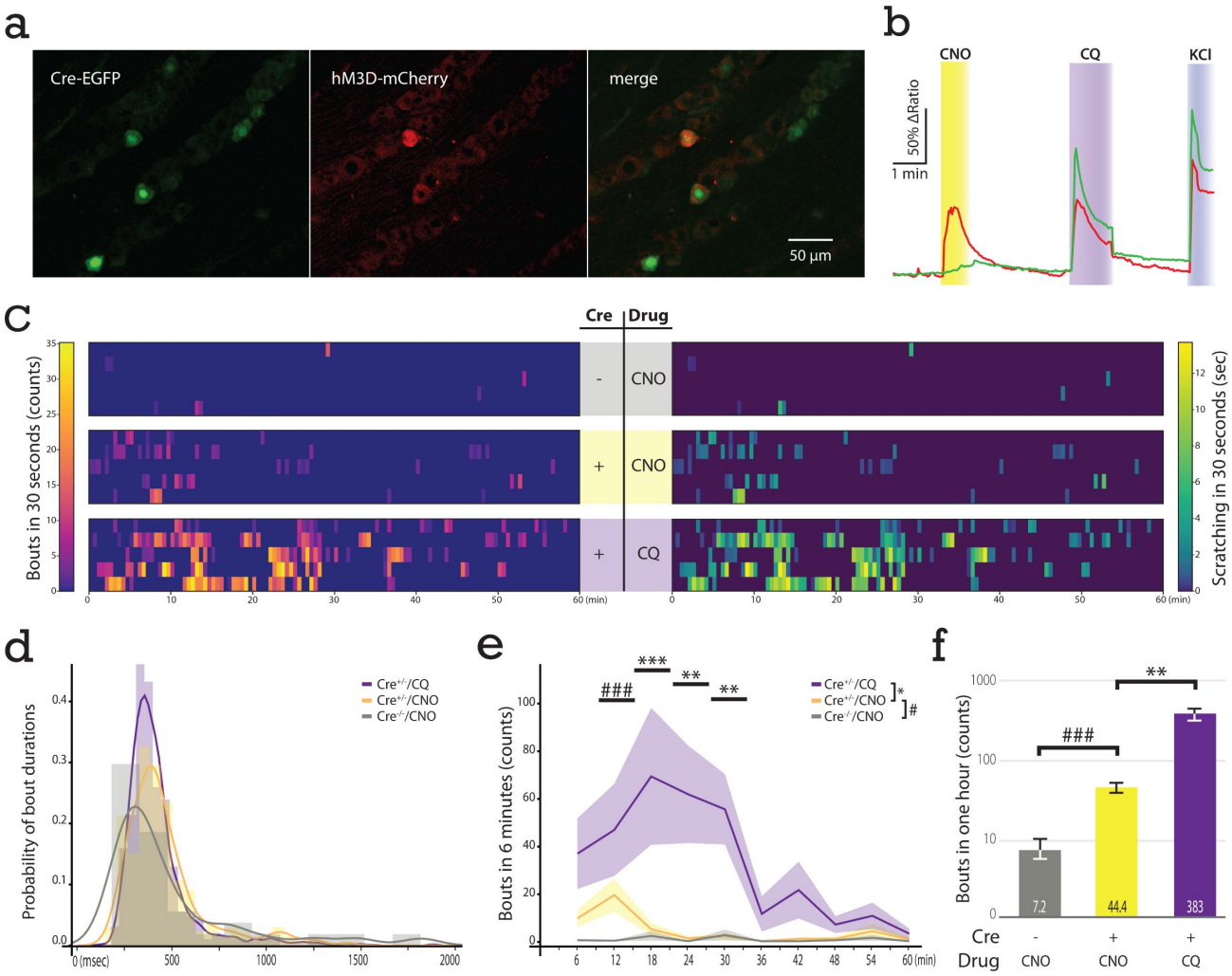

Figure 1- Selective stimulation of MrgprA3 C-afferents via activation of endogenous or heterologous metabotropic receptors induces scratching. *a) AAV transduction induces selective Cre-dependent expression of hM3Dq-mCherry in MrgprA3Cre-eGFP cells. Cre-eGFP signal, predominantly localized in the nucleus, and mCherry signal, amplified with a monoclonal antibody against mCherry. b) Calcium transients evoked by CNO (5 µM) or CQ (2 mM) validate the selective activation of MrgprA3 neurons in vitro. Representative traces from a Cre-eGFP+:mCherry- cell (green trace) and a Cre-eGFP+:mCherry+ cell (red trace). KCl (50 mM) was used as positive control. c) CNO (3 mM) induces*

hM3Dq-mediated scratching behavior similar but not as intense as CQ (10 mM). Time-course of scratching behavior induced by intradermal injection of CNO in Cre-/- animals (top), CNO in Cre+/- cage-/litter-mates (middle), and CQ in the same Cre+/- animals (bottom). Each row in every panel is an individual mouse (n= 5 for each condition). Compounds were injected at time = 0 and every colored block indicates the number of scratching bouts (left), or the time spent scratching (right) in the corresponding 30 second bin, as defined by the color maps. Rare sporadic baseline scratching behavior in Cre-/-/CNO group shows a different profile compared to that of Cre+/-/CNO and Cre+/-/CQ groups that display significant responses closer to injection time. d) Probability distributions of scratching bout durations show that, although total counts are different (36, 222, 1946 for the Cre-/-/CNO, Cre+/-/CNO, and Cre+/-/CQ groups, respectively), mean durations of individual bouts are similar (495.4, 471.9, 429.5 msec for the Cre-/-/CNO, Cre+/-/CNO, and Cre+/-/CQ groups respectively). e) Native MrgprA3 or Gq-coupled DREADD activation induces comparable build-up and wind-down of scratching behavior over time albeit with different intensities. Timeline of scratching bout counts indicates that unlike Cre-/-/CNO group, metabotropic activation in Cre+/-/CNO and Cre+/-/CQ groups induces scratching behavior closer to injection time. While CNO induces significantly more scratching bouts in Cre+/- than in Cre-/- animals, CQ effects in the same Cre+/- animals last longer and build up to a higher extent. Two-way ANOVA, and Bonferroni post-Hoc tests were used for comparison of Cre (#) or drug effects (*) over time. The one-hour period of observation (compound injection at time = 0) was divided into 10 equal 6-minute bins in order to perform the statistical tests. f) CNO induces itch only in presence of hM3Dq, and in lower intensities than CQ. Total numbers of scratching bouts over the one-hour period following CNO injection shows significant scratching behavior in Cre+/- vs Cre-/- animals (unpaired t-test, $p < 0.001$). The itch behavior induced by CQ is significantly more intense than the one induced by CNO (paired t-test, $p < 0.01$).

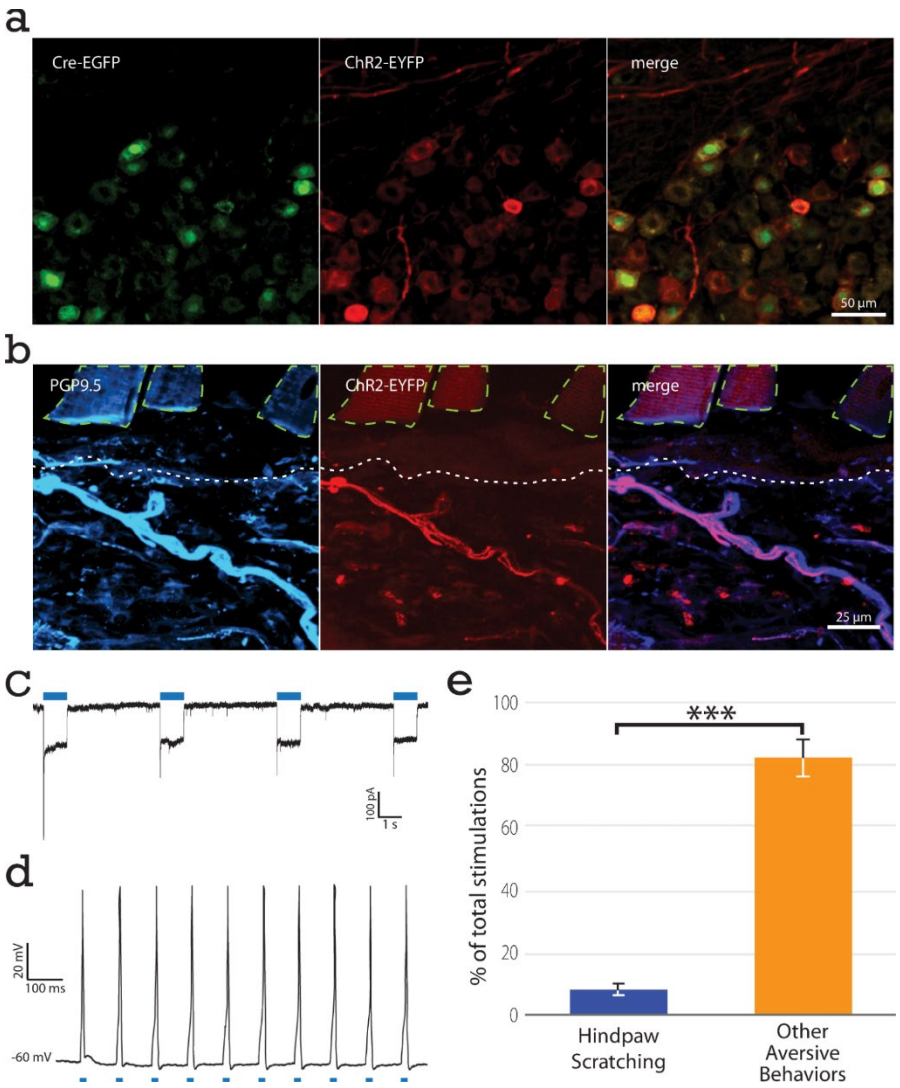

Figure 2- Optical ionotropic stimulation of ChR2-expressing MrgprA3 C-afferents mainly induces aversive behaviors other than scratching. *a) MrgprA3Cre-eGFP+/-:Rosa26ChR2-eYFP+ animals express channelrhodopsin-2 in MrgprA3+ primary afferents in cervical dorsal root ganglia. Representative image showing nuclear Cre-EGFP while eYFP signal in the same neurons shows the expression of ChR2 on the cell membrane and in processes (Supplementary figure 2a). b) ChR2 is trafficked to the peripheral terminals in the skin of the nape of the neck. ChR2-eYFP is detected in peripheral nerve endings (stained by PGP9.5) in the*

hairy skin. Hair shafts are indicated by dashed lines, the dermis-epidermis border is indicated by a dotted line. c) ChR2 photocurrents evoked by blue light in response to 4 one-second long stimulations in voltage clamp. d) Generation of a train of action potentials by 20 msec short pulses of blue light confirms the capability of these cells to follow frequencies up to 10 Hz reliably. e) In vivo photostimulation of the nape of the neck induces behavioral responses in most trials (89.93 ± 0.05% SEM of all stimulations, 6 animals, 15 stimulations each). A majority of these responses correspond to aversive behaviors such as escaping, aggressive approaches, or vocalization (other aversive behaviors) instead of stereotypical itch behaviors (rapid scratching bouts with the hindpaws) ($p < 0.001$).

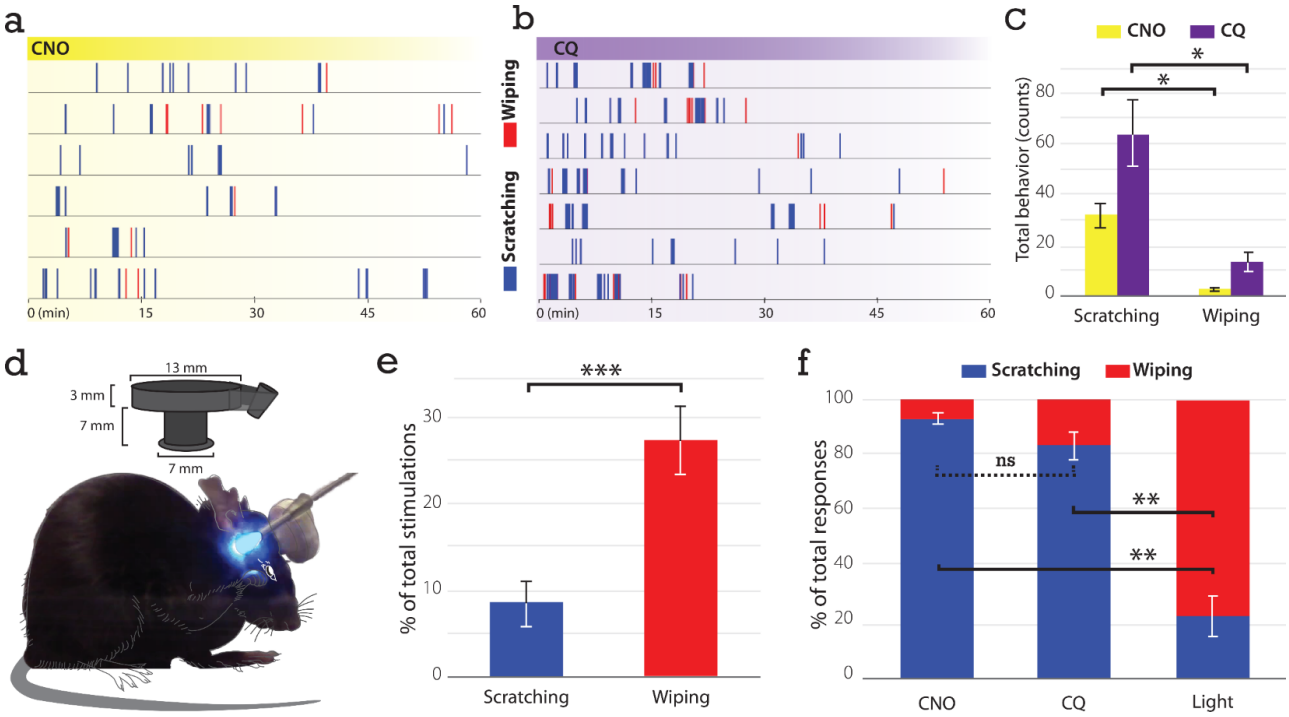

Figure 3- Distinct stimulation modes of cutaneous MrgprA3 C-afferents differentially evoke itch or pain with stereotypical behavioral responses. *Time-course of pruriceptive hindpaw scratching bouts (blue), and nocifensive forepaw wipes (red) following injection of a) CNO (3 mM), and b) CQ (10 mM) in the cheek. Each row represents an individual animal (n = 6-7) and each behavioral event is represented by colored bars at the corresponding time. c) Compilation of behavioral responses ($p < 0.05$). d) 3D-printed headposts (top) as fiber optic holders for consistent cheek illumination. Transdermal blue laser illumination on the cheek induces stereotypical nocifensive wiping behavior (bottom, Supplementary video 4). e) Probability of light-induced wiping and scratching (5 animals, 15 test sessions, 8 trials each, $p < 0.001$). f) Behavioral phenotype in metabotropic (i.e. CNO and CQ) vs. ionotropic (i.e. blue light) stimulation ($p < 0.01$ for both, One-way ANOVA with Bonferroni post-hoc test).*

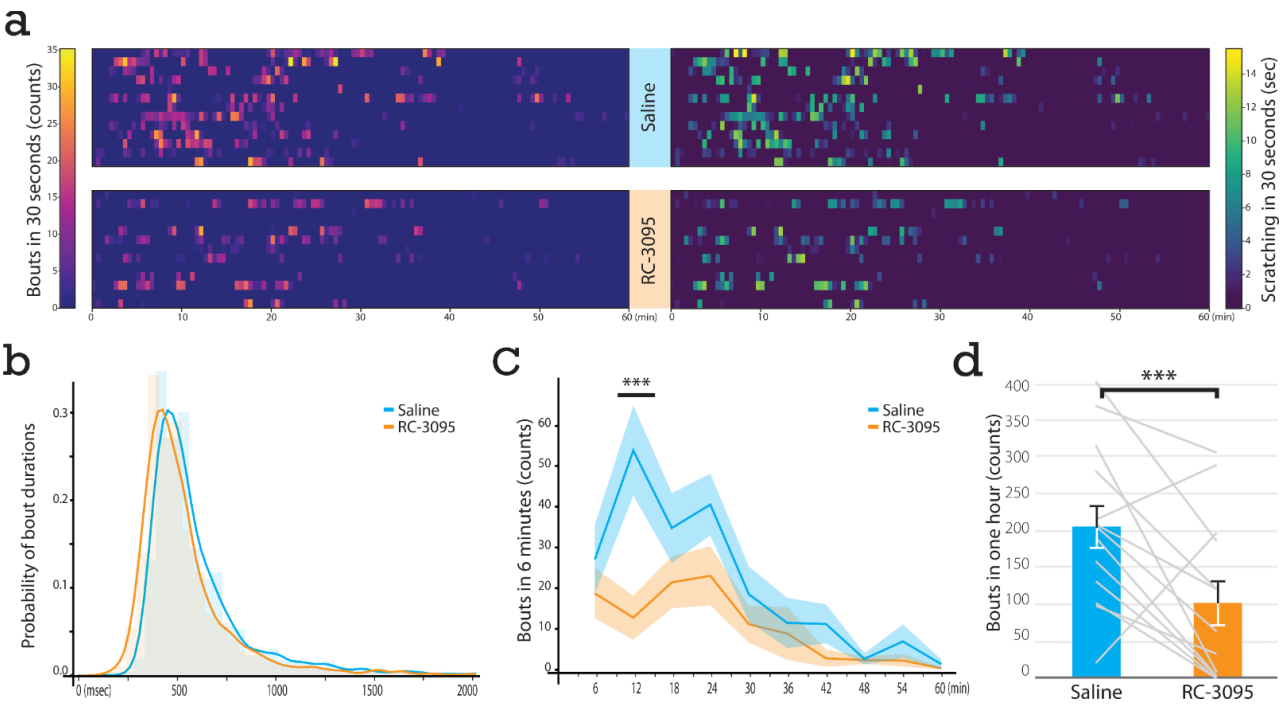

Figure 4- Pruriception mediated by MrgprA3 C-afferents is GRPR-dependent. *a) Chloroquine-induced itch is inhibited by the selective GRPR blocker RC-3095 (50 pmol i.c.). Time-course of scratching behavior induced by CQ (10 mM) in the nape of the neck (at time = 0) 15 minutes after i.c. injection of saline (top) or RC-3095 (bottom). Each row represents an individual C57Bl6 mouse (n = 13) and every block indicates the number of scratching bouts (left), or time spent scratching (right) in the corresponding 30 second bin, as defined by the color maps. b) Similar distribution of individual scratching bout durations (552.6, 536.7 msec in average for saline and RC-3095 groups, respectively), despite different total counts (2711 vs 1348 for saline and RC-3095 groups, respectively), indicates no significant changes in the scratching behavior phenotype. c) Timeline of scratching behavior indicates that GRPR blockade decreases scratching at early time points. Average counts in 6-minute time bins are displayed with shades indicating SEMs (Two-way ANOVA test with Bonferroni post-tests). d) Total number of*

scratching bouts following CQ injection indicates itch suppression by pharmacological blockade of GRPR ($p < 0.001$, paired t-test). Each line corresponds to an individual mouse in two different conditions.

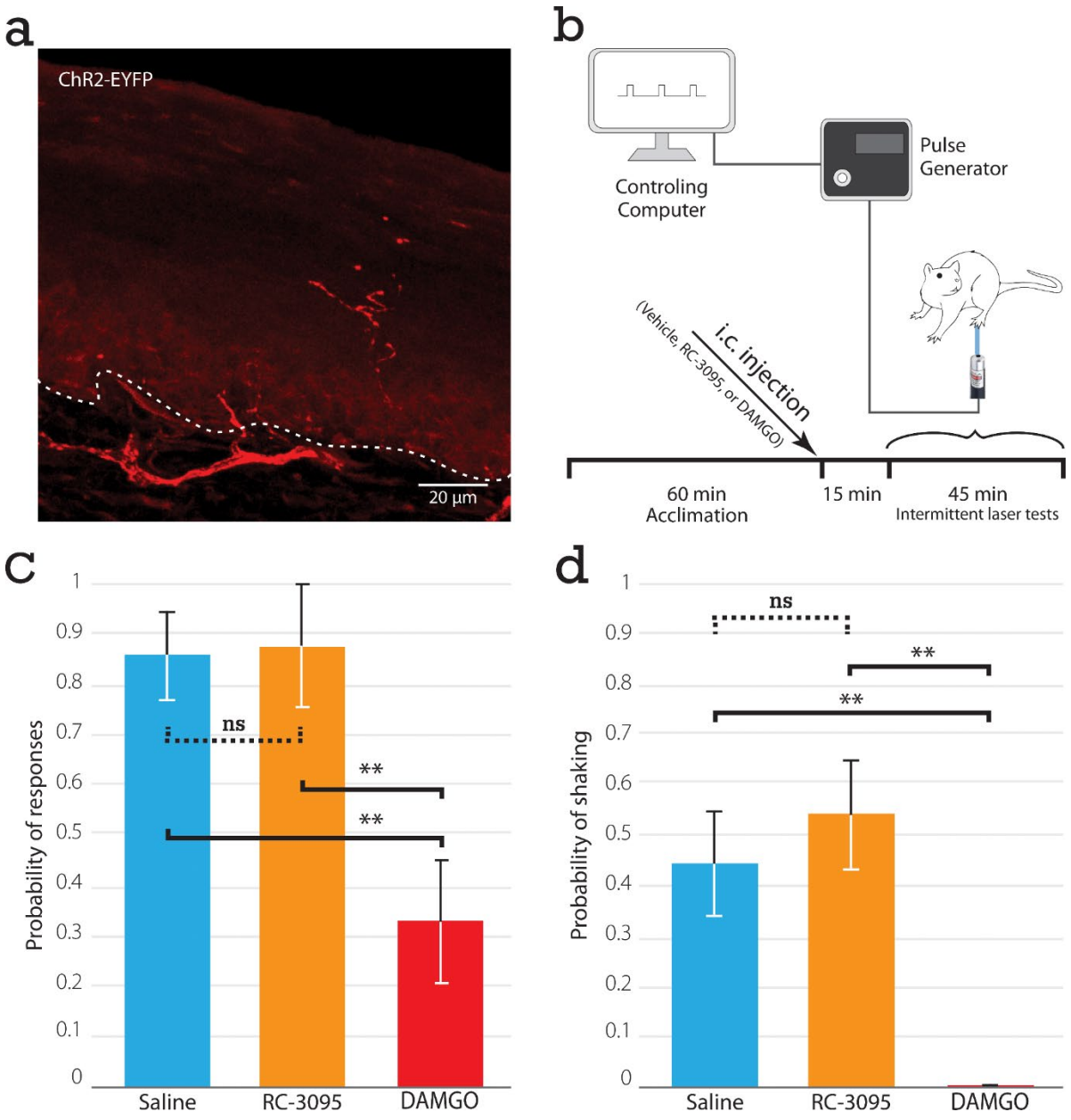

Figure 5- Nociception mediated by MrgprA3 C-afferents is sensitive to mu opioid receptor signaling, but not to GRPR blockade. *a) MrgprA3-expressing afferents innervate the glabrous skin of the paw. Representative image showing direct eYFP fluorescence in MrgprA3Cre-eGFP+/-:Rosa26ChR2-eYFP+ animals in the plantar surface of the hindpaw. The dermis-epidermis border is indicated by a dotted line. b) Experimental design for quantification*

of optically-induced pain responses. Acclimated animals received intra-cisternal injections of 50 pmol RC-3095 or 100 pmol DAMGO, 15 minutes before the start of optical stimulation trials (12 animals, 3 trials per treatment). c) Probability of all evoked behavioral responses upon transdermal photostimulation of the hindpaw is not affected by GRPR blockade yet is significantly reduced by treatment with the μ–opioid agonist DAMGO ($p < 0.01$, One-way ANOVA with Bonferroni post-Hoc test). d) Light-evoked shaking is suppressed by DAMGO while RC-3095 does not cause any significant changes in the probability of this high-intensity pain behavior ($p < 0.01$, One-way ANOVA with Bonferroni post-test).

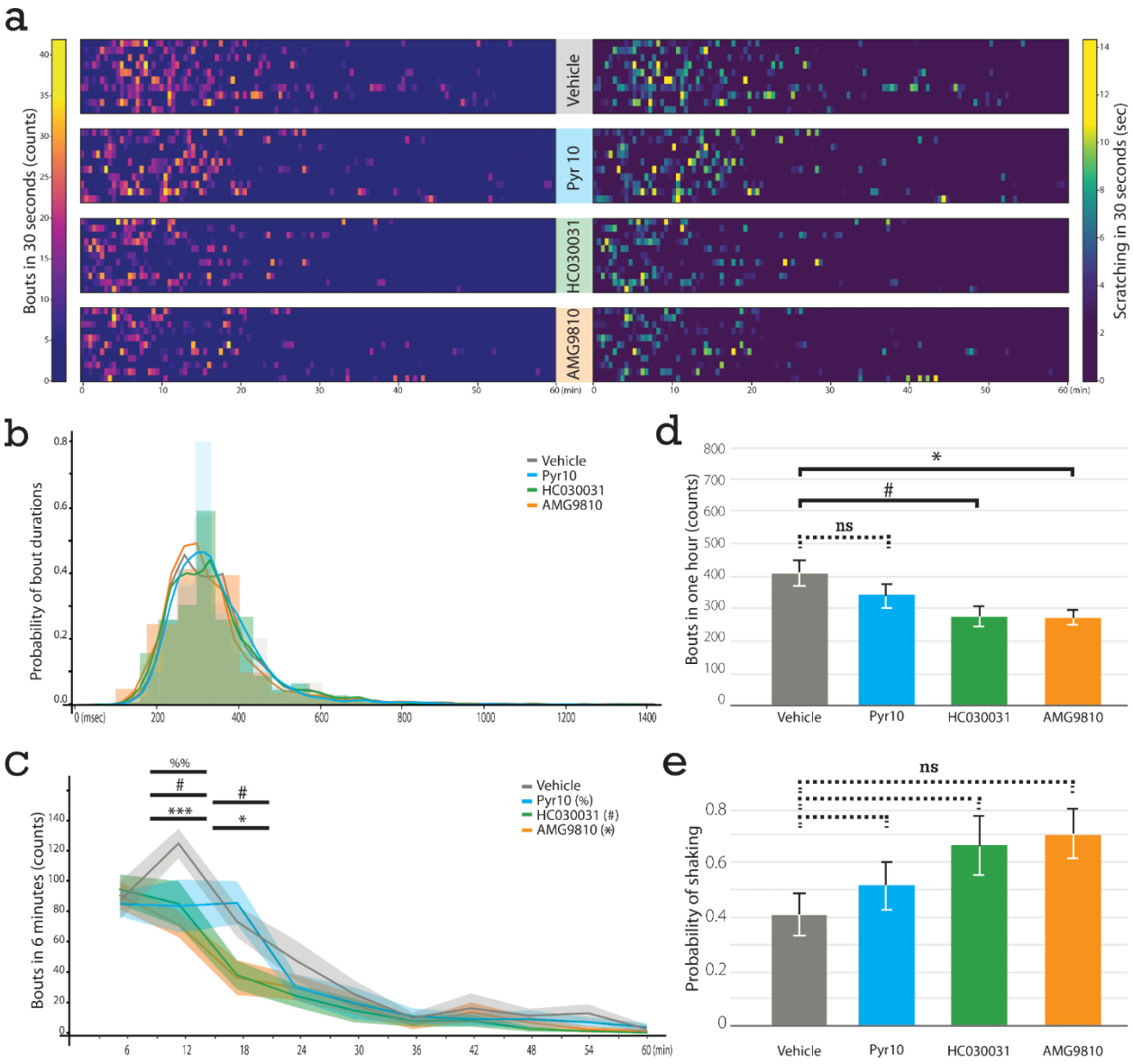

Figure 6- Pharmacological blockade of peripheral TRP channels reduces pruriception, but not nociception, mediated by MrgprA3 C-afferents. *a) Time-course of scratching behavior induced by injection of CQ (10 mM) in the nape of the neck (at time = 0) 10 minutes after s.c. injection of 1 mM solution of Pyrazole 10 (Pyr10), HC030031 or AMG9810 (selective blockers of TRPC3, TRPA1, and TRPV1, respectively) or vehicle. Each line represents an individual C57Bl6 mouse (n = 10-11) and every block indicates the number of scratching bouts (left), or time spent*

*scratching (right) in the corresponding 30 second bin, as defined by the color maps. b) Probability distribution of bout durations showing similar scratching phenotypes (mean bout durations of 356.0, 348.9, 347.2, and 339.4 msec for vehicle, Pyr10, HC030031, and AMG9810, respectively). c) Timeline of scratching counts after injection of CQ (at time = 0) in animals pretreated by selective TRP channel blockers (at time = -10 min) (Two-way ANOVA with Bonferroni post-hoc test, %, #, and * symbols depict significance levels for comparison of the vehicle vs. Pyr10, HC030031, or AMG9810 groups, respectively). d) Total number of scratching bouts in the one-hour period following CQ injection shows that pharmacological blockade of TRPA1 or TRPV1 channels inhibits the pruriception triggered by MrgprA3 C-afferents (One-way ANOVA with Bonferroni post-hoc test). e) The probability of shaking behavior induced by photostimulation of the hindpaw, as a readout for pain, indicates that pretreatment of MrgprA3Cre-eGFP+/-:Rosa26ChR2-eYFP+ animals with TRP channel blockers does not inhibit light-evoked nociception (n=9, One-way ANOVA with Bonferroni post-Hoc test).*

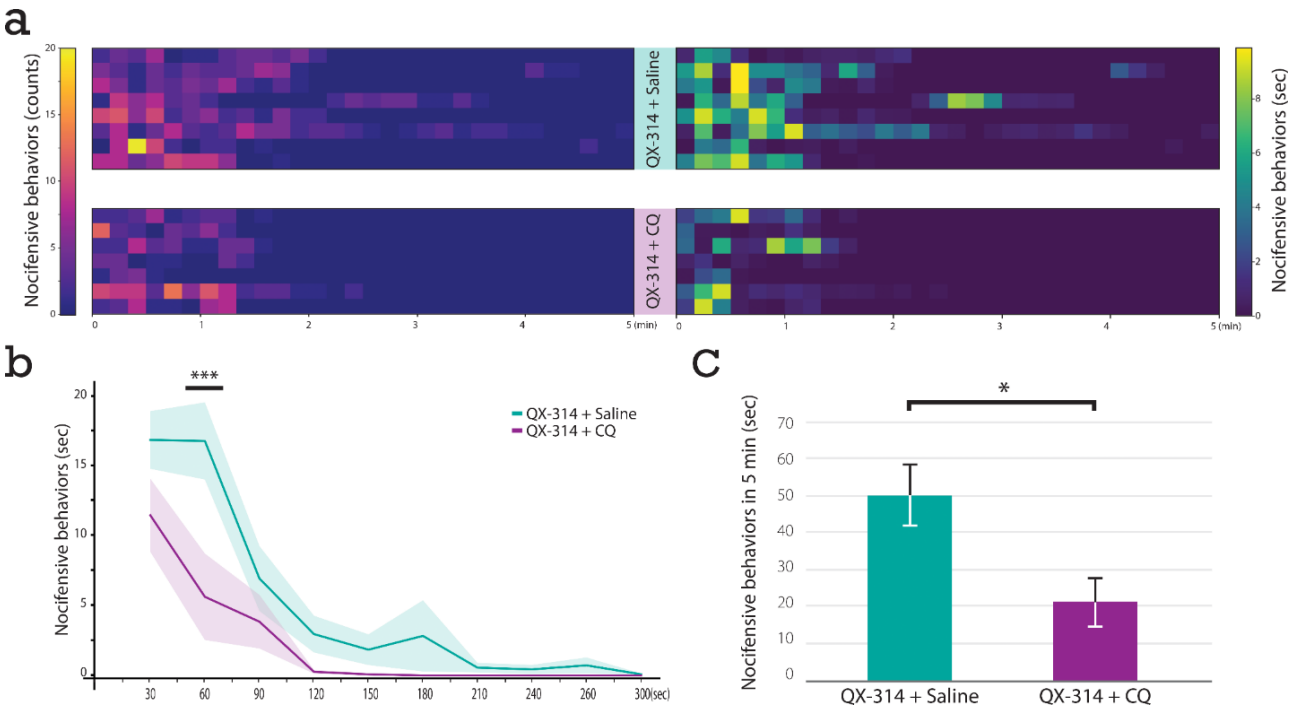

Figure 7- Selective silencing of MrgprA3 C-afferents significantly reduces acute purinergic pain. *a) Time-course of nocifensive behavior induced by intraplantar injection of αβmeATP (20 mM) in the hindpaw 30 minutes after conditioning with coinjection of QX-314 with saline or CQ (5 mM). Each line represents an individual wildtype C57Bl6 mouse (n= 7-8) and every block indicates the number of lifting or licking behaviors observed (left panel), or time spent behaving (right panel) in 10-second time bins, as defined by the heat maps. b) Timeline of nocifensive behaviors observed (lifting and licking), showing that QX-314-mediated silencing the CQ-responsive cells blunts the expression of nocifensive behaviors evoked by αβmeATP. Average durations in 30-second time bins are displayed with shades indicating SEMs. Two-way ANOVA test with Bonferroni post-tests was used for statistical comparison (p <0.001). c) Conditional silencing of CQ-responsive afferents reduces the total duration of purinergic nocifensive behaviors. Animals receiving QX-314 + CQ 30 minutes before αβmeATP spend significantly less*

time manifesting nocifensive behaviors (licking and lifting their paw) in the 5 minutes period post algogen injection ($p < 0.05$, unpaired t-test).

STAR Methods

LEAD CONTACT AND MATERIALS AVAILABILITY

Further information and requests for resources and reagents should be directed to and will be fulfilled by the Lead Contact, Philippe Séguéla (philippe.seguela@mcgill.ca).

This study did not generate new unique reagents.

EXPERIMENTAL MODEL AND SUBJECT DETAILS

Mouse strains

All animal procedures were approved by the McGill animal care committee and in compliance with the Canadian Council on Animal Care guidelines. Mice were kept in 12-hour light-dark cycle, 22 °C air-filtered cages (194 mm x 178 mm x 397mm) in groups up to 5 per cage with access to food and water *ad libitum*. All animals were kept at least for 10 days in their home cages before any procedures.

Wild-type C57Bl6 mice (Charles River Canada) were used for heterozygous breedings or behavioral tests at 3-4 weeks of age. The transgenic MrgprA3$^{Cre\text{-}eGFP}$ mouse line was kindly provided by Xinzhong Dong (Johns Hopkins University, HHMI). Hemizygotes were bred in house by crossing to wild-type C57Bl6. The Ai32 mouse line (JAX) was used as the optogenetic reporter line, homozygotes were bred in-house.

Viral constructs and transduction

Adeno associated virus serotype 9 (AAV9) was used for expression of hM3Dq-mCherry cDNA in Cre-expressing animals. AAV9-hSYN-DIO-hM3D(Gq)-mCherry (titer: 2-5E13 GC/mL) was produced by the Canadian Neurophotonics Platform, Quebec, Canada. Newly born pups (postnatal day 0-2) were anesthetized on ice and administered intra-peritoneally by 10 µL of the viral construct using a Hamilton syringe connected to a 30G syringe tip (Becton Dickinson) through a Polyethylene tube (PE-10/10, Warner Instruments). Pups were returned to their parent cages and weaned after 21-28 days.

METHOD DETAILS

Ligands and administration routes

Intra-dermal (i.d.) injections (20 µL, unless otherwise specified) were made either in the cheek or in the nape of the neck using low volume insulin syringes (Becton Dickinson). Intra-cisternal (i.c.) injections were made in 5 µL volumes using a bent 30G syringe tips (Becton Dickinson) attached to a 10 µL Hamilton syringe (Ueda et al., 1979). Intra-plantar and subcutaneous (s.c.) injections were made in 10 µL volumes and 50 µL respectively, using insulin syringes (Becton Dickinson).

Chloroquine diphosphate (Sigma) was prepared in 100 mM stock solution in deionized distilled water and was kept in aliquots at -20 °C before dilution in saline (*in vivo* tests) or extracellular recording solution (*in vitro* tests). CNO (Tocris) was prepared in 5 mg/mL stock solution in

deionized distilled water and was kept in aliquots at -80 °C before dilution in saline (*in vivo* tests) or extracellular recording solution (*in vitro* tests). RC3095 (Adooq Bioscience) was prepared in 10 mM stock solution in deionized distilled water and was kept in aliquots at -80 °C before dilution in saline for i.c. injections. DAMGO (Tocris) was prepared in 1 mM stock solution in deionized distilled water and was kept in aliquots at -80 °C before dilution in saline. TRP channel blockers pyrazole 10 (Sigma), HC-030031 (Tocris), and AMG9810 (Tocris), were prepared in 5 mM stock solutions and stored at -20 °C in aliquots before dilution to the final concentration of 1 mM in 10% ethanol and 10% DMSO at the time of experiments. α,β-methylene adenosine 5'-triphosphate trisodium salt (αβmeATP, Tocris) was prepared in 20 mM stock solution in saline and was kept in aliquots at -20 °C before use. QX-314 chloride (abcam) was prepared in 100 mM stock solution in deionized distilled water and aliquots were kept at -20 °C before use.

Headpost implants

Polylactic acid (PLA) was used for 3D printing of headposts (1h x 7d in mm at the base, 7h x 6d in mm at the shaft, and 3h x 13d in mm at the top). Adult mice were anesthetized by isoflurane and stabilized on a warming pad after shaving the hair on the top of their hair and application of lubricant eye ointment (Alcon). After application of disinfecting agent (chlorhexidine 2%) a 1.5-2 cm incision was made in the midline over the skull. After cleansing the surface of the skull, the headpost was placed on the skull in between the ears and was secured using dental cement (LangDental). For reinforcing the headpost placement for longitudinal studies, a bone anchor screw (Stoelting) was put in the bone surface beside the headpost shaft before applying the dental cement. After the cement cured, the skin was

sutured around the base of the headpost and local anesthetic cream was applied (emla: Lidocaine 2.5% & Prilocaine 2.5%) before the animals were left to wake up. All animals received pre (right before surgery) and post (for 4 days) surgical analgesics (20 mg/kg/day Carprofen s.c. for 3 days) and were monitored for wound healing and proper hydration. Once the animals recovered from this procedure they would undergo a light anesthesia during which a cut pipet tip was glued to the top of the headpost to make an optic fiber holder keeping the light localized to the cheek. Animals were given at least two weeks of recovery before behavioral tests.

Laser sources and light guides

A 473 nm diode-pumped solid-state (DPSS) laser (max 120 mW, LaserGlow) was used for selective activation of ChR2 while a 589 nm DPSS laser (max 100 mW, Changchun Dragon Lasers) was used as a yellow light source for control experiments. Light was guided through a 1 mm-diameter optical fiber (NA= 0.5) for skin (transdermal) stimulations and through a 0.2 mm-diameter optical fiber (NA= 0.37) for *in vitro* tests. For transdermal stimulations, unless otherwise stated, the lasers were set to 3.5-4.5 mW (constant power output) at the tip of the optical fiber and the tip was placed 2-5 mm away from the skin. A TTL pulse train generator (Prizmatix) was used for driving the lasers with 20 msec short pulses. For screening purposes, 3-second trains of 0.5-10 Hz pulses (20-500 msec on-time) with 0.01-90 mW powers were used in random orders to avoid desensitization due to prior exposures.

Behavioral assays

For all behavioral studies, adult male mice were familiarized with the experimenter, handling and injection types, and the environment of the experiment for at least one week, daily. Tests were done during the light cycle between 10am and 4pm. When needed, animals were shaved using a small electric shaver 2 days prior to the recording. All chemical interventions were followed by multi-angle video recordings for off-line behavioral analysis. Video scorings were performed by trained experimenters blind to treatments. To further decrease possible bias within each experiment, long recordings were randomly cut into 8-15 minute clips, shuffled and mixed and put together after evaluations. Videos were scored manually using an in-house time stamping software which allowed precise recording of several behavioral responses and their duration within each clip.

For the cheek model of itch/pain discrimination, each scratching bout was defined as rapid brushing of the face by the hindpaw on the ipsilateral side. Each episode starts from the time scratching begins and ends with the hindpaw back on the ground or in the mouth. Pain behavior was defined as unilateral wiping of the ipsilateral side of the face by the forepaw. This behavior was distinct from grooming, defined as bilateral wiping of the face or any other actions on nonspecific sites of the body, e.g. rapid licking and biting of the chest, limbs and side areas. Contralateral scratching and wipings were not included in the behavioral analysis. For the nape of the neck model of itch quantification, scratching bouts were defined as rapid scuffing of the back area with either hindpaw.

For laser-evoked behaviors on the nape of the neck, scratching was defined similarly to the scratching behavior observed after chemical interventions: rapid treatment of the illuminated area by the hind paw. All other behavioral responses elicited by blue light were categorized as aversive: rapid avoidance, aggressive biting approaches towards the fiber optic, running and vocalization. It is noteworthy that wiping was not observed in these experiments as the nape is physically inaccessible by the forepaws of the animal. All animals received the different frequency-intensity protocols. No consistent relationship between illumination protocols and the evoked behavioral responses was observed.

For cheek illumination experiments, animals were acclimated to the observation chamber and the fiber optic attachment for at least one week. For each session of cheek illumination experiment, animals were brought to the testing chamber to acclimate for at least 30 min. In each session 8-10 trials of laser illumination protocols (i.e. different frequency, pulse duration, and intensity) were randomly applied for 3-5 seconds. At least 3 minutes of separation was allowed between trials and sessions were separated by at least 2 days for each animal. Although responses were more likely to be observed at the beginning of each session, no significant relationship was deduced between the illumination protocols and the probability of behavior induction.

For hindpaw illumination studies, animals were acclimated to the behavior observation chambers (10w x 5d x 8h cm) placed on a wire mesh for at least one hour in presence of the experimenter and the laser devices. Laser illumination pulses of 3 seconds were delivered to the plantar site of the hindpaws allowing at least 3 minutes in between stimulations on one paw.

For purinergic pain studies, animals were acclimated on the recording platform for at least 30 minutes. QX-314 conditioning injection in the plantar surface of the right hindpaw were made in 10 µL volumes and the animals were returned to their recording chambers. 30 minutes after the conditioning injection 10 µL of 20 mM αβmeATP was injected intraplantary in the same paw and the animals were recorded for 5 minutes. Close observation of the animals from 3 different angles was performed in slow-motion by blind experimenters to detect exact start and end points of lifting or licking of the right hindpaw.

In vitro preparations and assays

Trigeminal ganglia (TG) or dorsal root ganglia (DRG) were dissected from adult mice for primary culture and *in vitro* assays. In short, the animals were decapitated under isoflurane anesthesia, the sensory ganglia were removed and stored in ice-cold HBSS solution (Invitrogen). After treating with dispase (1.4 mg/mL, Sigma) and collagenase type II (1.1 mg/mL, Sigma) for 45 min on a shaker (37 °c), ganglia were washed twice with 10 mL of F-12 media (Invitrogen) containing 10% FBS, 1% L-glutamine, 1% penicillin and 1% streptomycin. The ganglia were then triturated using fire polished glass pipets with incrementally decreasing tip sizes. Dishes (35 mm) with 14 mm glass centers (MatTek) were coated with laminin (BD Biosciences) and poly-d-lysine (Sigma) for at least 2 h at 4 °C. Cells were then plated for at least 30 min in the incubator (37 °C, 5% CO_2) before addition of 2 mL culture medium. Cultured cells were used for Ca imaging or electrophysiology 24-48 hours post-plating.

For calcium imaging, cultured primary DRG and TG sensory neurons were loaded for 45 minutes in 2 mM Fura2-acetoxymethyl ester. Cells were then washed and kept for an additional 45

minutes in extracellular medium with no Fura-2 (37 °C, 5% CO_2) for desesterification. Loaded cells were imaged every 2 seconds with 340 nm and 380 nm excitation filters using a Nikon (Eclipse TE300) widefield microscope and Metafluor software (Molecular Devices). Background corrected normalized ratios of emission under 340 nm excitation divided by emission under 380 nm excitation are reported as proxies of relative intracellular calcium levels. Cultures were under constant perfusion of external solution (pH 7.4) consisting of 152 mM NaCl, 5 mM KCl, 2 mM $CaCl_2$, 1 mM $MgCl_2$, 10 mM HEPES, and 10 mM glucose with or withouth test drugs. Response criteria was defined as drug-induced Δratios 5 times larger than baseline fluctuations. All responsive cell traces were manualy verified after experiments.

For electrophysiology studies on neuronal excitability and controllability by blue light, cultured primary sensory neurons were patched onto with glass pipets (5-9MΩ) in whole cell configuration and perfused with artificial cerebrospinal fluid (pH 7.4) containing 152 mM NaCl, 5 mM KCl, 2 mM $CaCl_2$, 1 mM $MgCl_2$, 10 mM HEPES, and 10 mM glucose. Recording patch pipets were filled with internal solution (pH 7.2) containing 130 mM K-gluconate, 1 mM $MgCl_2$, 10 mM HEPES, 5 mM EGTA, 3 mM MgATP, and 0.4 mM GTP. Responses to blue light delivered by optic fiber were measured in voltage and current clamp modes in pClamp 9 on an amplifier Axopatch 200B connected to a digitizer Digidata 1320A (Molecular Devices).

Ex vivo tissue preparations and morphology

For expression and histological validations, animals were perfused by intracardiac perfusion of 10 mL phosphate buffer saline followed by 30 mL 4% formaldehyde solution (pH 7.4) after deep isoflurane anesthesia. DRGs, TGs, spinal cords and skin samples were collected and post-fixed

for 2-4 hours in formaldehyde solution before they were transferred to a 30% sucrose solution for minimum 48 hours. Sections were cut embedded and frozen in optimal cutting temperature (OCT) solution on a Leica cryostat (DRG and TG: 14 µm; skin and spinal cord: 30 µm). Skin and ganglia sections were mounted directly on microscope slides while spinal cord sections were transferred to 24 well dishes for staining procedures.

For immunohistochemistry, free-floating or mounted sections were washed three times for 10 minutes each with phosphate buffer solution containing 0.2% Triton X-100 (PBST) before blocking with 10% normal serum (goat or donkey). Sections were left in 5% normal serum containing primary antibodies (dilution 1:2000) on a shaker in a cold room (4°C) overnight. Rabbit anti-PGP9.5 (Ultraclone RA95101) as a marker for overall skin innervation and monoclonal rat anti-mCherry (Life Technologies M11217) were used as primary antibodies. After 3 washes with PBST, secondary antibodies (1:500) was added to the sections for 2 hours at room temperature. Donkey anti-rat conjugated to Cy-5 (Jackson Immunoresearch) and goat anti-rabbit conjugated to Alexa 568 (Life Technologies) were used as secondary antibodies. Finally, the sections were mounted and imaged with Zeiss LSM710 or Leica SP8 confocal microscopes.

QUANTIFICATION AND STATISTICAL ANALYSIS

All statistical tests were performed by MATLAB software. Individual tests, their respective tests and n are indicated in the results section and the figure legends. Errors are presented as the standard error of mean (SEM) and significance levels are mentioned in each comparison.

DATA AND CODE AVAILABILITY

Original data are available upon request.

KEY RESOURCES TABLE

REAGENT or RESOURCE	SOURCE	IDENTIFIER
Antibodies		
PGP9.5	Ultraclone	Cat# RA95101
mCherry	Life Technologies	Cat# M11217
Bacterial and Virus Strains		
AAV9-hSYN-DIO-hM3D(Gq)-mCherry (DREADD)	Addgene and Canadian Neurophotonic Platform	Cat# 44361
Chemicals, Peptides, and Recombinant Proteins		
Chloroquine diphosphate	Sigma	Cat# C6628
Clozapine N-Oxide	Tocris	Cat# 4936
RC-3095	Adooq	Cat# A12753
DAMGO	Tocris	Cat# 1171
HC-030031	Tocris	Cat# 2896
AMG9810	Tocris	Cat# 2316
Pyrazole 10	Sigma	Cat# SML1243
αβmeATP	Tocris	Cat# 3209
QX-314	abcam	Cat# Ab144493
Experimental Models: Organisms/Strains		
Wildtype C57Bl6 Mice	Charles River Canada	C57Bl6
ChR2-EYFP Mice	Jackson Laboratory	Ai32
MrgprA3-CreEGFP Mice	Dong Laboratory (JHU)	

- **Supplemental video 1-** *Optical stimulation of the nape of the neck of MrgprA3Cre-eGFP+/-:Rosa26ChR2-eYFP mice evokes predominantly aversive behaviors distinct from scratching (related to Figure 2).*

- **Supplemental video 2-** *Optical stimulation of the nape of the neck of MrgprA3Cre-eGFP-/-:Rosa26ChR2-eYFP cagemate littermates evokes no behavior (related to Figure 2).*

- **Supplemental video 3-** *Frame-by-frame quantification of different behaviors in the cheek assay in mice (related to Figure 3).*

- **Supplemental video 4-** *Optical stimulation of the cheek with blue light evokes stereotypical wiping behavior in MrgprA3Cre-eGFP+/-:Rosa26ChR2-eYFP mice (related to Figure 3).*

- **Supplemental video 5-** *Control optical stimulation of the cheek with yellow light does not induce any behavior in MrgprA3Cre-eGFP+/-:Rosa26ChR2-eYFP mice (related to Figure 3).*

- **Supplemental video 6-** *Optical stimulation of the cheek with blue light evokes no behavior in MrgprA3Cre-eGFP-/-:Rosa26ChR2-eYFP cagemate littermates (related to Figure 3).*

- **Supplemental video 7-** *Optical stimulation of the hindpaw with blue light evokes nocifensive responses in MrgprA3Cre-eGFP+/-:Rosa26ChR2-eYFP mice (related to Figure 5).*

- **Supplemental video 8-** *Optical stimulation of the hindpaw with blue light evokes no behavior in MrgprA3Cre-eGFP-/-:Rosa26ChR2-eYFP cagemate littermates (related to Figure 5).*

References

Albisetti, G.W., Pagani, M., Platonova, E., Hösli, L., Johannssen, H.C., Fritschy, J.-M., Wildner, H., and Zeilhofer, H.U. (2019). Dorsal Horn Gastrin-Releasing Peptide Expressing Neurons Transmit Spinal Itch But Not Pain Signals. J. Neurosci. 39, 2238–2250.

Bautista, D.M., Wilson, S.R., and Hoon, M.A. (2014). Why we scratch an itch: the molecules, cells and circuits of itch. Nat. Neurosci. 17, 175–182.

Bland-Ward, P.A., and Humphrey, P.P. (1997). Acute nociception mediated by hindpaw P2X receptor activation in the rat. Br. J. Pharmacol. 122, 365–371.

Brull, S.J., Atanassoff, P.G., Silverman, D.G., Zhang, J., and Lamotte, R.H. (1999). Attenuation of experimental pruritus and mechanically evoked dysesthesiae in an area of cutaneous allodynia. Somatosens Mot Res 16, 299–303.

Daou, I., Tuttle, A.H., Longo, G., Wieskopf, J.S., Bonin, R.P., Ase, A.R., Wood, J.N., De Koninck, Y., Ribeiro-da-Silva, A., Mogil, J.S., et al. (2013). Remote optogenetic activation and sensitization of pain pathways in freely moving mice. J. Neurosci. 33, 18631–18640.

Davidson, S., and Giesler, G.J. (2010). The multiple pathways for itch and their interactions with pain. Trends Neurosci. 33, 550–558.

Dong, X., and Dong, X. (2018). Peripheral and central mechanisms of itch. Neuron 98, 482–494.

Dong, X., Han, S., Zylka, M.J., Simon, M.I., and Anderson, D.J. (2001). A diverse family of GPCRs expressed in specific subsets of nociceptive sensory neurons. Cell 106, 619–632.

Feng, J., Yang, P., Mack, M.R., Dryn, D., Luo, J., Gong, X., Liu, S., Oetjen, L.K., Zholos, A.V., Mei, Z., et al. (2017). Sensory TRP channels contribute differentially to skin inflammation and persistent itch. Nat. Commun. 8, 980.

Forster, C., and Handwerker, H.O. (2014). Central nervous processing of itch and pain. In Itch: mechanisms and treatment, E. Carstens, and T. Akiyama, eds. (Boca Raton (FL): CRC Press/Taylor & Francis), Chapter 24.

Green, D., and Dong, X. (2016). The cell biology of acute itch. J. Cell Biol. 213, 155–161.

Green, A.D., Young, K.K., Lehto, S.G., Smith, S.B., and Mogil, J.S. (2006). Influence of genotype, dose and sex on pruritogen-induced scratching behavior in the mouse. Pain 124, 50–58.

Han, S.-K., and Simon, M.I. (2011). Intracellular signaling and the origins of the sensations of itch and pain. Sci. Signal. 4, pe38.

Han, L., Ma, C., Liu, Q., Weng, H.-J., Cui, Y., Tang, Z., Kim, Y., Nie, H., Qu, L., Patel, K.N., et al. (2013). A subpopulation of nociceptors specifically linked to itch. Nat. Neurosci. 16, 174–182.

Hill, R.Z., Morita, T., Brem, R.B., and Bautista, D.M. (2018). S1PR3 Mediates Itch and Pain via Distinct TRP Channel-Dependent Pathways. J. Neurosci. 38, 7833–7843.

Hong, S., Ratté, S., Prescott, S.A., and De Schutter, E. (2012). Single neuron firing properties impact correlation-based population coding. J. Neurosci. 32, 1413–1428.

Kakimoto, S., Nagakura, Y., Tamura, S., Watabiki, T., Shibasaki, K., Tanaka, S., Mori, M., Sasamata, M., and Okada, M. (2008). Minodronic acid, a third-generation bisphosphonate, antagonizes purinergic P2X(2/3) receptor function and exerts an analgesic effect in pain models. Eur. J. Pharmacol. 589, 98–101.

Kato, A., Ohkubo, T., and Kitamura, K. (2002). Algogen-specific pain processing in mouse spinal cord: differential involvement of voltage-dependent Ca(2+) channels in synaptic transmission. Br. J. Pharmacol. 135, 1336–1342.

Klein, A., Carstens, M.I., and Carstens, E. (2011). Facial injections of pruritogens or algogens elicit distinct behavior responses in rats and excite overlapping populations of primary sensory and trigeminal subnucleus caudalis neurons. J. Neurophysiol. 106, 1078–1088.

LaMotte, R.H., Shimada, S.G., and Sikand, P. (2011). Mouse models of acute, chemical itch and pain in humans. Exp. Dermatol. 20, 778–782.

LaMotte, R.H., Dong, X., and Ringkamp, M. (2014). Sensory neurons and circuits mediating itch. Nat. Rev. Neurosci. 15, 19–31.

Lembo, P.M.C., Grazzini, E., Groblewski, T., O'Donnell, D., Roy, M.-O., Zhang, J., Hoffert, C., Cao, J., Schmidt, R., Pelletier, M., et al. (2002). Proenkephalin A gene products activate a new family of sensory neuron--specific GPCRs. Nat. Neurosci. 5, 201–209.

Liu, Q., Tang, Z., Surdenikova, L., Kim, S., Patel, K.N., Kim, A., Ru, F., Guan, Y., Weng, H.-J., Geng, Y., et al. (2009). Sensory neuron-specific GPCR Mrgprs are itch receptors mediating chloroquine-induced pruritus. Cell 139, 1353–1365.

Liu, Q., Sikand, P., Ma, C., Tang, Z., Han, L., Li, Z., Sun, S., LaMotte, R.H., and Dong, X. (2012). Mechanisms of itch evoked by b-alanine. J. Neurosci. 32, 14532–14537.

Luo, J., Feng, J., Liu, S., Walters, E.T., and Hu, H. (2015). Molecular and cellular mechanisms that initiate pain and itch. Cell Mol. Life Sci. 72, 3201–3223.

Mack, M.R., and Kim, B.S. (2018). The Itch-Scratch Cycle: A Neuroimmune Perspective. Trends Immunol. 39, 980–991.

McMahon, S.B., and Koltzenburg, M. (1992). Itching for an explanation. Trends Neurosci. 15, 497–501.

Moore, C., Gupta, R., Jordt, S.-E., Chen, Y., and Liedtke, W.B. (2018). Regulation of pain and itch by TRP channels. Neurosci. Bull. 34, 120–142.

Nilsson, H.J., Levinsson, A., and Schouenborg, J. (1997). Cutaneous field stimulation (CFS): a new powerful method to combat itch. Pain 71, 49–55.

Pagani, M., Albisetti, G.W., Sivakumar, N., Wildner, H., Santello, M., Johannssen, H.C., and Zeilhofer, H.U. (2019). How Gastrin-Releasing Peptide Opens the Spinal Gate for Itch. Neuron 103, 102–117.e5.

Le Pichon, C.E., and Chesler, A.T. (2014). The functional and anatomical dissection of somatosensory subpopulations using mouse genetics. Front. Neuroanat. 8, 21.

Ratté, S., Hong, S., De Schutter, E., and Prescott, S.A. (2013). Impact of neuronal properties on network coding: roles of spike initiation dynamics and robust synchrony transfer. Neuron 78, 758–772.

Roberson, D.P., Gudes, S., Sprague, J.M., Patoski, H.A.W., Robson, V.K., Blasl, F., Duan, B., Oh, S.B., Bean, B.P., Ma, Q., et al. (2013). Activity-dependent silencing reveals functionally distinct itch-generating sensory neurons. Nat. Neurosci. 16, 910–918.

Ru, F., Sun, H., Jurcakova, D., Herbstsomer, R.A., Meixong, J., Dong, X., and Undem, B.J. (2017). Mechanisms of pruritogen-induced activation of itch nerves in isolated mouse skin. J. Physiol. (Lond.) 595, 3651–3666.

Scherrer, G., Imamachi, N., Cao, Y.-Q., Contet, C., Mennicken, F., O'Donnell, D., Kieffer, B.L., and Basbaum, A.I. (2009). Dissociation of the opioid receptor mechanisms that control mechanical and heat pain. Cell 137, 1148–1159.

Schmelz, M. (2015). Itch and pain differences and commonalities. Handb Exp Pharmacol 227, 285–301.

Shimada, S.G., and LaMotte, R.H. (2008). Behavioral differentiation between itch and pain in mouse. Pain 139, 681–687.

Simone, D.A., Zhang, X., Li, J., Zhang, J.-M., Honda, C.N., LaMotte, R.H., and Giesler, G.J. (2004). Comparison of responses of primate spinothalamic tract neurons to pruritic and algogenic stimuli. J. Neurophysiol. 91, 213–222.

Song, J., Xian, D., Yang, L., Xiong, X., Lai, R., and Zhong, J. (2018). Pruritus: Progress toward Pathogenesis and Treatment. Biomed Res. Int. 2018, 9625936.

St Sauver, J.L., Warner, D.O., Yawn, B.P., Jacobson, D.J., McGree, M.E., Pankratz, J.J., Melton, L.J., Roger, V.L., Ebbert, J.O., and Rocca, W.A. (2013). Why patients visit their doctors: assessing the most prevalent conditions in a defined American population. Mayo Clin. Proc. 88, 56–67.

Stantcheva, K.K., Iovino, L., Dhandapani, R., Martinez, C., Castaldi, L., Nocchi, L., Perlas, E., Portulano, C., Pesaresi, M., Shirlekar, K.S., et al. (2016). A subpopulation of itch-sensing neurons marked by Ret and somatostatin expression. EMBO Rep. 17, 585–600.

Sun, Y.-G., and Chen, Z.-F. (2007). A gastrin-releasing peptide receptor mediates the itch sensation in the spinal cord. Nature 448, 700–703.

Sun, S., Xu, Q., Guo, C., Guan, Y., Liu, Q., and Dong, X. (2017). Leaky Gate Model: Intensity-Dependent Coding of Pain and Itch in the Spinal Cord. Neuron 93, 840–853.e5.

Sun, Y.-G., Zhao, Z.-Q., Meng, X.-L., Yin, J., Liu, X.-Y., and Chen, Z.-F. (2009). Cellular basis of itch sensation. Science 325, 1531–1534.

Tang, M., Wu, G., Wang, Z., Yang, N., Shi, H., He, Q., Zhu, C., Yang, Y., Yu, G., Wang, C., et al. (2016). Voltage-gated potassium channels involved in regulation of physiological function in MrgprA3-specific itch neurons. Brain Res. 1636, 161–171.

Than, J.Y.-X.L., Li, L., Hasan, R., and Zhang, X. (2013). Excitation and modulation of TRPA1, TRPV1, and TRPM8 channel-expressing sensory neurons by the pruritogen chloroquine. J. Biol. Chem. 288, 12818–12827.

Tsuda, M., Shigemoto-Mogami, Y., Ueno, S., Koizumi, S., Ueda, H., Iwanaga, T., and Inoue, K. (2002). Downregulation of P2X3 receptor-dependent sensory functions in A/J inbred mouse strain. Eur. J. Neurosci. 15, 1444–1450.

Ueda, H., Amano, H., Shiomi, H., and Takagi, H. (1979). Comparison of the analgesic effects of various opioid peptides by a newly devised intracisternal injection technique in conscious mice. Eur. J. Pharmacol. 56, 265–268.

Urban, D.J., and Roth, B.L. (2015). DREADDs (designer receptors exclusively activated by designer drugs): chemogenetic tools with therapeutic utility. Annu. Rev. Pharmacol. Toxicol. 55, 399–417.

Usoskin, D., Furlan, A., Islam, S., Abdo, H., Lönnerberg, P., Lou, D., Hjerling-Leffler, J., Haeggström, J., Kharchenko, O., Kharchenko, P.V., et al. (2015). Unbiased classification of sensory neuron types by large-scale single-cell RNA sequencing. Nat. Neurosci. 18, 145–153.

Vos, T., Allen, C., and Arora, M. (2016). Global, regional, and national incidence, prevalence, and years lived with disability for 310 diseases and injuries, 1990-2015: a systematic analysis for the Global Burden of Disease Study 2015. Lancet 388, 1545–1602.

Wang, Y., Wu, Q., Hu, M., Liu, B., Chai, Z., Huang, R., Wang, Y., Xu, H., Zhou, L., Zheng, L., et al. (2017). Ligand- and voltage-gated Ca2+ channels differentially regulate the mode of vesicular neuropeptide release in mammalian sensory neurons. Sci. Signal. 10.

Wilson, S.R., Gerhold, K.A., Bifolck-Fisher, A., Liu, Q., Patel, K.N., Dong, X., and Bautista, D.M. (2011). TRPA1 is required for histamine-independent, Mas-related G protein-coupled receptor-mediated itch. Nat. Neurosci. 14, 595–602.

Xie, Z., and Hu, H. (2018). TRP channels as drug targets to relieve itch. Pharmaceuticals (Basel) 11.

Zeisel, A., Hochgerner, H., Lönnerberg, P., Johnsson, A., Memic, F., van der Zwan, J., Häring, M., Braun, E., Borm, L.E., La Manno, G., et al. (2018). Molecular architecture of the mouse nervous system. Cell 174, 999–1014.e22.

Zeldenrust, F., Wadman, W.J., and Englitz, B. (2018). Neural Coding With Bursts-Current State and Future Perspectives. Front. Comput. Neurosci. 12, 48.

Zylka, M.J., Dong, X., Southwell, A.L., and Anderson, D.J. (2003). Atypical expansion in mice of the sensory neuron-specific Mrg G protein-coupled receptor family. Proc. Natl. Acad. Sci. USA 100, 10043–10048.

Supplemental Information

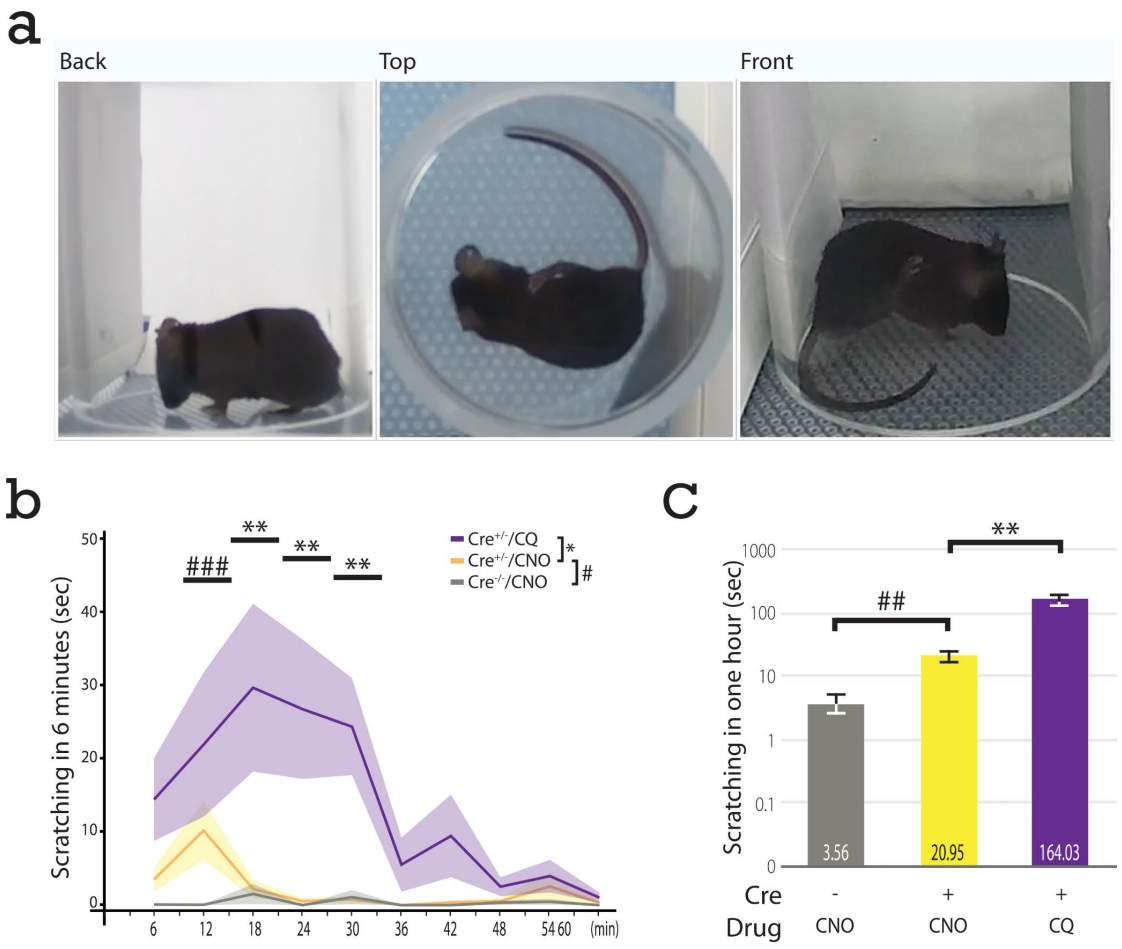

Supplemental figure 1- Multi-angle frame-by-frame video annotation allows precise analysis of scratching behavior (related to Figure 1). *a) Unilateral hindpaw scratching behavior can be observed and corroborated from different angles. The same mouse is shown from three different angles (Back, Top, and Front) during a scratching bout. The behavior is not detectable from the back angle camera while it can be detected in the two other angles. b) Timeline of time spent scratching demonstrates similar build-up and wind-down pattern of behavior in Cre+/-/CNO and Cre+/-/CQ groups but not in Cre-/-/CNO, confirming induction of itch by CQ and by*

CNO in Cre-expressing AAV-transduced animals. Observation of sporadic and irregular scratching bouts in the Cre-/-/CNO group, in comparison to Cre+/-/CNO cage-/litter-mates, confirms the dependence of CNO on DREADD expression to induce itch. Similarity to figure 1e is due to individual scratching bout durations being comparable (Figure 1d). Two-way ANOVA, and Bonferroni post-hoc tests were used for comparison of Cre (#) or drug effects (*) over time. The one-hour period of observation (injection at time = 0) was divided into 10 equal 6-minute bins for statistical comparisons. c) DREADD-mediated metabotropic stimulation of MrgprA3 C-afferents evokes pruriception. Total time spent scratching over the 1-hour period following CNO injection indicates that scratching behavior is Cre-dependent (unpaired t-test, $p < 0.01$). Activation of endogenous MrgprA3 by CQ evokes a significantly higher intensity of pruriception (paired t-test, $p < 0.01$).

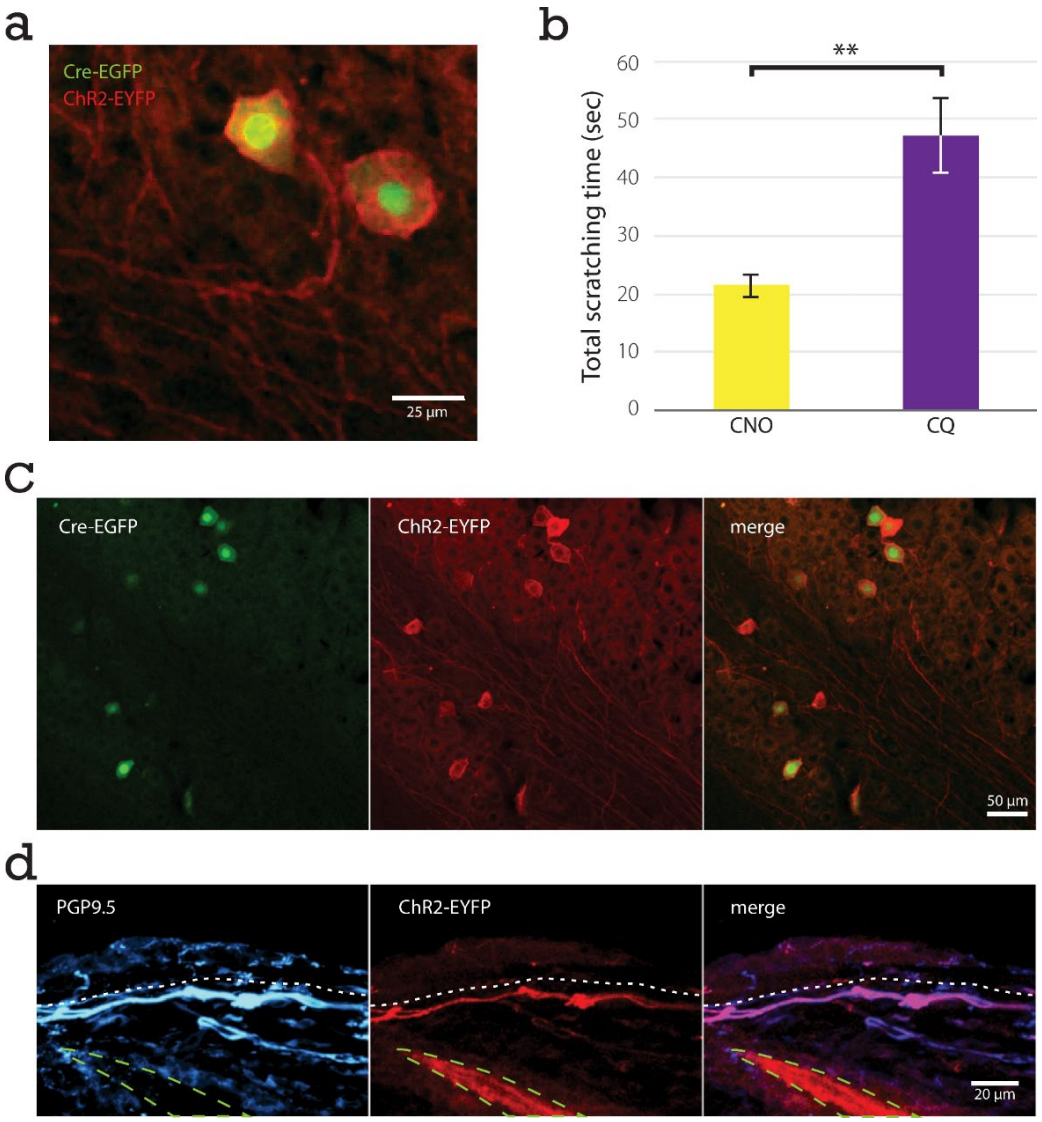

Supplemental figure 2- Proper expression of opsins and DREADDs in trigeminal MrgprA3 C-afferents validates the cheek behavioral discrimination assay (related to Figure 2).

a) Resolving eYFP and eGFP signals demonstrated by compartmentalization of Cre-eGFP mainly in the nucleos and ChR2-eYFP on the membrane of primary sensory neurons. b) CQ induces higher itch intensities than CNO in the cheek assay. Similar to the nape of the neck (Figure 1f), metabotropic activation of all MrgprA3 C-afferents through their endogenous GPCR induces more total time spent scratching than activation of a subset of afferents through DREADDs

(paired t-test, $p < 0.01$, n=6-7). These results are derived from the experiment represented in Figure 3. c) ChR2 is expressed in the trigeminal ganglia of MrgprA3Cre-eGFP+/-:Rosa26ChR2-eYFP+ animals in a Cre-dependent fashion. Similar to the cervical dorsal root ganglia (Figure 2a), membrane-bound ChR2 is expressed in Cre-expressing trigeminal afferents innervating the cheek hairy skin. d) ChR2-EYFP opsins are trafficked to the hairy skin of the cheek. Opsin expression in the cheek epidermis of MrgprA3Cre-eGFP+/-:Rosa26ChR2-eYFP+ mice is confirmed by the eYFP signal located in a subset of peripheral nerve endings (stained with PGP9.5). A hair shaft is indicated by dotted lines and the border between dermis and epidermis is indicated by dotted lines.

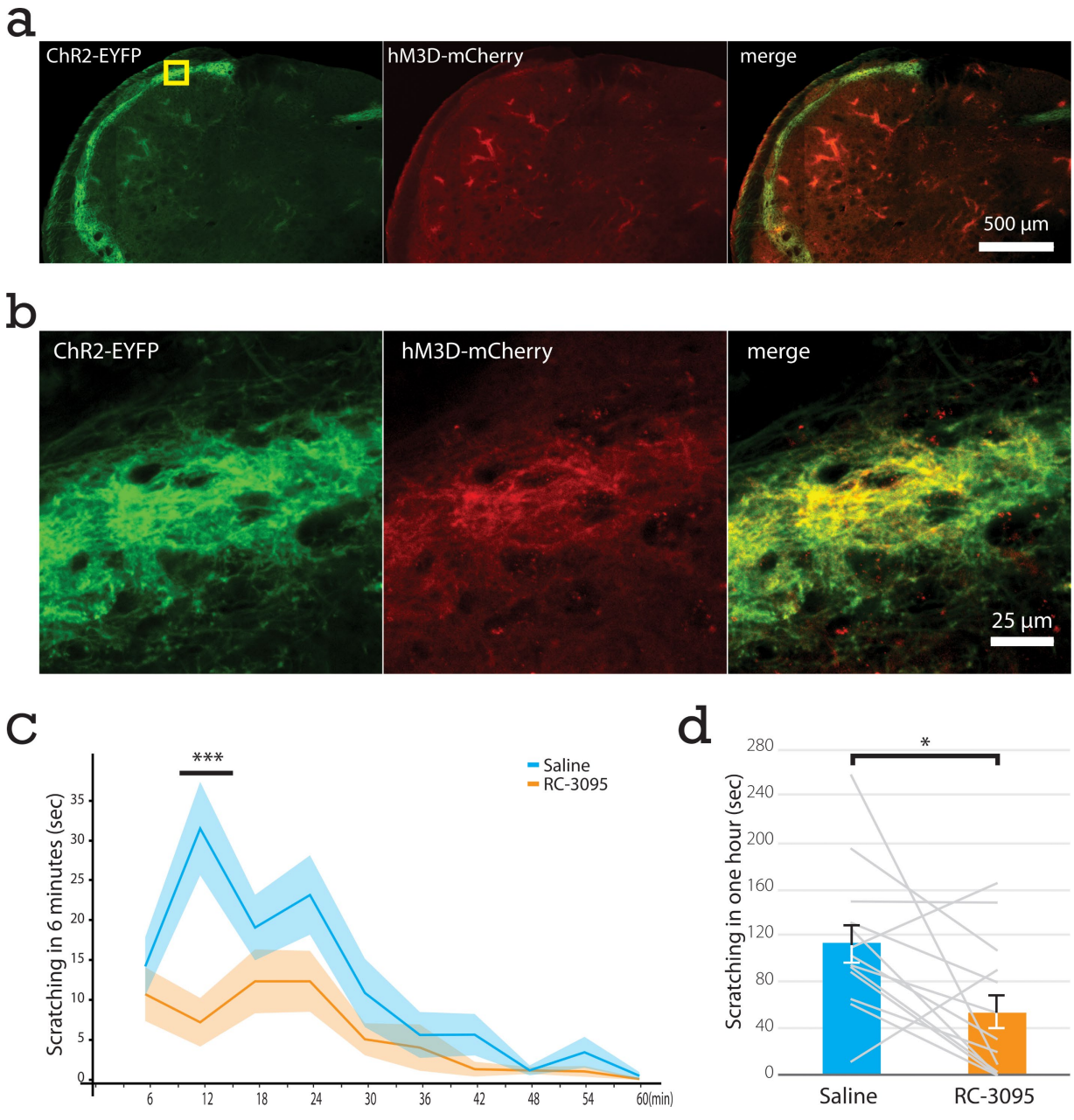

Supplemental figure 3- MrgprA3 C-afferents innervate the substantia gelatinosa in spinal cord (related to Figure 4). *a) Tiled coronal section of the medullary spinal cord from an AAV-transduced MrgprA3Cre-eGFP+/-:Rosa26ChR2-eYFP mouse shows termination of MrgprA3 afferents in lamina II. b) Zoomed view of the superficial laminae (yellow box in a) confirms expression of hM3Dq in eYFP-expressing terminals. c) i.c. administration of the GRPR blocker RC-*

3095 blunts CQ-induced itch. Timeline of time spent scratching, similar to the timeline of scratching bout counts (Figure 4c), indicates that GRPR blockade alleviates pruriception more effectively at earlier time points. Average counts in 6-minute time bins are displayed with shades indicating SEMs. Two-way ANOVA test with Bonferroni post-tests was used for statistical comparison. d) Total time spent scratching also confirms the inhibitory effect of RC-3095 in the 1 hour post CQ injection in the nape of the neck ($p < 0.05$, paired t-test, n=13).

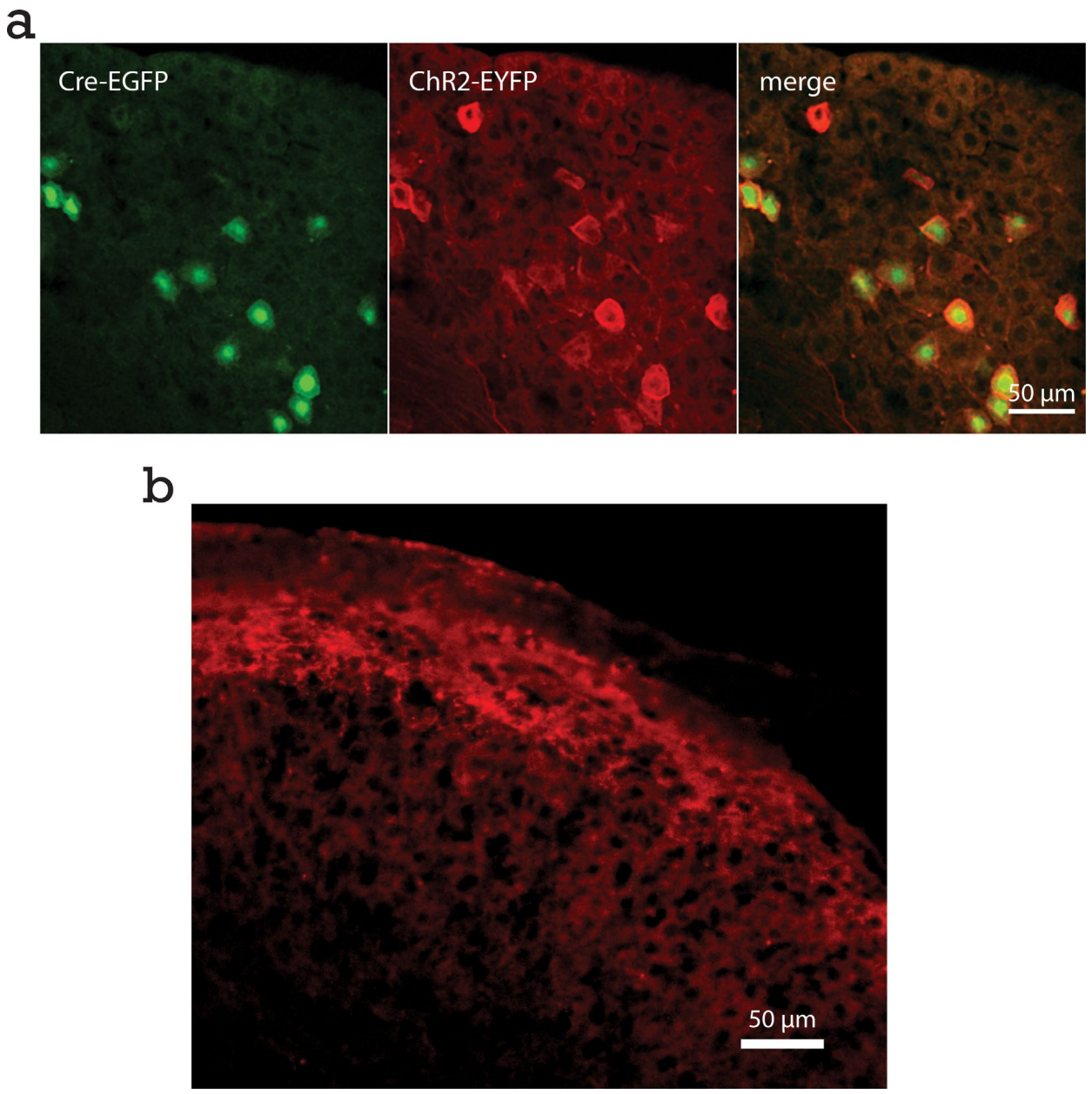

Supplemental figure 4- ChR2 expression in MrgprA3 C-afferents innervating the hindpaw underlies light-evoked nociception by transdermal illumination of the plantar surface (related to Figure 5). *a) MrgprA3Cre-eGFP+/-:Rosa26ChR2-eYFP+ mice express channelrhodopsin-2 in MrgprA3+ primary afferents in lumbar dorsal root ganglia. b) The central terminals of transgenic ChR2-expressing eYFP-positive MrgprA3 C-afferents are located in the substantia gelatinosa in lumbar spinal cord.*

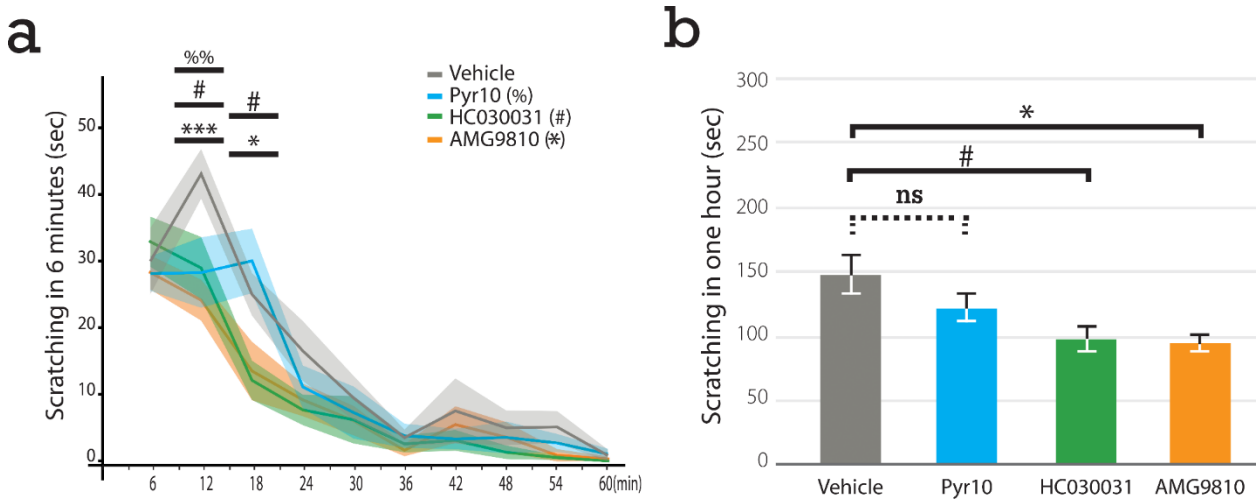

Supplemental figure 5- Pharmacological blockade of TRPC3, TRPA1, and TRPV1 channels reduces CQ-evoked itch mediated by MrgprA3 C-afferents (related to Figure 6). *a) TRP channel blockers reduce CQ-induced pruriception by changing the kinetics of the scratching behavior. Similar to the timeline of scratching bout counts (Figure 6c), the timeline of time spent scratching shows that pharmacological blockade of the TRP channels reduces the itch behavior more effectively at earlier time points (Two-way ANOVA with Bonferroni post-hoc test, %, #, and * symbols depict significance levels for comparison of the vehicle vs. Pyr10, HC030031, or AMG9810 groups, respectively). b) Total durations of time spent scratching in the 1 hour period post CQ injection, showing a significant decrease of scratching intensity by TRPA1 and TRPV1 blockers (One-way ANOVA with Bonferroni post-Hoc test).*

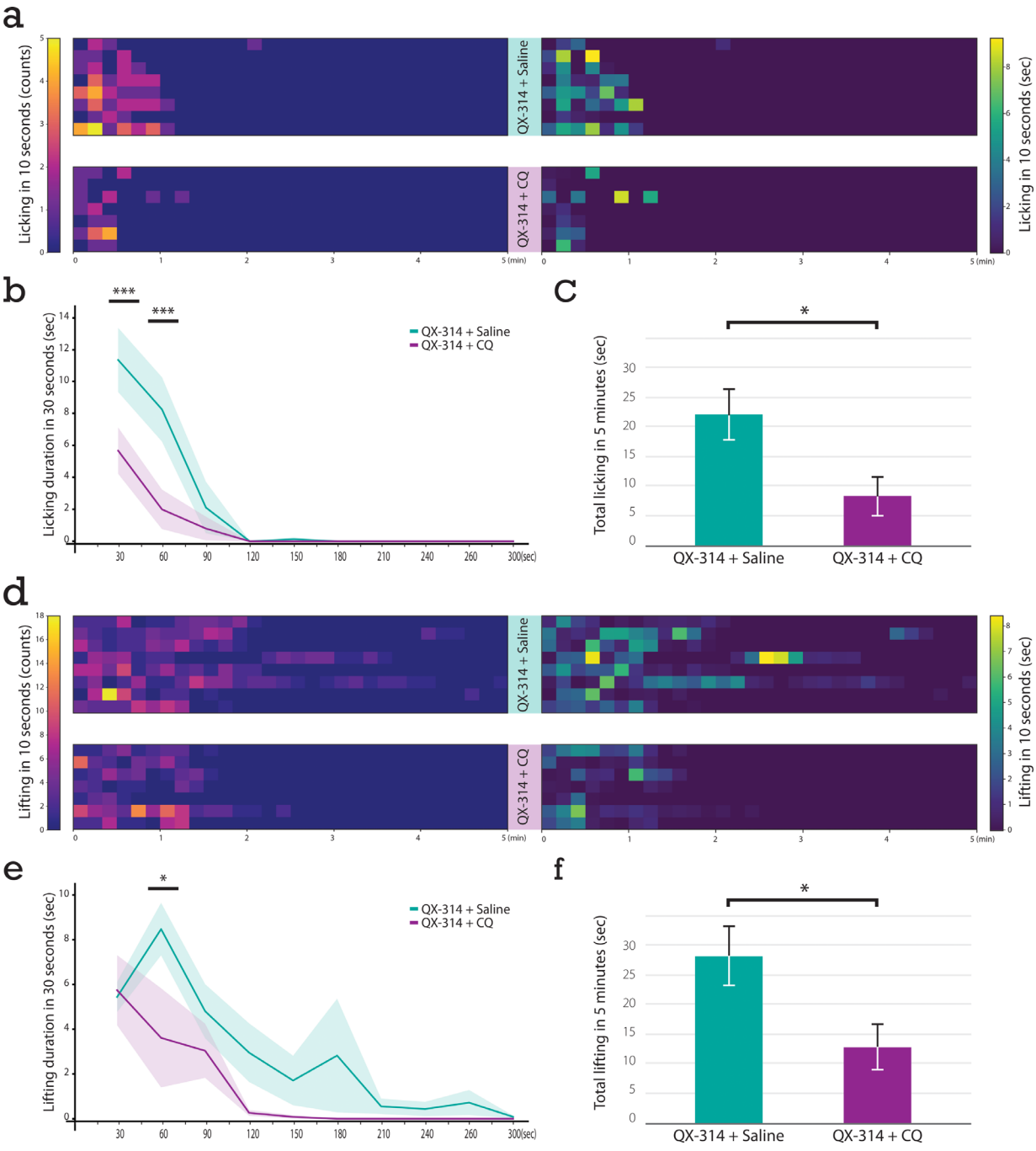

Supplemental figure 6- Protective and site-directed nocifensive behaviors are reduced by specific silencing of MrgprA3 C-afferents after purinergic activation (related to Figure 7). *a) Detailed time-course of licking behavior induced by intraplantar injection of αβmeATP (20 mM) in the hindpaw 30 minutes after conditioning with coinjection of QX-314 with saline or CQ (5*

mM). Each line represents an individual wildtype C57Bl6 mouse (n = 7-8) and every block indicates the number of licking behaviors observed (left panel), or time spent behaving (right panel) in 10-second time bins, as defined by the heat maps. b) Timeline of the licking bouts observed, showing that QX-314-mediated silencing of CQ-responsive cells reduces this site-directed coping behavior after αβmeATP-evoked pain. Average durations of licking in 30-second time bins are displayed with shades indicating the SEM. Two-way ANOVA test with Bonferroni post-tests was used for statistical comparison ($p < 0.001$). c) Conditional silencing of CQ-responsive afferents reduces the total duration of purinergic licking behavior. Animals receiving QX-314 + CQ 30 minutes before αβmeATP spend significantly less time licking the site of injection in the 5 minutes period after algogen administration ($p < 0.05$, unpaired t-test). Similar to licking behavior, details of lifting behavior are demonstrated in panels d, e, and f. In the time progression (e) the difference of lifting behavior in the QX-314 + CQ group is significantly less in the earlier time bins ($p < 0.05$) and this behavior is almost not observed after 2 minutes from algogen injection (d & e).

Supplemental video 1- Optical stimulation of the nape of the neck of MrgprA3$^{Cre\text{-}eGFP+/-}$:Rosa26$^{ChR2\text{-}eYFP}$ mice evokes predominantly aversive behaviors distinct from scratching (related to Figure 2).

https://ars.els-cdn.com/content/image/1-s2.0-S0896627320302282-mmc2.mp4

Supplemental video 2- Optical stimulation of the nape of the neck of MrgprA3$^{Cre\text{-}eGFP-/-}$:Rosa26$^{ChR2\text{-}eYFP}$ cagemate littermates evokes no behavior (related to Figure 2).

https://ars.els-cdn.com/content/image/1-s2.0-S0896627320302282-mmc3.mp4

Supplemental video 3- Frame-by-frame quantification of different behaviors in the cheek assay in mice (related to Figure 3). *Blue: hindpaw scratching of the cheek ipsilateral to the injection. Red: Unilateral forepaw wiping of the injected cheek. Green: Bilateral forepaw grooming behavior.*

https://ars.els-cdn.com/content/image/1-s2.0-S0896627320302282-mmc4.mp4

Supplemental video 4- Optical stimulation of the cheek with blue light evokes stereotypical wiping behavior in MrgprA3$^{Cre\text{-}eGFP+/-}$:Rosa26$^{ChR2\text{-}eYFP}$ mice (related to Figure 3).

https://ars.els-cdn.com/content/image/1-s2.0-S0896627320302282-mmc5.mp4

Supplemental video 5- Control optical stimulation of the cheek with yellow light does not induce any behavior in MrgprA3$^{Cre\text{-}eGFP+/-}$:Rosa26$^{ChR2\text{-}eYFP}$ mice (related to Figure 3).

https://ars.els-cdn.com/content/image/1-s2.0-S0896627320302282-mmc6.mp4

Supplemental video 6- Optical stimulation of the cheek with blue light evokes no behavior in MrgprA3$^{Cre\text{-}eGFP-/-}$:Rosa26$^{ChR2\text{-}eYFP}$ cagemate littermates (related to Figure 3).

https://ars.els-cdn.com/content/image/1-s2.0-S0896627320302282-mmc7.mp4

Supplemental video 7- Optical stimulation of the hindpaw with blue light evokes nocifensive responses in MrgprA3$^{Cre\text{-}eGFP+/-}$:Rosa26$^{ChR2\text{-}eYFP}$ mice (related to Figure 5).

https://ars.els-cdn.com/content/image/1-s2.0-S0896627320302282-mmc8.mp4

Supplemental video 8- Optical stimulation of the hindpaw with blue light evokes no behavior in MrgprA3$^{Cre\text{-}eGFP-/-}$:Rosa26$^{ChR2\text{-}eYFP}$ cagemate littermates (related to Figure 5).

https://ars.els-cdn.com/content/image/1-s2.0-S0896627320302282-mmc9.mp4

Linker

Whether the primary afferents send specific signals or relay signals pertaining to multiple modalities, the cellular heterogeneities of the sensory ganglia contribute to these signals. As shown in the previous chapter, modulations through effectors such as TRP channels can hold key information about how the sensory stimuli are differentially encoded. Understanding the heterogeneities and the molecular capacities of the cells in the primary sensory ganglia can further clarify the mechanisms through which somatosensation is achieved.

Chapter 3:

Comprehensive cellular atlas of human dorsal root ganglia using single-nucleus RNA and ATAC sequencing

Behrang Sharif[1,2,3], Spyros Oikonomopoulos[4], Jiannis Ragoussis[4,5] and Philippe Séguéla[1,2]

[1] Montreal Neurological Institute, Department of Neurology & Neurosurgery, McGill University, Montreal H3A 2B4, Quebec, Canada

[2] Alan Edwards Centre for Research on Pain, Montreal H3A 0G1, Quebec, Canada

[3] Department of Physiology, McGill University, Montreal H3G 1Y6, Quebec, Canada

[4] McGill Genome Centre, Department of Human Genetics, McGill University, Montreal H3A 0C7, Quebec, Canada

[5] Department of Bioengineering, McGill University, Montreal H3A 0E9, Quebec, Canada

IN PREPARATION

Summary

Primary afferents, with their terminals at the outermost frontiers of the nervous system, transmit the first-order sensory signals detected in the periphery. Cell bodies of these unique neurons reside in the sensory ganglia where they are closely chaperoned by various non-neuronal cells which can contribute to information processing and modulation. Understanding the cellular roster of human sensory ganglia can significantly improve our knowledge of how sensory modalities are coded in health and are altered in disease conditions. Here we aim to provide the first comprehensive cellular atlas of human dorsal root ganglia (DRG) as a resource for pain research and sensory neuroscience. In order to capture the genomic landscape of DRGs in states closely similar to *in vivo* conditions, we opted to use single-nucleus RNA sequencing from flash frozen postmortem samples. To further enrich the data set, we also include epigenomic information from individual nuclei by performing assay for transposase-accessible chromatin using sequencing (scATAC-seq). Preliminary results show the feasibility of this dual approach and the possibility of resolving physiologically relevant and expected cellular clusters from human DRGs.

Keywords

Human dorsal root ganglia (DRG), Single nucleus RNA sequencing (snRNA-seq), Single cell ATAC sequencing (scATAC-seq), pain, ion channels, transcriptome, epigenetics

Introduction

The cell bodies of primary afferents, the frontiers of somatosensory nervous system in vertebrates, reside in primary sensory ganglia. These pseudo-unipolar neurons extend one axon to their receptive fields in peripheral organs such as the skin, muscle, bones and viscera, while they send another axon to the central nervous system, mainly the spinal cord. The unique characteristics of these neurons with their extensive axonal processes, require special anatomical, metabolic, and autonomic support structures exclusively present in sensory ganglia (Devor, 1999; Haberberger et al., 2019; Matsuda et al., 2005; Nascimento et al., 2018). Different neurons of the peripheral sensory ganglia innervate receptive fields with different spatial and density characteristics and neurons from each ganglion tend to cover similar areas on the body called dermatomes (Foerster, 1933; Lee et al., 2008). Other than distinctive receptive fields, primary afferents display transcriptomic, cellular, and cytochemical diversities which have been correlated with their distinct functionalities (Carr and Nagy, 1993; Gatto et al., 2019; Le Pichon and Chesler, 2014). Whereas highly myelinated Aβ afferents with large cell-bodies are believed to be primarily responsible for transmission of touch and vibration modalities, unmyelinated C fibers with small cell bodies are mainly nociceptors, i.e. pain sensing, with distinct modality sensitivity (Todd and Koerber, 2006). To better characterize the connection of these neuronal types to their function, there has been various attempts in recent years for categorizing peripheral somatosensory afferents based on their transcriptome (Kupari et al., 2021; Nguyen et al., 2021; Usoskin et al., 2015). These categories, if shown to be reliable and consistent, can significantly affect the identification of therapeutic targets for sensory

modality specific treatments. As most previous studies in this field were done in animal models, mainly due to specific technical requirements of human sensory ganglia samples, in this project we aimed to provide high quality single-cell transcriptomic data from human DRGs.

The primary neurons are not unaccompanied in the sensory ganglia. On the contrary, sensory neuronal cell bodies are tightly embraced by satellite glial cells and other distinctive cellular structures such as Dogiel's pericellular nests, and Cajal's initial glomeruli (Devor, 1999; Matsuda et al., 2005). The non-neuronal cells in the sensory ganglia include satellite glial cells (SGCs), mesenchymal cells such as fibroblasts, hematopoietic cells such as B cells, T cells, and macrophages, Schwann cells, vascular smooth muscle and endothelial cells. These cells are known to be essential in maintenance and homeostatic support of the sensory neurons (Esposito et al., 2019; Pannese, 1964). Moreover, recently the non-neuronal cells of the primary sensory ganglia are becoming important topics of research as they are shown to significantly contribute to the neurons' function and their excitability states (Feldman-Goriachnik and Hanani, 2021; Hanani, 2005; Hanani and Spray, 2020). SCGs and macrophages, for instance, have also been indicated in various chronic disease states (Iwai et al., 2021; De Logu et al., 2021; Warwick and Hanani, 2013). In this single-cell profiling study, we decided to also include transcriptomic information on the non-neuronal cells as they may also serve as therapeutic targets for treating sensory diseases such as chronic pain or pruritus.

Due to the tight anatomical enmeshment of the primary sensory neurons by SGCs, the highly fibrous nature of the sensory ganglia, and their high myelin content, the dissociation of whole single neuronal cells requires a combination of harsh mechanical, enzymatic, and chemical treatments (Valtcheva et al., 2016). These treatments may introduce multiple confounding

factors in the transcriptomic profiling of the cells in sensory ganglia. For instance, the large and fragile sensory neurons that exist in the sensory ganglia represent a smaller fraction of the neuronal population in the single-cell RNA sequencing (scRNA-seq) studies compared to what is expected from the immune-histochemical studies performed on fixed tissue (Kupari et al., 2021; Usoskin et al., 2015). Moreover, as living axotomized cells go through these relatively long dissociation and isolation procedures, the native transcriptomic content of these cells may be affected by the time the RNA is captured and cDNA is generated. One readily available indicator of such impact is the increase in stressed induced transcription factors like activating transcription factor 3 (ATF3) or excessive presence of mitochondrial genes in the captured cells (Wangzhou et al., 2020). To ensure proper separation of cellular entities, reduce the dissociation and isolation biases towards certain cell types, and to minimize the post-mortem transcriptomic deviation from *in vivo* conditions, for this project we flash froze and protected the human sensory ganglia shortly after cross-clamp of the donors. We also opted to perform both single-nucleus RNA sequencing (snRNA-seq) and nuclear captures of these rare samples.

The dynamic nature of the cellular components of the peripheral sensory system has been demonstrated in studies comparing the transcriptomic repertoire of these cells in healthy and disease conditions (Cobos et al., 2018; Nguyen et al., 2019; Shin et al., 2019). Key information about targetability of the sensory afferent subpopulations, or their supporting cells in the sensory ganglia may be in their capability to change. The epigenomic characteristics of the cells in the sensory ganglia, and the chromatin accessibility loci can be valuable indicators of genetic flexibility in these cells. Hence, in order to enrich our data set in a unique way, in the current

study we are including ATAC sequencing (assay for transposase-accessible chromatin using sequencing) information for all cellular subpopulations of primary sensory ganglia.

ATAC-seq was originally developed for investigation of open chromatin regions in the genome (Buenrostro et al., 2013) and with advances in the field of single-cell technologies, it is now possible to perform these studies at the single-cell level (Sinha et al., 2021). Integration of single-cell transcriptomic and ATAC information can make cell-specific genomic research possible in ways not explored before (Stuart et al., 2019). Processed data from such experiments can be used not only for taxonomic listing of clusters, or a snapshot of their expression patterns, but also for analysis of cis-regulatory elements such as promoters and enhancers, and trans-regulatory elements like transcription factors, in every cellular cluster population. This can unravel genetic capacities of key cell types while providing estimates for gene activity and genetic variants' accessibility as well (Satpathy et al., 2019).

Studying epigenetic heterogeneity and transcriptomic capacity of cells within DRGs, as prototypical primary sensory ganglia, is essential for understanding the dynamic mechanisms of somatosensation, can improve our understanding of sensory disorders, and may lead to identification of novel therapeutic targets for conditions such as chronic pain and itch. In this paper we aim to provide the comprehensive genetic landscape of human dorsal root ganglia (DRG) as a valuable resource for sensory research. We believe this can clarify various hypotheses pertaining to sensory mechanisms in health and disease, can be used for ideation of many novel sensory research, and can serve as a reference for peripheral nervous system genetic studies.

Results

Quality of captured transcriptomes is of critical importance for any RNA sequencing study. For single-cell and single-nucleus RNA sequencing studies, the importance of RNA integrity and quality is even more pronounced as many steps in the analysis pipelines rely on high confidence on captured RNA. For the current study, in order to produce meaningful sequencing results, after rigorous optimization, multiple quality control check points were defined and tested during each experiment (refer to material and methods, and Supplementary figures 1-4). First, the quality of each original tissue sample's transcriptomic content was quantified by direct (whole tissue) RNA extraction and RNA integrity number (RIN) measurement through Agilent TapeStation automated electrophoresis (Supplementary figure 1D). Only samples with RINs of 6 and higher were passed on to dissociation and isolation steps. In addition to the initial tissue quality, single-nucleus experiments require meticulous optimization of dissociation and isolation procedures. DRG tissue is highly fibrous with high myelin contents in unique organization of supporting cells closely connected and tightly surrounding sensory neurons (Supplementary figure 1A-C). Such entangled organization calls for optimization of the extensive dissociation required, which can be a combination of mechanical, enzymatic, and chemical interventions. Based on morphology and number of the nuclei isolated, along with RNA quality and yield, we narrowed the isolation methods to two protocols (see Materials and methods). In order to verify whether the final isolation detergents and protocols introduce biases in the captured genetic material, and to increase the total number of nuclei analyzed from each human DRG, for each capture both protocols were run in parallel on similar initial amounts of tissue. Before checking the profile of the nuclear RNA, the

quality of the nuclear samples was assessed by their morphology and numbers at multiple steps in the isolation procedure. Integrity of the nuclear membrane, low aggregation levels, low levels of cellular debris, and sufficient numbers of nuclei for efficient 10x genomic capture were verified before each capture (Supplementary figure 1E-F). Furthermore, the RNA content of the isolated nuclei were quantified by high sensitivity electrophoresis (Supplementary figure 1G). After microfluidic single-nucleus captures (10x Genomics), the quality of the cDNA libraries generated from each sample were further verified by a LabChip bioanalyzer (Supplementary figure 2A). cDNA libraries with expected profiles and high yields were processed for generation of sequencing-ready libraries. They were then quality controlled for library profiles, measured for precise concentrations, and were submitted for sequencing (Supplementary figure 2B, Materials and methods).

Sequencing results were aligned to a human genome reference (NCBI GRCh38) and cell calling was performed by CellRanger software (see Materials and methods for details). From the single-nucleus RNA sequencing captures, a total of 63,931 nuclei were detected from 8 different experiments. General quality control steps were taken for defining the quality of the assigned nuclei (Supplementary figure 3). After sorting the nuclei based on their unique genes (features) and unique RNAs (UMI counts), barcodes with low numbers of UMIs or high number of features were excluded (see Materials and methods). All in all, a total of 46,079 nuclei were passed on to clustering steps.

Single-nucleus RNA sequencing of whole human DRG tissue

In order to regress out the effect of capture experiments and inter-subject variations, data from different captures were integrated by mapping onto defined anchor points. 10 major cell types were defined in an initial clustering (Figure 1A). Contribution of each capture experiment to all clusters (and subclusters) was verified by per-experiment plotting of final UMAPs (Supplementary figure 4A-C). Furthermore, we verified that the clustering was not biased by depth of capture and sequencing for various experiments, by plotting the UMAPS colored by the counts of features and UMIs (Supplementary figure 4D-E). About one third (32.8%) of the nuclei from the DRG expressed genes such as Fibronectin Leucine Rich Transmembrane Protein 2 (FLRT2) that are previously described as marker genes for fibroblasts (Franzén et al., 2019; Lacy et al., 1999). Another large set of nuclei (27.2%) could be described by genes known to be expressed in satellite glial cells, e.g. neural cell adhesion molecule 1 (NCAM1) (Fukada et al., 2007; Illa et al., 1992). Hematopoietic cells expressing genes reported as macrophage markers, such as CD163 Molecule (Abraham and Drummond, 2006; Komohara et al., 2006), were the next large cluster of nuclei (18.8%). Neuronal nuclei, defined by markers such as Tubulin Beta 3 Class III (TUBB3) (Lee et al., 1990), constituted 8.3% of the total nuclei. About 6% of the nuclei could be clustered as endothelial cells as they expressed genes such as Fms Related Receptor Tyrosine Kinase 1 (FLT1) (Lau et al., 2020). Nuclei expressing high levels of genes such as Src Kinase Associated Phosphoprotein 1 (SKAP1) were tagged as T cells (2.5%) (Dadwal et al., 2021; Marie-Cardine et al., 1997) while those expressing genes like Myelin Protein Zero (MPZ) were called myelinating Schwann cells (2.2%) (Jessen and Mirsky, 2019; Su et al., 1993). Less than 1% of the nuclei belonged to clusters that were enriched for Myosin Heavy Chain 11 (MYH11),

Adiponectin, C1Q and Collagen Domain Containing (ADIPOQ), and B lymphocyte kinase (BLK), genes respectively associated with smooth muscle cell (0.9%) (Chakraborty et al., 2019; Matsuoka et al., 1993), adipocytes (0.8%) (Hu et al., 1996; Levina et al., 2021), and B cells (0.6%) (Dymecki et al., 1990). Numbers of the captured nuclei are detailed in Figure 1B. The distribution of expression for some of the marker genes in individual nuclei of every cluster is shown in Figure 1C heatmap. The top 20 differentially expressed genes in satellite glial cells nuclei (SGCs) and neuronal nuclei are also shown in Figure 1D dot plots. Detailed dot plots for all clusters are included in supplementary information (Supplementary figure 5). To demonstrate the differential presence of some well-known marker genes in various clusters, the highly expressed markers genes Protein Tyrosine Phosphatase Receptor Type Z1 (PTPRZ1), and Synaptosome Associated Protein 25 (SNAP25), as markers of SCGs (Fukada et al., 2007; Milev et al., 1994; Snyder et al., 1996) and neurons (Oyler et al., 1989; Tang, 2021) respectively, are shown in the feature plots (Figure 1E-F). Feature plots for all major clusters are provided in Supplementary figure 5.

Single-nucleus RNA sequencing of human DRG neurons

Out of the 46079 nuclei analyzed, 3811 were transcriptionally defined as neurons. In order to verify the feasibility of further clustering neurons into smaller cellular categories, we performed principal component analysis (PCA) for dimensionality reduction and clustering on the neuronal nuclei. Preliminary clustering algorithms suggest more than a dozen subcategories of these nuclei, requiring further validation (Figure 2A). However, based on these crude groupings and several classically known markers in the top highly expressed genes, we believe the data set

identifies at least 436 proprioceptors, 386 peptidergic nociceptors, and 202 pruriceptors. Feature plots of some of the well-known markers for these subpopulations, namely parvalbumin gene (PVALB) as a marker of proprioceptors, substance P gene (TAC1) as a marker of peptidergic nociceptors, and IL31 receptor gene (IL31RA) as a marker of pruriceptors are shown in Figure 2B. More of these marker genes and their expression distribution in individual nuclei are shown in Figure 2C heat map. The top uniquely expressed genes in these clusters are also included in the dot plots (Figure 2D).

Multi-modal single-nucleus sequencing (RNAseq plus ATACseq)

Single-cell RNA experiments can provide rich data for studies at population levels but as their sampling is very sparse, RNA distribution over cell compartments and time are not homogenous, and as RNA life span is relatively short, common sample sizes do not allow constructing a comprehensive map of cellular transcriptomic landscape. In particular, for cells like neurons that are post-mitotic, terminally differentiated, and spatially extended, the genetic capacity may not be depicted as thoroughly by the transcriptome as by the epigenome. Here we are presenting some preliminary data from few multiome experiments that we performed for integrating single-nucleus RNA sequencing and single-nucleus ATAC sequencing of human DRG. As we have optimized most steps of these experiments, we aim to increase the sample sizes to significantly enrich the resource that this study can provide for the sensory research community. The main purpose of this section is to prove the feasibility of such experiments with the current samples and technical setups.

From the total 12,296 nuclei detected by preliminary cell-calling algorithms, 10,454 passed the quality control criteria for further analyses (See Materials and Methods). Whole DRG nuclei were clustered after dimensionality reduction based on the gene expression data and 6 general biologically known populations were detected (Figure 3A). A breakdown of the populations is shown in Figure 3B. Some of the top differentially expressed marker genes are shown in Figure 3C heatmap.

One of the primary advantages of scATAC-seq in parallel to snRNA-seq is the increased confidence and accuracy of clustering. For instance, although the sample size and the count of nuclei in the analyzed dataset is still low, we can verify clusters by searching for known lineage-specific transcription factors (TFs) and counting the open chromatin regions that bear their motifs. Here, we looked at the macrophage lineage-specific transcription factor, PU.1 (REFghisletti2010&Heinz2010) which is coded by SPI1 gene. Interestingly, in this case, although there are very few copies of the mRNA detected by the transcriptomic capture (Figure 3D), there is clear and statistically significant increased levels of SPI1 motif counts detected in the macrophage cluster (Figure 3E). Another advantage of the combined transcriptomic and chromatin accessibility single cell analyses is to detect novel links between these components. Positive and negative correlation between sites with increased accessibility with other open areas or detected transcripts can lead to discoveries of cis and trans regulatory elements in the genome. Unfortunately, with current sample sizes, the dataset is still immature for such purposes but an example of such links is shown in supplementary figure 7.

Discussion

Primary sensory ganglia, including DRGs, are important therapeutic sites for sensory disorders (Esposito et al., 2019). Understanding the cellular environment of these ganglia is a focus of many researchers as it undoubtedly improves our knowledge about the biology of primary afferents and how they function in health and disease. Here we are providing a unique and thorough atlas of the genomic landscape of DRGs. This resource can be used for refining previously debated theories such as the labeled line theory retrospectively or for development of novel ways to study and target the function of primary sensory cells. Moreover, the multimodal approach taken in this study can redefine and fine-tune the labels and markers used for such compartmental strategies towards the sensory afferents, as the differences might not be necessarily based on transcriptome or protein expressions, and rather be in the epigenomic capacities of the cells.

Single-cell sequencing data are intrinsically noisy and sparse (Eraslan et al., 2019; Lähnemann et al., 2020) hence they require large sample sizes or combinatorial approaches that can complement each other. In this study we are aiming to have statistically acceptable sample sizes (at least 8 subjects in total) and also increase the power and quality of the data by including multiple information modalities. Other than the single-nucleus RNA sequencing and ATAC sequencing data discussed in the current report, we have also optimized the usage of single-cell full-length cDNA sequencing (Oxford Nanopore Technologies). Combined with whole tissue long-read RNA sequencing, this information can lead to detection of splicing variants in specific subpopulation of cells, improving the depth of the transcriptome databases.

Inclusion of all cellular subtypes present in the DRG ("the DRG ecosystem"), significantly distinguishes the current study from previously published studies in the field. This is long overdue as there are several studies showing the contribution of non-neuronal cells of the sensory ganglia to chronic sensory disorders, e.g. the role of macrophages in neuropathic pain (Iwai et al., 2021; De Logu et al., 2021; Yu et al., 2020; Zhang et al., 2016a), or the participation of SGCs in peripheral sensitization (Hanani and Spray, 2020; Pannese et al., 2003; Warwick and Hanani, 2013). Understanding these non-neuronal cell types and their respective subcategories has also the potential to facilitate the identification of novel therapeutic targets for the treatment of sensory disorders.

We are aiming to balance the male and female samples included in this study. Distinct from most previous works in the field, this can provide the possibility of studying sex differences in the neuronal, as well as non-neuronal, populations of cells in the primary sensory ganglia. Although there are studies showing sexual dimorphism regarding important genes such as opioid receptors (Liu et al., 2007; Lomas et al., 2007; Midavaine et al., 2021) and some cytokines (Gregus et al., 2021; Yu et al., 2020), to our knowledge there is no comprehensive studies addressing these differences at the single-cell resolution. Using our dual approach, we will be able to investigate whether sex differences are present at the transcriptomic level or among the non-coding genomic elements that are mostly involved in epigenetic regulation of gene expression.

Acknowledgments

The funding for this study is provided by Eli Lilly USA. We thank Mr. Yu Chang Wang and Mr. Haïg Djambazian, for their technical support in library preparation and sequencing. We thank Ms. Stéphanie Mouchbahani-Constance for initial processing and storage of human DRG samples.

Author Contributions

B.S. performed the experiments, ran the data analyses, and prepared the manuscript.

S.O. assisted with the experiments and analyses.

P.S. and J.R. supervised the study.

All authors contributed to the design, troubleshooting, interpretation of experiments, and to the editing of the manuscript.

Declaration of Interests

The authors declare no conflict of interests.

Figures & Legends

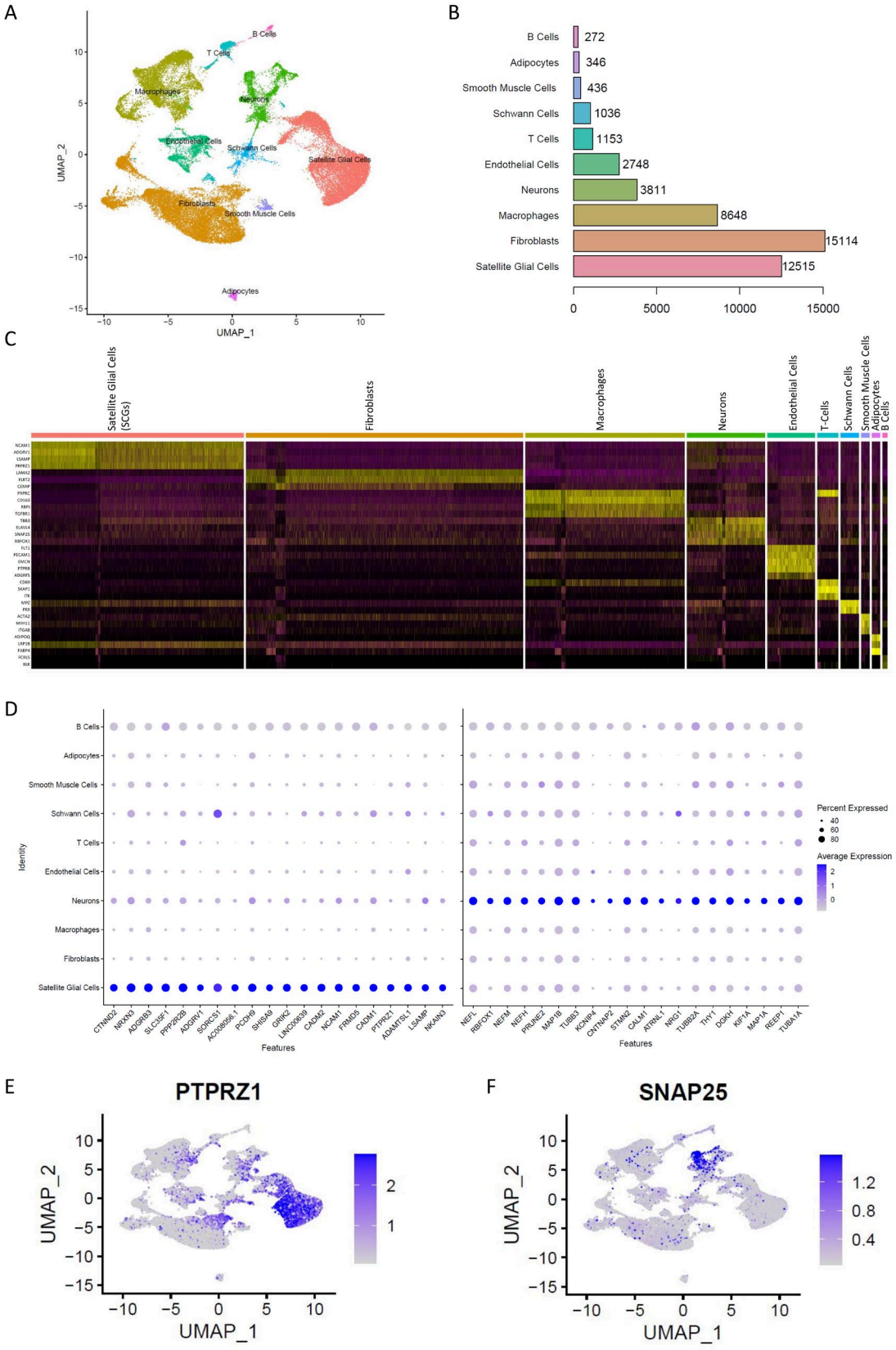

Figure 1- Single-nucleus RNA sequencing of whole human dorsal root ganglia indicates the presence of multiple cell types with distinct population sizes.

A) Low-resolution clustering of more than 46,000 single nuclei based on their transcriptomic profile defines 10 different categories of cells.

B) Breakdown of major cell types tally in whole DRGs. While almost one third of the nuclei counts belong to SGC and fibroblast categories, neurons make close to 8% of the total population.

C) Heatmap of top marker genes expressed in each cluster.

D) Dot plots showing the top differentially expressed genes in the SGC and neuron clusters.

E) Distribution of PTPRZ1 gene expression in all nuclei, overlaid on the UMAP dimensionality reduction graphs showing the enrichment of this marker in the SGC cluster.

F) Feature plot demonstrating SNAP25 gene expression enrichment in the neurons cluster.

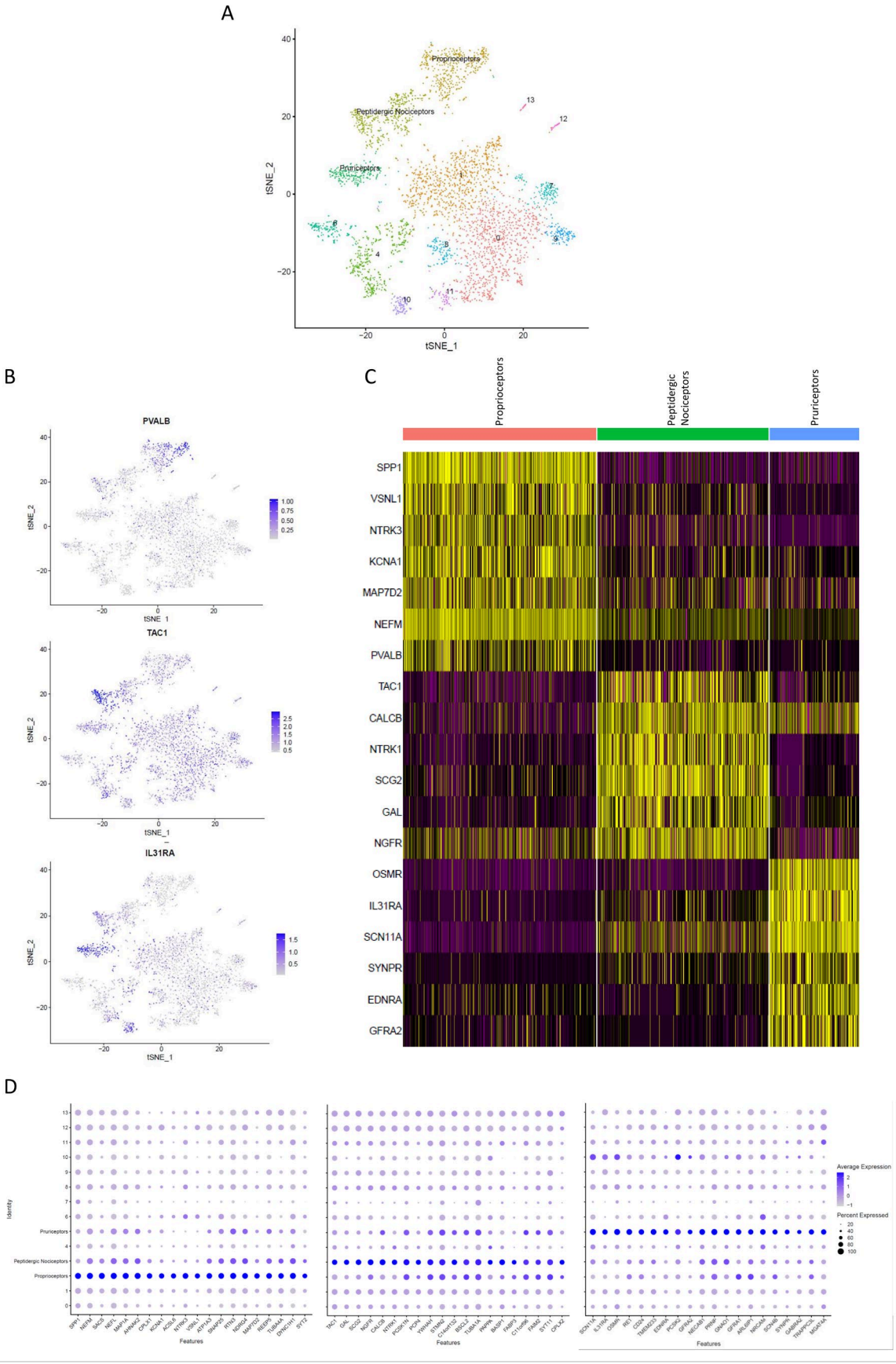
A
Proprioceptors
Peptidergic Nociceptors
Pruriceptors
tSNE_1
tSNE_2
B
PVALB
TAC1
IL31RA
C
Proprioceptors
Peptidergic Nociceptors
Pruriceptors
SPP1
VSNL1
NTRK3
KCNA1
MAP7D2
NEFM
PVALB
TAC1
CALCB
NTRK1
SCG2
GAL
NGFR
OSMR
IL31RA
SCN11A
SYNPR
EDNRA
GFRA2
D
Identity
Features
Average Expression
Percent Expressed

Figure 2- Sub-clustering of human DRG neurons based on single-nucleus transcriptomics.

A) Unsupervised clustering of 3811 neuronal nuclei suggests 14 categories of cellular subtypes.

B) Known markers such as parvalbumin, substance P, and interleukin 31 receptor genes are enriched in three separate initial clusters.

C) Heatmaps showing distribution of typically enriched genes in the proprioceptor, peptidergic nociceptor, and pruriceptor subpopulations.

D) Dot plots showing top differentially expressed genes from named clusters.

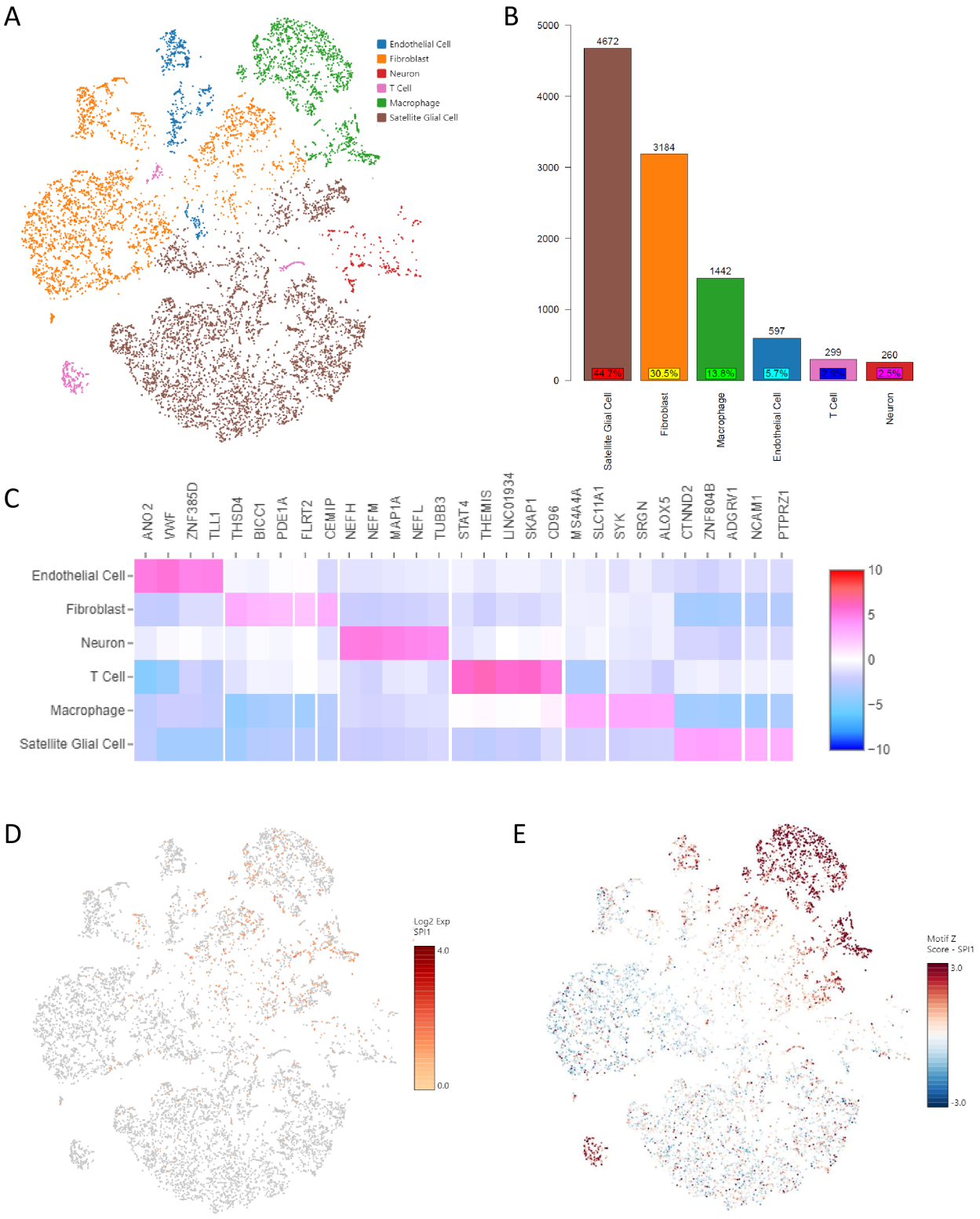
A
Endothelial Cell
Fibroblast
Neuron
T Cell
Macrophage
Satellite Glial Cell
B
5000
4000
3000
2000
1000
0
4672
3184
1442
597
299
260
44.7%
30.5%
13.8%
5.7%
2.8%
2.5%
Satellite Glial Cell
Fibroblast
Macrophage
Endothelial Cell
T Cell
Neuron
C
ANO2
VWF
ZNF385D
TLL1
THSD4
BICC1
PDE1A
FLRT2
CEMIP
NEFH
NEFM
MAP1A
NEFL
TUBB3
STAT4
THEMIS
LINC01934
SKAP1
CD96
MS4A4A
SLC11A1
SYK
SRGN
ALOX5
CTNND2
ZNF804B
ADGRV1
NCAM1
PTPRZ1
Endothelial Cell
Fibroblast
Neuron
T Cell
Macrophage
Satellite Glial Cell
10
5
0
−5
−10
D
Log2 Exp
SPI1
4.0
0.0
E
Motif Z
Score - SPI1
3.0
-3.0

Figure 3- Single-nucleus RNA-seq and scATAC-seq of whole human DRG provides reliable clustering and epigenomic information on cell types.

A) Preliminary clustering of nuclei based on gene expression data derived from multiome single-nucleus captures results in similar clustering to that of single-nucleus transcriptomic captures.

B) Distribution of cell type populations in the DRG (one subject, two capture experiments)

C) Heatmap showing the expression levels of some of the top differentially expressed transcriptomes.

D) Feature plot showing the expression levels of PU.1 transcription factor (SPI1 gene). Note the low amount of mRNA levels captured.

E) Feature plot showing the normalized sum of accessible regions containing PU.1 transcription factor motif regions derived from single nucleus ATAC data, confirming the high levels of macrophage lineage specific transcription factor accessibility in the macrophage cluster.

Materials and methods

Resources Table

REAGENT or RESOURCE	SOURCE	IDENTIFIER
Antibodies and dyes		
DRAQ-5	Thermo Scientific	62251
Chemicals, Peptides, and Recombinant Proteins		
Tris pH 7.4	Rockland Immunochemicals	CAMB-002
Tris pH 8	Fisher Scientific	BP1758-500
NaCl	Invitrogen	AM9760G
MgCl2	Invitrogen	AM9530G
CaCl2	VWR Life Sciences	E506-100ML
BSA	Bioshop Canada Inc.	ALB001.500
Tween-20	Sigma	P7949-500mL
Nuclease free water	Applied Biosystems	901578
10X PBS	ThermoFisher	AM9624
NP-40	Abcam Inc	ab142227-100ML
CHAPS	Fisher BioReagents	FLBP5715
Digitonin	Invitrogen	LSBN2006
Sigma Protector RNase inhibitor	Roche	3335402001
RNase Inhibitor	Enzymatics /Qiagen	Y9240L
RNaseIN plus	Promega	PRN2615
SuperaseIN	Invitrogen	AM2696
RNA protect tissue reagent	Qiagen	76104
RNase free DNase Set	Qiagen	79254
Other consumables		

Chromium Next GEM Single Cell 3' Kit v3.1,16 rxns	10X Genomics Inc.	1000268
Chromium Next GEM Single Cell MultiomeATAC + Gene Expression Reagent Bundle,16 rxns	10X Genomics Inc.	1000283
pluriStrainer Mini 40µ	Fisher Scientific	NC1469671
pluriStrainer Mini 20µ	Fisher Scientific	NC1423042
MACS SmartStrainer	Miltenyi Biotec	130-110-915
Hemacytometers	SKC Inc.	DHCN015
HT DNA 1K/12K/HI SENS LABCHIP	PerkinElmer Health Sciences Canada, Inc.	760517
Qubit RNA high sensitivity	ThermoFischer Scientific	Q32852
Qubit 1X dsDNA high sensitivity	ThermoFischer Scientific	Q33230
High Sensitivity RNA ScreenTape	Agilent	5067-5579-81
D5000 DNA screentape	Agilent	5067-5588-90
RNeasy Plus Mini kit	Qiagen	74134
RNeasy Plus Micro kit	Qiagen	74034
QiaShredder	Qiagen	79654
Ligation Sequencing kit	Oxford Nanopore Technologies	SQK-LSK109
PromethION flowcell	Oxford Nanopore Technologies	FLO-PRO002
Non-consumables		
Tissue Grinder Douncer 7ML CS2	Kimble	62400-620
Bessman Tissue Pulverizers	Fisher Scientific	08-418-2

Experimental Tissue and Subjects Details

Subjects

Lumbar DRGs (L4-L5) from de-identified male and female organ donors were harvested through a collaboration with Transplant Quebec Organ Donation according to the protocols approved by McGill University ethical review board (IRB#s A04-M53-08B). Multiple DRG samples from male and female subjects aged between 25 to 78 were used for optimization of the dissociation and isolation protocols. Two female subjects (68 and 78 years of age) and one male subject (35 years of age) were included in the data shown in this manuscript. Subjects did not have any history of chronic sensory disease and no known medical conditions related to peripheral nervous system.

Harvest protocol

The lumbar DRGs were harvested within 2 hours of cross-clamp (Valtcheva et al., 2016) and were flash frozen in cold isopentane after removal of surrounding connective tissue. The DRGs where transferred to -80 °C deep freezers before isolation of nuclei.

Isolation of nuclei

As the DRG tissue is a fibrous tissue with unique structural and organizational anatomy, several optimization steps were taken to improve the nuclei purification and increase the yield of nuclei from the tissue. To ensure that the isolation protocols did not affect the quality of the genetic content of the isolated nuclei, two different protocols with different primary detergents (NP-40 and CHAPS) and different RNase inhibitors were selected for single nuclei captures. Each DRG sample was dissociated according to both isolation protocols in parallel in order to better compare the resulting captures and possible biases.

NP-40 based isolation

This isolation method was adapted from, and optimized based on the protocol introduced by 10x genomics for multiome captures (CG000375 | Rev B) (10xGenomics, 2021a). In short, 20-30 mg of one lumbar DRG was manually chopped by a surgical pair of scissors for 7 minutes before 10 minutes of lysis in 1 mL of lysis buffer containing pH 7.4 Tris (10 mM), NaCl (10 mM), MgCl2 (3 mM), NP-40 (0.1 %), DTT (1 mM), BSA (1 %), Sigma Protector RNase inhibitor (1 U/µL). The sample was then strained through 40 µ pore size strainers and were centrifuged at 500 g for 6 minutes at 4 °C. The supernatant was removed and the nuclei were resuspended in 1 mL of PBS based wash buffer containing 1 % BSA and 1 U/µL RNase Inhibitor before centrifugation for 5 minutes at 500 g at 4 °C. For 3’ transcriptomic captures, the pelleted nuclei were then resuspended in 30-80 µL of the same PBS based wash buffer before 10x genomics capture by Chromium Next GEM Single Cell 3' Kit v3.1 chips using a Chromium controller machine. Before capture, the nuclei were quality controlled, counted, and if need be reconcentrated in the same

PBS based buffer based on their morphological analysis on hemocytometers using a EVOS FL Auto microscope (Life Technologies) and 5 µM DRAQ-5 nuclear staining (Supplementary figure 1).

CHAPS based isolation

This isolation method was adapted from, and optimized based on the protocol introduced by Drokhlyanski et. al (Drokhlyansky et al., 2020). In short, 20-30 mg of the DRG samples were manually chopped by a pair of surgical scissors for 7 minutes before addition of 1 mL CST lysis buffer containing pH 8 Tris (10 mM), NaCl (146 mM), CaCl2 (1 mM), MgCl2 (21 mM), BSA (0.1 %), CHAPS (0.49 %), RNaseIN plus (0.2 U/µL), SuperaseIN (0.1 U/µL). Samples were lysed in this solution for 10 minutes on ice with gentle stirring every 2 minutes. The suspension was then strained through 40 µ strainers and the lysis was quenched by addition of 3 mL of ST wash buffer containing 8 Tris (10 mM), NaCl (146 mM), CaCl2 (1 mM), MgCl2 (21 mM), and Enzymatics Inhibitor (0.1 %). Samples were then centrifuged for 6 minutes at 500 g at 4 °C. Supernatant was removed and the pellets were resuspended in 1 mL of the same ST wash buffer before another centrifugation at 500 g for 5 minutes at 4 °C. For 3’ transcriptomic captures, the nuclei in the pellets were reconstituted in 30-80 µL of PBS based buffer containing 1 % BSA and 1 U/µL RNase Inhibitor. The suspension was then stained by 5 µM DRAQ-5 nuclear stain and were quality checked and counted before 10x genomics capture through Chromium Next GEM Single Cell 3' Kit v3.1 chips with a 10x chromium controller machine. If required, the samples were centrifuged at 500 g for 5 minutes at 4 °C and were reconcentrated in appropriate volume of the same PBS based buffer before single nucleus captures.

Permeabilization for ATAC Captures

For multiome captures, after the washing steps nuclei were permeabilized for 1-3 minutes depending on the quality of the nuclear membranes in 100 µL of permeabilization buffer containing pH 7.4 Tris (10 mM), NaCl (10 mM), MgCl2 (3 mM), BSA (1 %), DTT (1 mM), Tween-20 (0.1 %), NP-40 (0.1 %), Digitonin (0.01 %), and RNase Inhibitor (1 U/µL). The end point for the permeabilization was chosen from separate experiments based on the high magnification phase contrast imaging of the nuclei (CG000375 | Rev B) (10xGenomics, 2021a). The permeabilization was quenched by addition of 1 mL of wash buffer containing pH 7.4 Tris (10 mM), NaCl (10 mM), MgCl2 (3 mM), BSA (1 %), DTT (1 mM), Tween-20 (0.1 %), and RNase Inhibitor (1 U/µL). The permeabilized nuclei were then pelleted by centrifugation at 500 g for 5 minutes at 4 °C. After removal of the supernatant, the nuclei were resuspended in 10-60 µL of diluted nuclei buffer containing 10x Genomics Nuclei Buffer, DTT (1 mM), RNase Inhibitor (1 U/µL). Nuclei were then quality checked and counted based on their morphological characteristics after staining by DRAQ-5 and imaging. If need be, the nuclei were reconcentrated in the same diluted nuclei buffer after 5 minutes of centrifugation at 500 g at 4 °C before capturing single nuclei by Chromium Next GEM Single Cell MultiomeATAC + Gene Expression Reagent Bundle kits with a 10x chromium controller machine.

Single-nuclei Capture and Barcoding

3’ captures

3’ transcriptome captures were performed according to recommended protocols by 10x Genomics (CG000204 | Rev D) (10xGenomics, 2019). In short, 1.7 times more nuclei than targeted cell recovery were loaded together with the master mix (containing RT reagents and enzyme, template switching oligos and reducing agents) in one well of the microfluidic chip (type G), in order to compensate for the nuclei capture efficiency in GEMs (gel bead-in emulsions). Barcoded gel beads and partitioning oil were loaded in other wells of the same columns before sealing the chips and capturing using a Controller device. Chips were checked after each run by wide field microscopes to confirm absence of fluidic line clogging, or wetting of the GEMs. Refer to supplementary table 1 for detailed information on captures.

Multiome captures

Multiome captures were performed according to 10x Genomics recommended protocols in Single cell ATAC and Gene expression guides (CG000338 | Rev E) (10xGenomics, 2021b). In short, permeabilized nuclei were counted and mixed with transposition reagents with 1.7 time more counts than the aimed capture numbers to compensate for capture efficiency. After 1 hour of transposition at 37 °C the nuclei were mixed with RT reagent mix and loaded on type J chromium chips. Barcoded gel beads and partitioning oil were loaded on other well of the same column before sealing the chip with the plastic gasket and placing it in the Chromium Controller machine (Supplementary table 1 for detailed statistics).

Library Preparations

3’ gene expression libraries

In accordance with 10x Genomics guides (CG000204 | Rev D) (10xGenomics, 2019), cDNA libraries originating from the in-GEM reverse transcription (RT) reactions were cleaned and amplified by 12 cycles of PCR according to the recommended protocols before quality control steps. cDNA library profiles were checked using automated electrophoresis before short-read sequencing ready gene expression library generation, i.e. fragmentation, and adaptor ligation, etc. Sequencing libraries profiles were also inspected before submission for sequencing (Supplementary figure 2).

ATAC libraries

As per the protocol provided by 10x Genomics (CG000338 | Rev E) (10xGenomics, 2021b), GEMs were placed in a thermal cycler for completion of enzymatic reactions and reverse transcription before quenching the reactions by 10x genomics provided quenching agent. After recommended cleaning and purification steps, the samples were pre-amplified for 7 PCR cycles before separation into ATAC and GEX (gene expression) allotments. ATAC libraries were then made by 8 more PCR cycles using sample index PCR mix before quality check and submission for sequencing. Gene expression cDNA libraries were separately cleaned and amplified through 8 extra PCR cycles. Similar to 3’ captures, the GEX libraries were quality checked, fragmented and end-prepped before submission to sequencing (Supplementary figure 2).

Full length libraries

In order to verify the quality of the captured cDNA and to pave the way for better detection of splicing variants, full length cDNA libraries produced from 10x captured GEMs were used for generation of Nanopore ready sequencing libraries. These libraries are also to be used for comparing to whole tissue and whole nuclei controls from prior to 10x captures in order to detect any procedural biases towards certain cellular populations.

Nanopore provided protocol for end repairing and ligation of sequencing adaptors were used for library generation (SQK-LSK109). In short, calculated numbers of double stranded cDNA amplicons were FFPE end-prepped, cleaned and size selected before ligation to sequencing adaptors containing motor proteins.

Libraries were measured and quality checked by electrophoresis before moving on to sequencing steps (data not shown).

Sequencing

In order to normalize the loading amounts of samples, all short read libraries were quantified by qPCR using a LightCycler 480 Real Time PCR instrument with the KAPA library quantification kit (Roche) prior to submission for sequencing. All data shown in this manuscript were sequenced by MGI sequencer model DNBSEQ-G400 (MGI Tech. Co.).

Gene expression short read sequencing

Short read libraries from 10x gene expression experiments (3' or multiome GEX captures) were converted to MGI libraries using the MGIEasy Universal Library Conversion Kit. The converted libraries were amplified by rolling circle amplification (RCA) to form balls of single stranded DNA (DNA nanoballs). These amplification products were then quantified by Qubit with the ssDNA HS Assay kit, normalized and loaded on the flowcells using MGI auto-loader (auto-loader MGI-DL-200R). Libraries were sequenced with MGI, DNBSEQ-G400RS PE100 kit with App-A primers.

Libraries were sequenced for 28 cycles for read1, 150 cycles for read2 and 8 cycles for the indexes. Sequencing depth and statistics are included in supplementary table 1.

ATAC sequencing

Single cell ATAC libraries, captured through 10x multiome kits, were also sequenced after ligation of MGI sequencing adaptors and RCA. For single cell ATAC libraries App-B primers of MGI, DNBSEQ-G400RS PE100 kit were used. These ATAC libraries were sequenced for 90 cycles for Read1, 90 cycles for Read2, 8 cycles for i7 index, and 24 cycles (including 8 dark cycles) for i5

index using a custom program provided by MGI Tech. Co. called PE90-dualBCDark (Supplementary table1 for detailed stats of sequencing).

Long-read sequencing

FLO-PR0002 flowcells and PromethION Sequencer were used for long read library sequencing. The “Genomic DNA by Ligation” SQK-LSK109 protocol (Version: GDE_9063_v109_revAE_14Aug2019) provided by Oxford Nanopore Technologies was used to prepare the library for sequencing. When more than one sample had to be barcoded and run together in the same flowcell, pairs of native barcodes from the EXP-NBD196 kit were used and the library preparation protocol followed was the “Native barcoding genomic DNA (with EXP-NBD104, EXP-NBD114, and SQK-LSK109; NBE_9065_v109_revAH_14Aug2019)”. During the sequencing run when the translocation speed fell below the accepted range, 200 µl of “Flush Buffer” was added to the flowcell. The high quality basecalling (HAC) was done with “Guppy v5” and the sequenced reads used were the ones with average basecalling quality above 9.

Data Analysis

All data analysis was done on Compute Canada servers. Software and packages used for analyses are freely available with open licenses. Detailed codes for individual analysis steps can be provided upon request.

FASTQ demultiplexing of short reads

The raw fastqs from MGI runs were demultiplexed by fastq-multx (https://github.com/brwnj/fastq-multx) and also fgbio/DemuxFastqs (http://fulcrumgenomics.github.io/fgbio/tools/latest/DemuxFastqs.html). In both cases we used a mismatch of 1.

3’ transcriptomic capture read alignment

Initial alignment of transcriptomic data from 3’ captures, combined with the gene expression information from the multiome captures were performed using CellRanger 6.1.1. Human genome reference GRCh38 downloadable from 10x genomics website (refdata-gex-GRCh38-2020-A) was used for mapping. Cell calling algorithms integrated in the software package were used for the data provided here, with the expected value included as per each capture; i.e. aimed nuclei counts at the loading step (refer to stats in supplementary information table 1).

Multiome capture read alignment

CellRanger-arc V2.0.0 was used for single cell multiome capture alignments and mapping to human genome reference (GRCh38). Based on preliminary quality checks, minimum genes and minimum ATAC reads per nuclei were set to 550 and 1000 respectively. Furthermore, nuclei

with features counts larger than 12k and cut sites more than 100k were also excluded from the current initial reports.

Data from 2 captures (one male subject), were aggregated using CellRanger-arc aggregate function for the downstream analyses included in this manuscript.

Long read alignment

Minimap2 (Li, 2018) was used for alignment of long reads to human reference genome (GRCh38).

Gene expression analyses

After alignment and cell calling by CellRanger, detected "cells" were aggregated using Seurat package in R (Hao et al., 2021; Stuart et al., 2019) for initial quality check and parameter verification (Supplementary figure 3). Based on these analyses, only barcodes with features counts between 550 and 4000 and total RNA counts between 1000 and 12000 were used for downstream analyses. As mitochondrial genes are not expected in nuclei captures, in order to remove their contribution to dimensionality reduction algorithms and clustering, all mitochondrial genes were also removed.

Dimensionality reduction, clustering, marker definition and visualization were all performed in R, using Seurat package. All normalized capture experiments were aggregated using find anchors and integrate functions. Whole DRG nuclei passed through principle component analysis (PCA) dimensionality reduction down to 30 PCs. T-distributed stochastic neighbor embedding (t-SNE) and uniform manifold approximation and projection (UMAP) using multiple

k-means were used and the markers of each clustering iteration were manually reviewed before a 10 biologically relevant crude clustering was chosen for further analyses (Figure 1). Cluster nomenclature and top marker genes were also manually selected based on the top list of significantly enriched genes in each cluster.

Neurons sub-analyses were performed on a subsetted data set of nuclei. Data was scaled, centered and verified for proper integration before PCA dimensionality reduction to 20. Initial clustering and analyses reported in this manuscript are performed with no further manual reclustering or parameter optimization. Three of the 14 suggested clusters were named based on their known markers as a demonstration of feasibility.

ATAC analyses

Initial analyses included in the current manuscript, including filtering, clustering, and feature statistics, were performed by Loupe Browser 6.0.0. Manual marker and cluster detections based on gene expression and chromatin accessibility were performed to detect biological relevant categories.

CellRanger-arc reanalyze function was used for sub-clustering of the neuronal population. As the sample sizes were limited, the downstream analyses are only shown in the supplementary figure 8 as a proof of feasibility.

Long-read analyses

Because of their premature nature, no analysis of long read sequencing is included in the current version of the report.

References

10xGenomics (2019). Chromium' ' Next GEM Single Cell 3 ’ Reagent Kits v3.1 . Rev D.

10xGenomics (2021a). Nuclei Isolation from Complex Tissues for' ' Single Cell Multiome ATAC + Gene Expression Sequencing.

10xGenomics (2021b). Chromium Next GEM Single Cell Multiome ATAC + Gene Expression. CG000338.

Abraham, N.G., and Drummond, G. (2006). CD163-Mediated hemoglobin-heme uptake activates macrophage HO-1, providing an antiinflammatory function. Circ. Res. 99, 911–914.

Buenrostro, J.D., Giresi, P.G., Zaba, L.C., Chang, H.Y., and Greenleaf, W.J. (2013). Transposition of native chromatin for fast and sensitive epigenomic profiling of open chromatin, DNA-binding proteins and nucleosome position. Nat. Methods 10, 1213–1218.

Carr, P.A., and Nagy, J.I. (1993). Emerging relationships between cytochemical properties and sensory modality transmission in primary sensory neurons. Brain Res. Bull. 30, 209–219.

Chakraborty, R., Saddouk, F.Z., Carrao, A.C., Krause, D.S., Greif, D.M., and Martin, K.A. (2019). Promoters to study vascular smooth muscle. Arterioscler. Thromb. Vasc. Biol. 39, 603–612.

Cobos, E.J., Nickerson, C.A., Gao, F., Chandran, V., Bravo-Caparrós, I., González-Cano, R., Riva, P., Andrews, N.A., Latremoliere, A., Seehus, C.R., et al. (2018). Mechanistic Differences in Neuropathic Pain Modalities Revealed by Correlating Behavior with Global Expression Profiling. Cell Rep. 22, 1301–1312.

Dadwal, N., Mix, C., Reinhold, A., Witte, A., Freund, C., Schraven, B., and Kliche, S. (2021). The Multiple Roles of the Cytosolic Adapter Proteins ADAP, SKAP1 and SKAP2 for TCR/CD3 - Mediated Signaling Events. Front. Immunol. 12, 703534.

Devor, M. (1999). Unexplained peculiarities of the dorsal root ganglion. Pain Suppl 6, S27–S35.

Drokhlyansky, E., Smillie, C.S., Van Wittenberghe, N., Ericsson, M., Griffin, G.K., Eraslan, G., Dionne, D., Cuoco, M.S., Goder-Reiser, M.N., Sharova, T., et al. (2020). The Human and Mouse Enteric Nervous System at Single-Cell Resolution. Cell 182, 1606–1622.e23.

Dymecki, S.M., Niederhuber, J.E., and Desiderio, S.V. (1990). Specific expression of a tyrosine kinase gene, blk, in B lymphoid cells. Science 247, 332–336.

Eraslan, G., Simon, L.M., Mircea, M., Mueller, N.S., and Theis, F.J. (2019). Single-cell RNA-seq denoising using a deep count autoencoder. Nat. Commun. 10, 390.

Esposito, M.F., Malayil, R., Hanes, M., and Deer, T. (2019). Unique characteristics of the dorsal root ganglion as a target for neuromodulation. Pain Med. 20, S23–S30.

Feldman-Goriachnik, R., and Hanani, M. (2021). How do neurons in sensory ganglia communicate with satellite glial cells? Brain Res. 1760, 147384.

Foerster, O. (1933). The dermatomes in man. Brain 56, 1–39.

Franzén, O., Gan, L.-M., and Björkegren, J.L.M. (2019). PanglaoDB: a web server for exploration of mouse and human single-cell RNA sequencing data. Database (Oxford) 2019.

Fukada, S., Uezumi, A., Ikemoto, M., Masuda, S., Segawa, M., Tanimura, N., Yamamoto, H., Miyagoe-Suzuki, Y., and Takeda, S. (2007). Molecular signature of quiescent satellite cells in adult skeletal muscle. Stem Cells 25, 2448–2459.

Gatto, G., Smith, K.M., Ross, S.E., and Goulding, M. (2019). Neuronal diversity in the somatosensory system: bridging the gap between cell type and function. Curr. Opin. Neurobiol. 56, 167–174.

Gregus, A.M., Levine, I.S., Eddinger, K.A., Yaksh, T.L., and Buczynski, M.W. (2021). Sex differences in neuroimmune and glial mechanisms of pain. Pain 162, 2186–2200.

Haberberger, R.V., Barry, C., Dominguez, N., and Matusica, D. (2019). Human dorsal root ganglia. Front. Cell Neurosci. 13, 271.

Hanani, M. (2005). Satellite glial cells in sensory ganglia: from form to function. Brain Res Brain Res Rev 48, 457–476.

Hanani, M., and Spray, D.C. (2020). Emerging importance of satellite glia in nervous system function and dysfunction. Nat. Rev. Neurosci. 21, 485–498.

Hao, Y., Hao, S., Andersen-Nissen, E., Mauck, W.M., Zheng, S., Butler, A., Lee, M.J., Wilk, A.J., Darby, C., Zager, M., et al. (2021). Integrated analysis of multimodal single-cell data. Cell 184, 3573–3587.e29.

Hu, E., Liang, P., and Spiegelman, B.M. (1996). AdipoQ is a novel adipose-specific gene dysregulated in obesity. J. Biol. Chem. 271, 10697–10703.

Illa, I., Leon-Monzon, M., and Dalakas, M.C. (1992). Regenerating and denervated human muscle fibers and satellite cells express neural cell adhesion molecule recognized by monoclonal antibodies to natural killer cells. Ann. Neurol. 31, 46–52.

Iwai, H., Ataka, K., Suzuki, H., Dhar, A., Kuramoto, E., Yamanaka, A., and Goto, T. (2021). Tissue-resident M2 macrophages directly contact primary sensory neurons in the sensory ganglia after nerve injury. J. Neuroinflammation 18, 227.

Jessen, K.R., and Mirsky, R. (2019). Schwann cell precursors; multipotent glial cells in embryonic nerves. Front. Mol. Neurosci. 12, 69.

Komohara, Y., Hirahara, J., Horikawa, T., Kawamura, K., Kiyota, E., Sakashita, N., Araki, N., and Takeya, M. (2006). AM-3K, an anti-macrophage antibody, recognizes CD163, a molecule associated with an anti-inflammatory macrophage phenotype. J. Histochem. Cytochem. 54, 763–771.

Kupari, J., Usoskin, D., Parisien, M., Lou, D., Hu, Y., Fatt, M., Lönnerberg, P., Spångberg, M., Eriksson, B., Barkas, N., et al. (2021). Single cell transcriptomics of primate sensory neurons identifies cell types associated with chronic pain. Nat. Commun. 12, 1510.

Lacy, S.E., Bönnemann, C.G., Buzney, E.A., and Kunkel, L.M. (1999). Identification of FLRT1, FLRT2, and FLRT3: a novel family of transmembrane leucine-rich repeat proteins. Genomics 62, 417–426.

Lähnemann, D., Köster, J., Szczurek, E., McCarthy, D.J., Hicks, S.C., Robinson, M.D., Vallejos, C.A., Campbell, K.R., Beerenwinkel, N., Mahfouz, A., et al. (2020). Eleven grand challenges in single-cell data science. Genome Biol. 21, 31.

Lau, S.-F., Cao, H., Fu, A.K.Y., and Ip, N.Y. (2020). Single-nucleus transcriptome analysis reveals dysregulation of angiogenic endothelial cells and neuroprotective glia in Alzheimer's disease. Proc. Natl. Acad. Sci. USA 117, 25800–25809.

Lee, M.K., Tuttle, J.B., Rebhun, L.I., Cleveland, D.W., and Frankfurter, A. (1990). The expression and posttranslational modification of a neuron-specific beta-tubulin isotype during chick embryogenesis. Cell Motil. Cytoskeleton 17, 118–132.

Lee, M.W.L., McPhee, R.W., and Stringer, M.D. (2008). An evidence-based approach to human dermatomes. Clin Anat 21, 363–373.

Levina, I.S., Kuznetsov, Y.V., Shchelkunova, T.A., and Zavarzin, I.V. (2021). Selective ligands of membrane progesterone receptors as a key to studying their biological functions in vitro and in vivo. J. Steroid Biochem. Mol. Biol. 207, 105827.

Li, H. (2018). Minimap2: pairwise alignment for nucleotide sequences. Bioinformatics 34, 3094–3100.

Liu, N.-J., von Gizycki, H., and Gintzler, A.R. (2007). Sexually dimorphic recruitment of spinal opioid analgesic pathways by the spinal application of morphine. J. Pharmacol. Exp. Ther. 322, 654–660.

De Logu, F., Marini, M., Landini, L., Souza Monteiro de Araujo, D., Bartalucci, N., Trevisan, G., Bruno, G., Marangoni, M., Schmidt, B.L., Bunnett, N.W., et al. (2021). Peripheral Nerve Resident Macrophages and Schwann Cells Mediate Cancer-Induced Pain. Cancer Res. 81, 3387–3401.

Lomas, L.M., Barrett, A.C., Terner, J.M., Lysle, D.T., and Picker, M.J. (2007). Sex differences in the potency of kappa opioids and mixed-action opioids administered systemically and at the site of inflammation against capsaicin-induced hyperalgesia in rats. Psychopharmacology 191, 273–285.

Marie-Cardine, A., Bruyns, E., Eckerskorn, C., Kirchgessner, H., Meuer, S.C., and Schraven, B. (1997). Molecular cloning of SKAP55, a novel protein that associates with the protein tyrosine kinase p59fyn in human T-lymphocytes. J. Biol. Chem. 272, 16077–16080.

Matsuda, S., Kobayashi, N., Terashita, T., Shimokawa, T., Shigemoto, K., Mominoki, K., Wakisaka, H., Saito, S., Miyawaki, K., Saito, K., et al. (2005). Phylogenetic investigation of Dogiel's pericellular nests and Cajal's initial glomeruli in the dorsal root ganglion. J. Comp. Neurol. 491, 234–245.

Matsuoka, R., Yoshida, M.C., Furutani, Y., Imamura, S., Kanda, N., Yanagisawa, M., Masaki, T., and Takao, A. (1993). Human smooth muscle myosin heavy chain gene mapped to chromosomal region 16q12. Am. J. Med. Genet. 46, 61–67.

Midavaine, É., Côté, J., Marchand, S., and Sarret, P. (2021). Glial and neuroimmune cell choreography in sexually dimorphic pain signaling. Neurosci. Biobehav. Rev. 125, 168–192.

Milev, P., Friedlander, D.R., Sakurai, T., Karthikeyan, L., Flad, M., Margolis, R.K., Grumet, M., and Margolis, R.U. (1994). Interactions of the chondroitin sulfate proteoglycan phosphacan, the extracellular domain of a receptor-type protein tyrosine phosphatase, with neurons, glia, and neural cell adhesion molecules. J. Cell Biol. 127, 1703–1715.

Nascimento, A.I., Mar, F.M., and Sousa, M.M. (2018). The intriguing nature of dorsal root ganglion neurons: Linking structure with polarity and function. Prog. Neurobiol. 168, 86–103.

Nguyen, M.Q., Le Pichon, C.E., and Ryba, N. (2019). Stereotyped transcriptomic transformation of somatosensory neurons in response to injury. Elife 8.

Nguyen, M.Q., von Buchholtz, L.J., Reker, A.N., Ryba, N.J., and Davidson, S. (2021). Single-nucleus transcriptomic analysis of human dorsal root ganglion neurons. Elife 10.

Oyler, G.A., Higgins, G.A., Hart, R.A., Battenberg, E., Billingsley, M., Bloom, F.E., and Wilson, M.C. (1989). The identification of a novel synaptosomal-associated protein, SNAP-25, differentially expressed by neuronal subpopulations. J. Cell Biol. 109, 3039–3052.

Pannese, E. (1964). Number and structure of perisomatic satellite cells of spinal ganglia under normal conditions or during axon regeneration and neuronal hypertrophy. Z. Zellforsch. Mikrosk. Anat. 63, 568–592.

Pannese, E., Ledda, M., Cherkas, P.S., Huang, T.Y., and Hanani, M. (2003). Satellite cell reactions to axon injury of sensory ganglion neurons: increase in number of gap junctions and formation of bridges connecting previously separate perineuronal sheaths. Anat. Embryol. (Berl.) 206, 337–347.

Le Pichon, C.E., and Chesler, A.T. (2014). The functional and anatomical dissection of somatosensory subpopulations using mouse genetics. Front. Neuroanat. 8, 21.

Satpathy, A.T., Granja, J.M., Yost, K.E., Qi, Y., Meschi, F., McDermott, G.P., Olsen, B.N., Mumbach, M.R., Pierce, S.E., Corces, M.R., et al. (2019). Massively parallel single-cell chromatin landscapes of human immune cell development and intratumoral T cell exhaustion. Nat. Biotechnol. 37, 925–936.

Shin, J.E., Ha, H., Kim, Y.K., Cho, Y., and DiAntonio, A. (2019). DLK regulates a distinctive transcriptional regeneration program after peripheral nerve injury. Neurobiol. Dis. 127, 178–192.

Sinha, S., Satpathy, A.T., Zhou, W., Ji, H., Stratton, J.A., Jaffer, A., Bahlis, N., Morrissy, S., and Biernaskie, J.A. (2021). Profiling Chromatin Accessibility at Single-cell Resolution. Genomics Proteomics Bioinformatics 19, 172–190.

Snyder, S.E., Li, J., Schauwecker, P.E., McNeill, T.H., and Salton, S.R. (1996). Comparison of RPTP zeta/beta, phosphacan, and trkB mRNA expression in the developing and adult rat nervous system and induction of RPTP zeta/beta and phosphacan mRNA following brain injury. Brain Res. Mol. Brain Res. 40, 79–96.

Stuart, T., Butler, A., Hoffman, P., Hafemeister, C., Papalexi, E., Mauck, W.M., Hao, Y., Stoeckius, M., Smibert, P., and Satija, R. (2019). Comprehensive Integration of Single-Cell Data. Cell 177, 1888–1902.e21.

Su, Y., Brooks, D.G., Li, L., Lepercq, J., Trofatter, J.A., Ravetch, J.V., and Lebo, R.V. (1993). Myelin protein zero gene mutated in Charcot-Marie-tooth type 1B patients. Proc. Natl. Acad. Sci. USA 90, 10856–10860.

Tang, B.L. (2021). SNAREs and developmental disorders. J. Cell Physiol. 236, 2482–2504.

Todd, A.J., and Koerber, H.R. (2006). Neuroanatomical substrates of spinal nociception. In Wall and melzack's textbook of pain, (Elsevier), pp. 73–90.

Usoskin, D., Furlan, A., Islam, S., Abdo, H., Lönnerberg, P., Lou, D., Hjerling-Leffler, J., Haeggström, J., Kharchenko, O., Kharchenko, P.V., et al. (2015). Unbiased classification of sensory neuron types by large-scale single-cell RNA sequencing. Nat. Neurosci. 18, 145–153.

Valtcheva, M.V., Copits, B.A., Davidson, S., Sheahan, T.D., Pullen, M.Y., McCall, J.G., Dikranian, K., and Gereau, R.W. (2016). Surgical extraction of human dorsal root ganglia from organ donors and preparation of primary sensory neuron cultures. Nat. Protoc. 11, 1877–1888.

Wangzhou, A., McIlvried, L.A., Paige, C., Barragan-Iglesias, P., Shiers, S., Ahmad, A., Guzman, C.A., Dussor, G., Ray, P.R., Gereau, R.W., et al. (2020). Pharmacological target-focused transcriptomic analysis of native vs cultured human and mouse dorsal root ganglia. Pain 161, 1497–1517.

Warwick, R.A., and Hanani, M. (2013). The contribution of satellite glial cells to chemotherapy-induced neuropathic pain. Eur. J. Pain 17, 571–580.

Yu, X., Liu, H., Hamel, K.A., Morvan, M.G., Yu, S., Leff, J., Guan, Z., Braz, J.M., and Basbaum, A.I. (2020). Dorsal root ganglion macrophages contribute to both the initiation and persistence of neuropathic pain. Nat. Commun. 11, 264.

Zhang, H., Li, Y., de Carvalho-Barbosa, M., Kavelaars, A., Heijnen, C.J., Albrecht, P.J., and Dougherty, P.M. (2016). Dorsal Root Ganglion Infiltration by Macrophages Contributes to Paclitaxel Chemotherapy-Induced Peripheral Neuropathy. J. Pain 17, 775–786.

Supplemental Information

QC results

Pre-capture quality controls

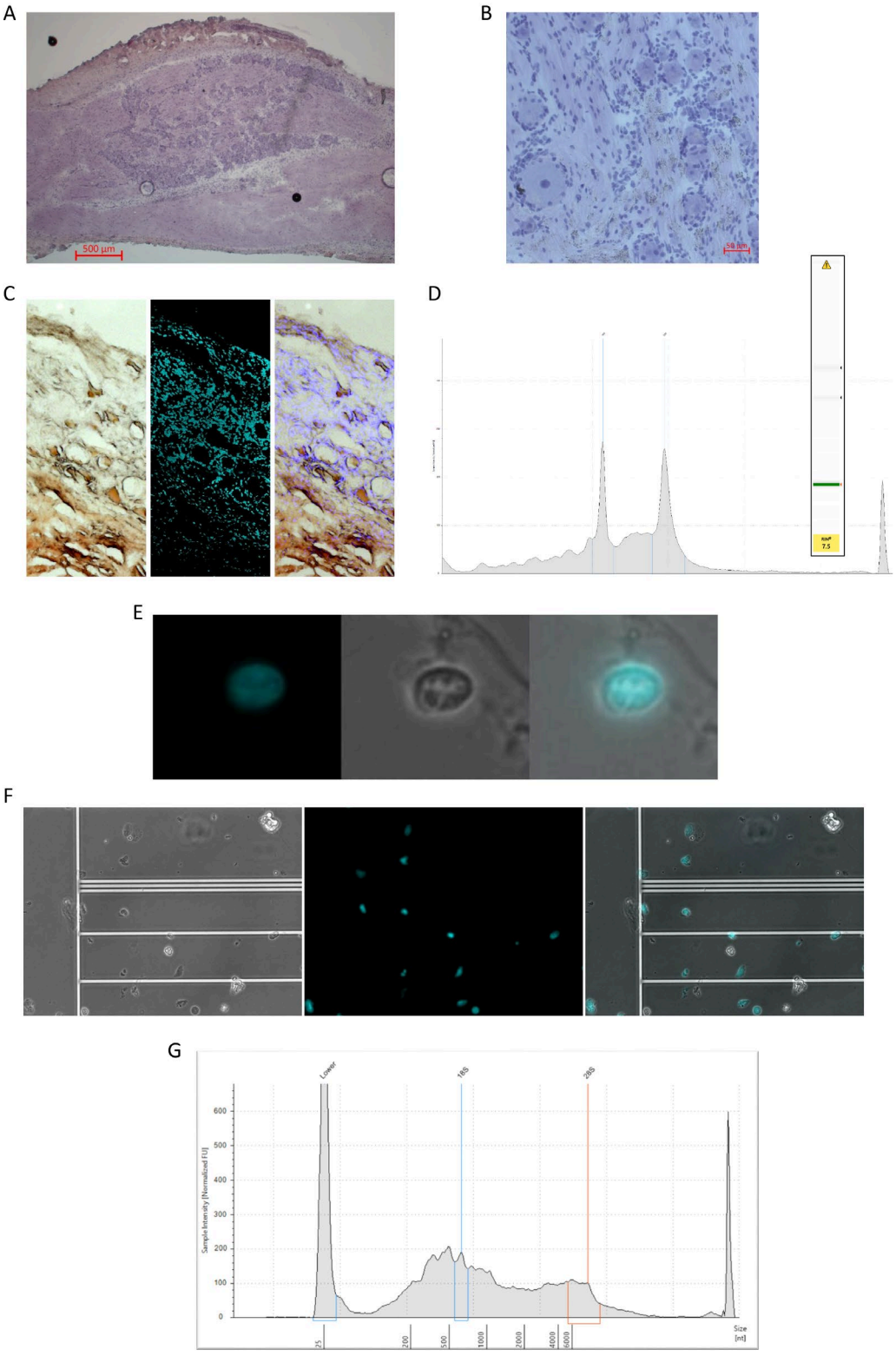

Supplementary figure 1- Quality control steps required before single-nucleus capture and barcoding of genetic material from DRGs.

A) Freshly harvested and prepared dorsal root ganglia from a non-human primate (Macaca) used as a control for morphological quality check.

B) Higher magnification of 20 µm-thick section of non-human primate DRG showing the close surrounding of satellite glial cells around the neurons. Note in A and B the abundance of non-neuronal nuclei in comparison to the total number of neurons.

C) Post-mortem human DRG section stained with Hoechst for nuclei.

D) Sample electropherogram of a good quality whole tissue RNA sample with RNA integrity number (RIN) 7.5. Note clear 18S and 28S peaks.

E) Example of single high quality nucleus stained with DRAQ-5 prior to microfluidic capture. Note round and defined membrane indicating the absence of over-permeabilization.

F) Example of nuclear suspension used for counting the total number of nuclei per µL (required for accurate calculation of loading material).

G) Whole nuclei RNA electropherogram indicating a wide range of RNA molecule sizes present in the purified nuclear samples.

Post-capture quality controls

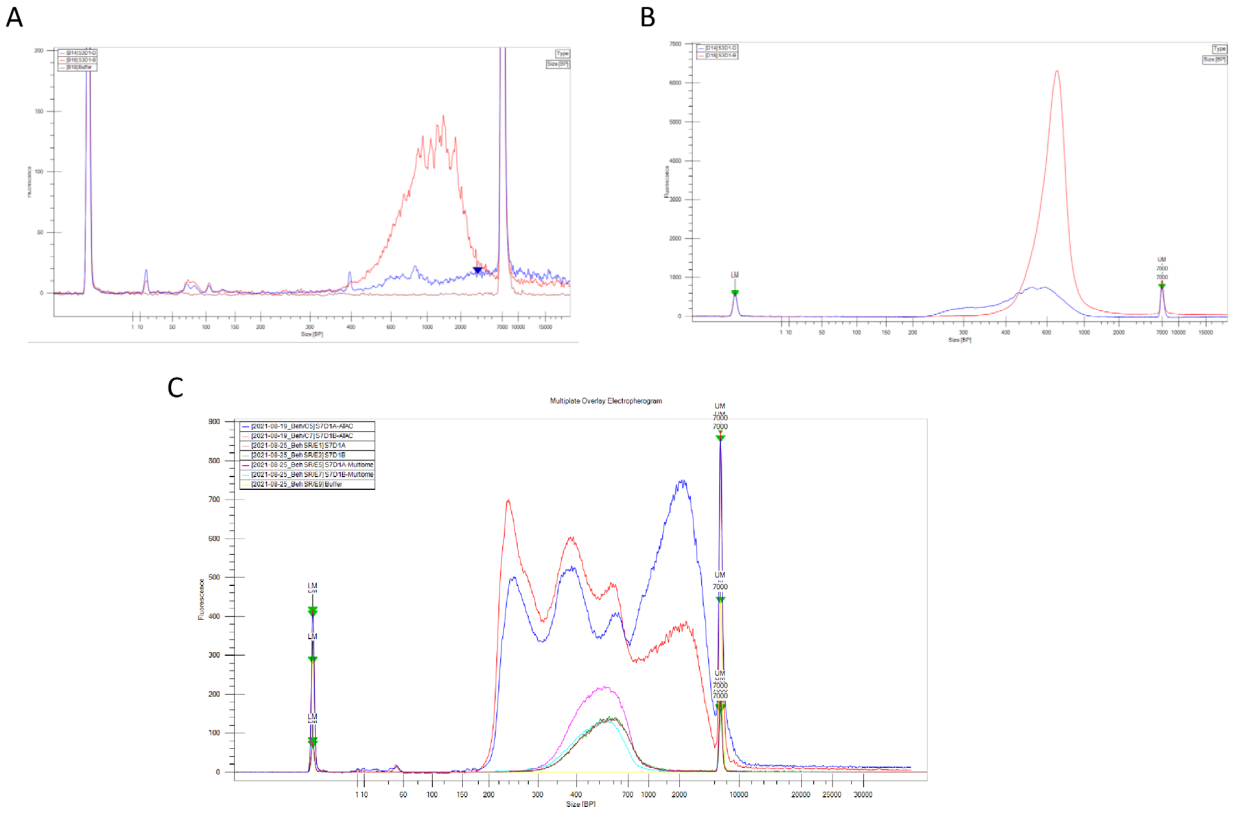

Supplementary figure 2- Genomic content captured from single-nucleus RNA and multiome experiments were quality controlled before proceeding to sequencing.

A) Sample trace from two full length cDNA libraries generated from in-GEM reverse transcription after PCR amplification. Only libraries with the expected size profiles were passed on to sequencing library generation steps.

B) Sample sequencing ready library electropherograms. Ready for sequencing short read libraries were made by fragmentation and Illumina adaptor ligation. Size distribution and yield of the libraries were measured before submission for sequencing.

C) Multiome captures (3' gene expression and ATAC) sequencing ready libraries electropherogram showing acceptable quality of samples for sequencing.

Post-alignment quality controls

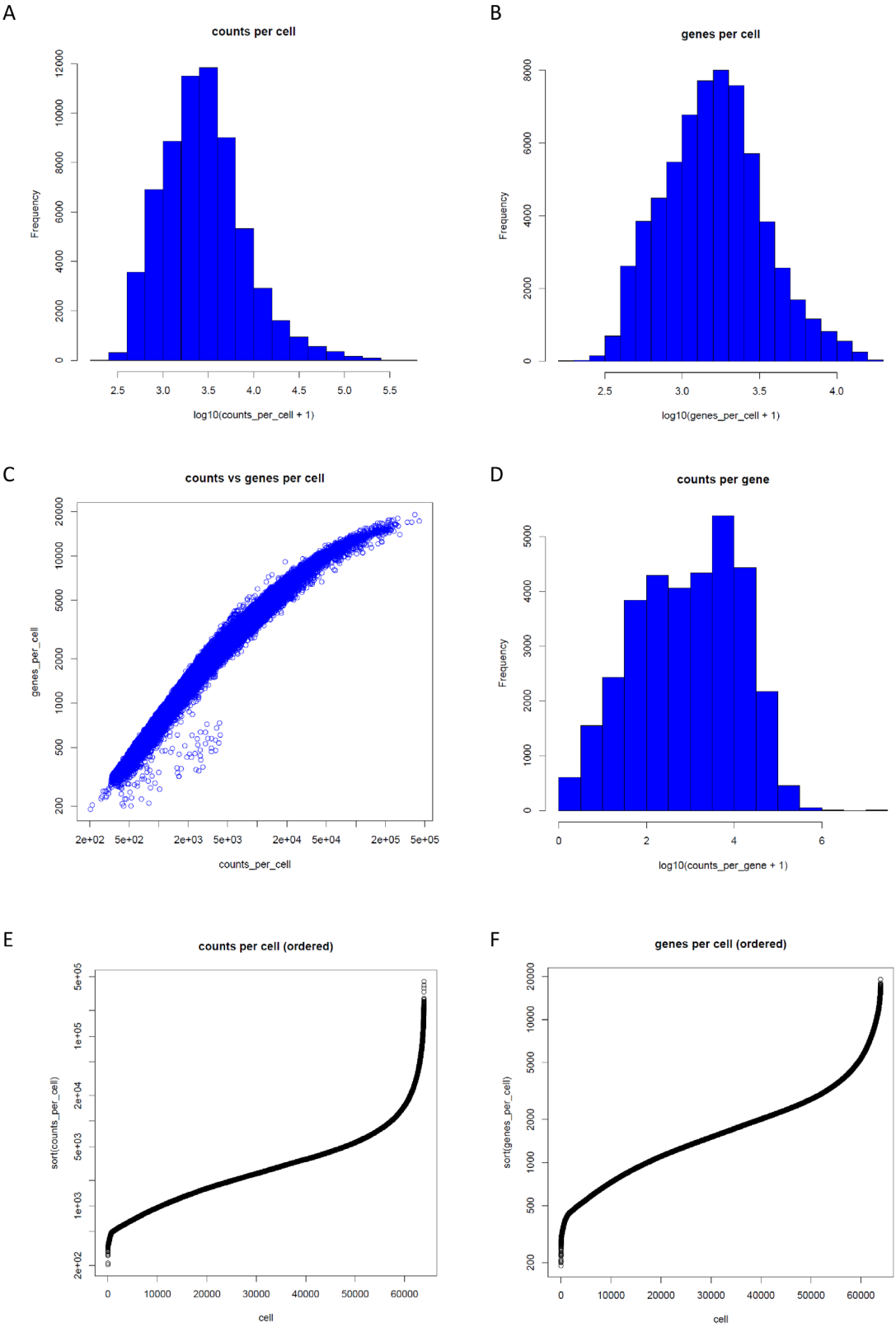

Supplementary figure 3- Quality control and general assessment of all ~64k single-nucleus 3' transcriptome captures.

A) Histogram showing the distribution of RNA counts (UMIs) in all 63931 nuclei captured through 8 different experiments that were cell called.

B) Distribution of count of unique genes (features) in each nucleus in the raw integrated dataset.

C) Correlation between the number of genes (features) and number of RNAs (UMI count) per nucleus.

D) Distribution of total RNAs belonging to similar genes in the combine population of nuclei.

E) Prevalence of nuclei based on RNA counts per nucleus sorted from the least to the most. Nuclei with RNA counts less than 1000 were excluded from downstream analyses.

F) Prevalence of nuclei based on gene count per nucleus sorted from the least to the most. Nuclei with feature counts of more than 4000 were excluded from downstream analyses.

Integration quality control

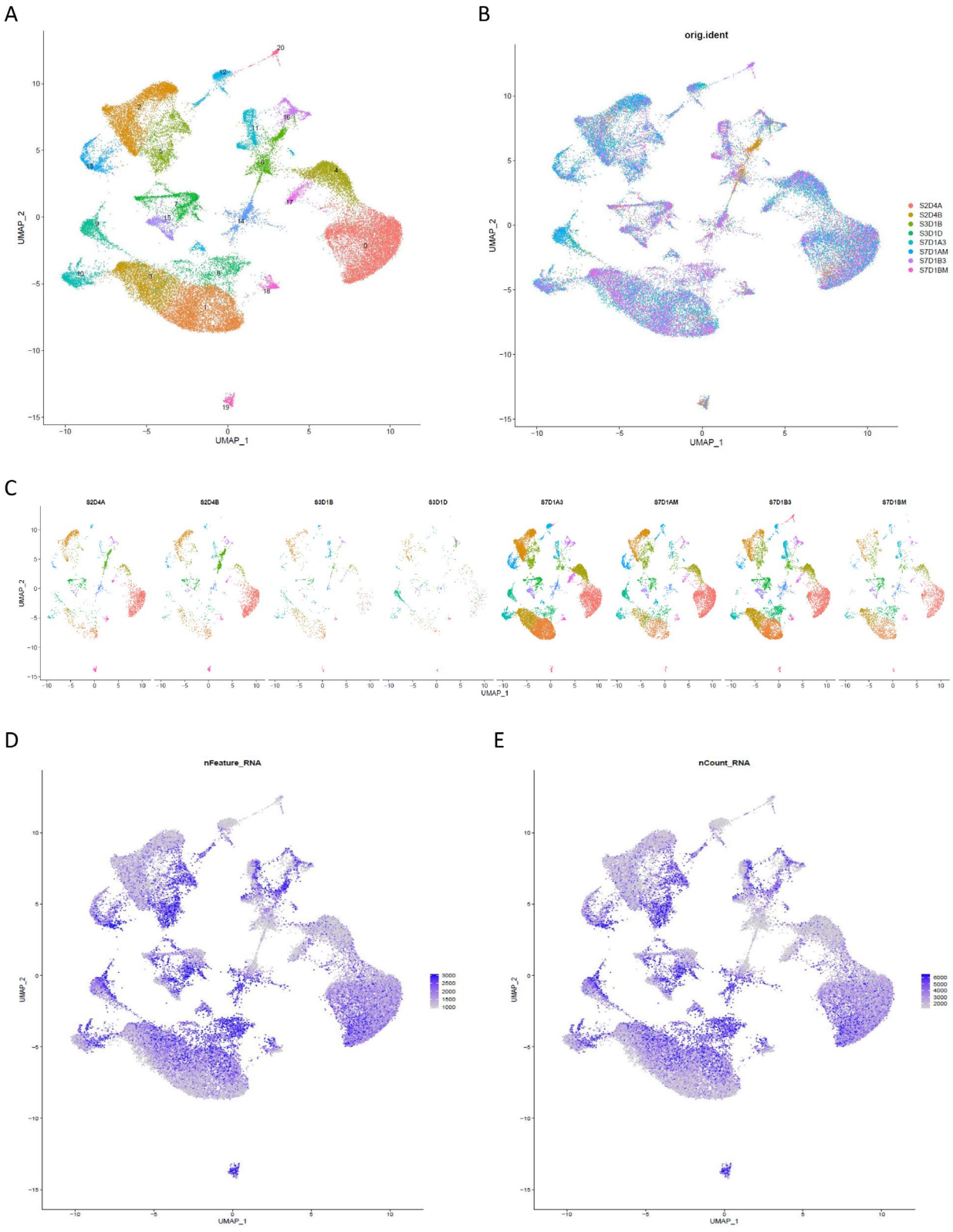

Supplementary figure 4- Batch effect correction verification for integrated data.

A) Initial automatic clustering performed on integrated data from 8 separate capture experiments resulted in suggestion of 21 clusters. In order to verify proper removal of batch effects (experiment-specific biases introduced as clustering criteria) this initial clustering is demonstrated. Some of these clusters were combined together based on their marker gene expressions in order to group the nuclei into the 10 biologically relevant clusters presented in Figure 1.

B) UMAP projection of the integrated dataset drawn with color depicting capture experiments.

C) Similar data as shown in B with each experiment visualized separately. Although the number of captured nuclei are different from each experiment, all experiments contribute to all clusters.

D) Feature plot showing the distribution of nuclei with high number of unique genes (features) detected on the same UMAP as previous panels. Although nuclei have diverse amounts of features, clusters are not formed solely based on feature counts.

E) Feature plot showing the total number of unique RNA (UMI counts) overlapped on the similar UMAP as previous panel. Similar to D, RNA counts per cells are diverse, yet original clusters are not formed by a significant bias of this measure.

Experiments summary

Capture	Type	Subject	Sex	Age	Sequencing Depth	Target Nuclei	Detected Nuclei	Analyzed Nuclei
24A-GEX	3’	F-820	F	68	450M	4278	3968	3012
24B-GEX	3’	F-820	F	68	450M	5086	3848	3060
31B-GEX	3’	F-1120	F	78	450M	9940	2359	1025
31D-GEX	3’	F-1120	F	78	200M	9950	2279	781
71A-GEX	3’	M-521	M	35	450M	10101	18010	15501
71B-GEX	3’	M-521	M	35	450M	10010	16414	10982
71Am-GEX	Multiome	M-521	M	35	450M	5600	11664	7864
71Am-ATAC	Multiome	M-521	M	35	900M	5600	9337	7904
71Bm-GEX	Multiome	M-521	M	35	450M	2900	5389	3854
71Bm-ATAC	Multiome	M-521	M	35	900M	2900	2959	2550

Supplementary table 1– Detailed statistics on human DRG capture experiments.

Details of each experiment. Capture: each experiment (column on 10x genomics chip) with data used for this manuscript. Type: 10x Genomics capture experiment type. Subject: de-identified donor codes. Sequencing depth: target sequencing reads. Target Nuclei: originally calculated number of nuclei expected to be captured based on the QC before loading each sample. Detected Nuclei: number of “cells” called by CellRanger or CellRanger-arc algorithms. Analyzed Nuclei: number of nuclei that passed quality control and were included in the clustering experiments.

Whole DRG (all nuclei) supplementary information

Top highly expressed genes in each cluster

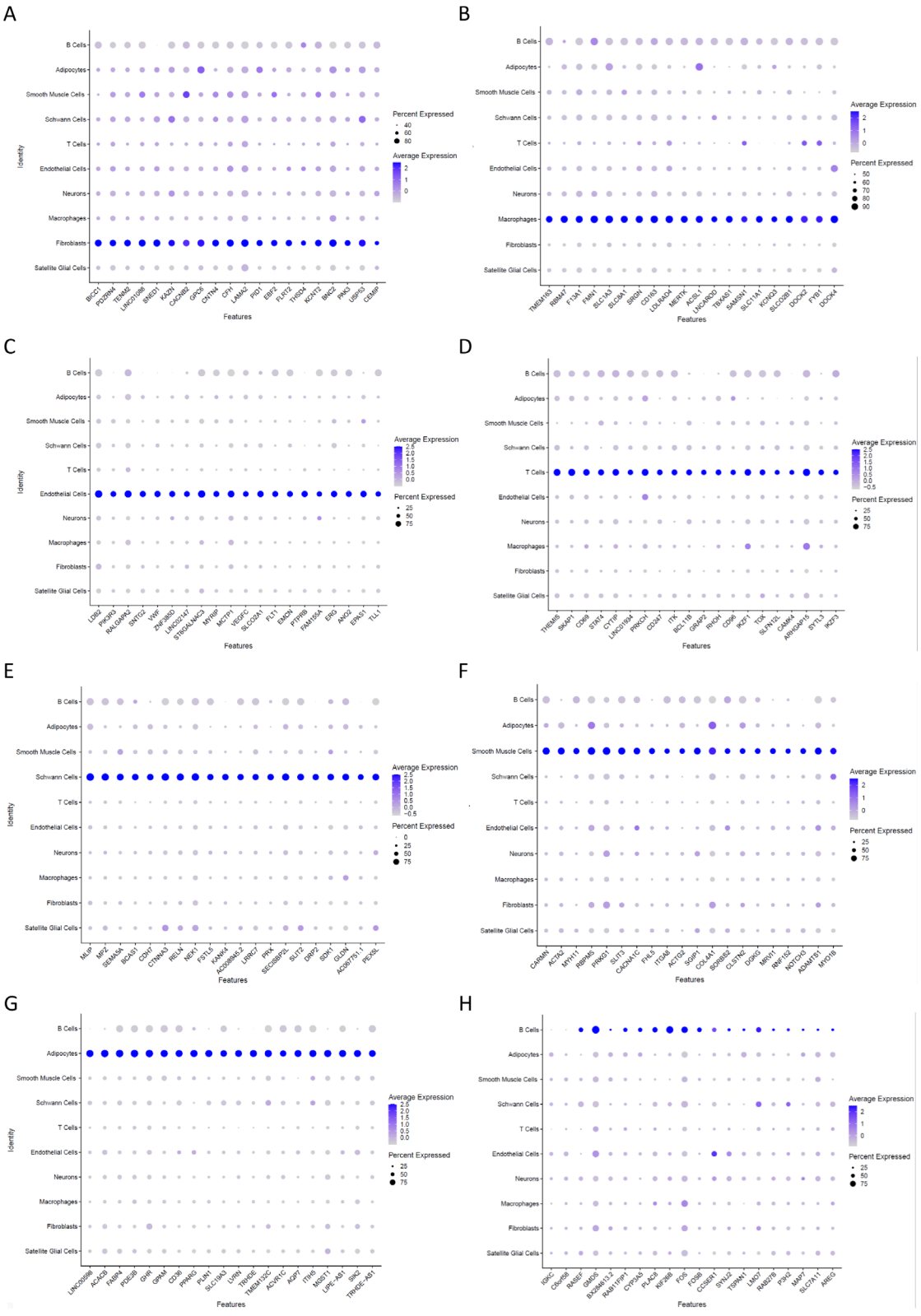

Supplementary figure 5- Differentially expressed genes in different clusters of nuclei from human dorsal root ganglia - related to figure 1.

A to H) Dot plots of top 20 differentially expressed genes from 8 different clusters of nuclei (in addition to the 2 clusters shown in figure 1).

Differentially expressed marker genes examples for each cluster

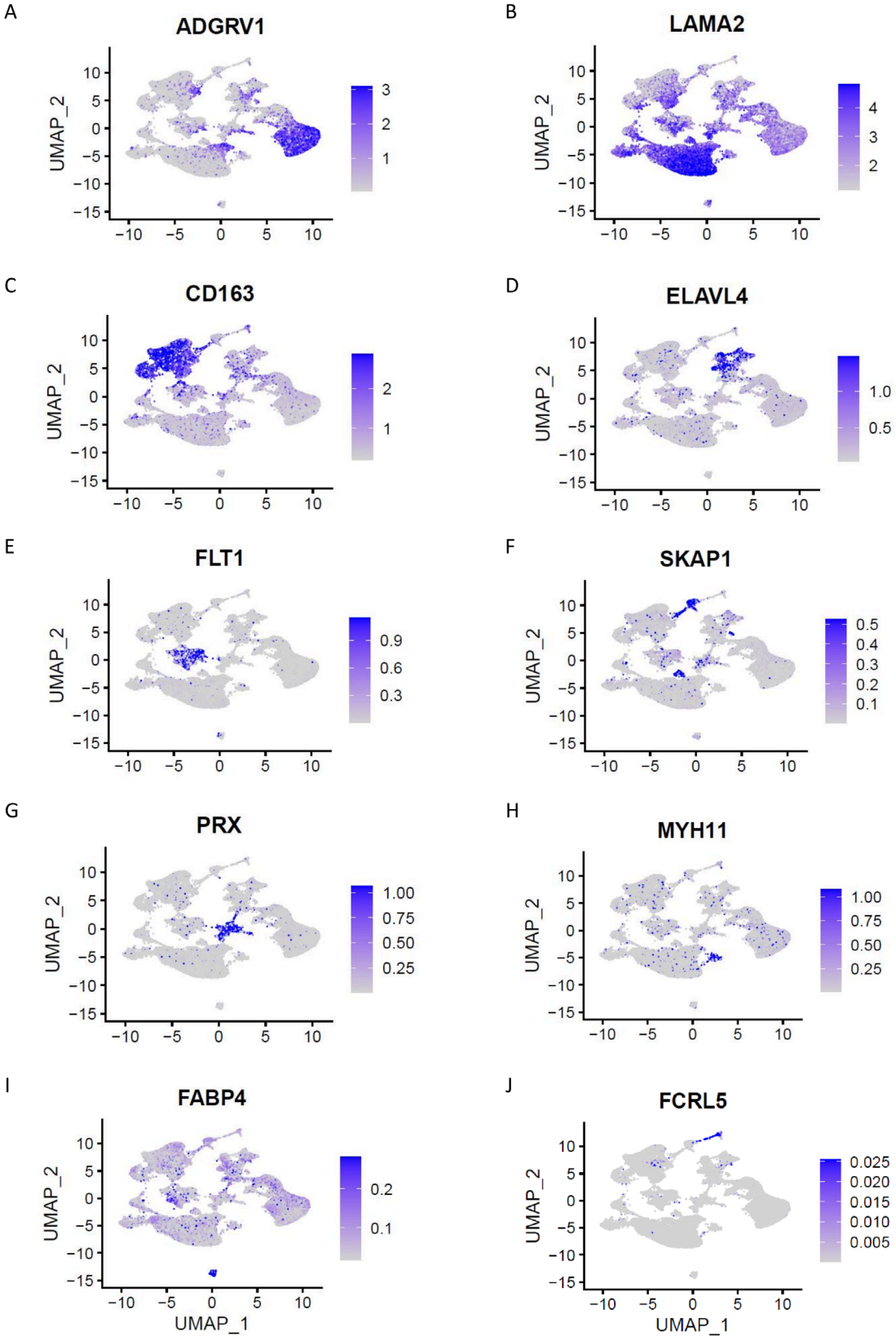

Supplementary figure 6- Distribution of differentially expressed marker genes from each cluster of nuclei from human DRG - related to figure 1.

A to J) Feature plots showing the expression distribution of known marker genes for each of the 10 general clusters of cell type.

Single nucleus multiome captures (RNA plus ATAC)

Open chromatin region linkage

Supplementary figure 7- Open chromatin region link to gene expression – feasibility stage (current sample size too small).

Example of an enriched accessible chromatin region among neuronal nuclei (compared to those of macrophages and T cells) and its negative links detected to genes nearby.

Subclustering using combined GEX and ATAC information

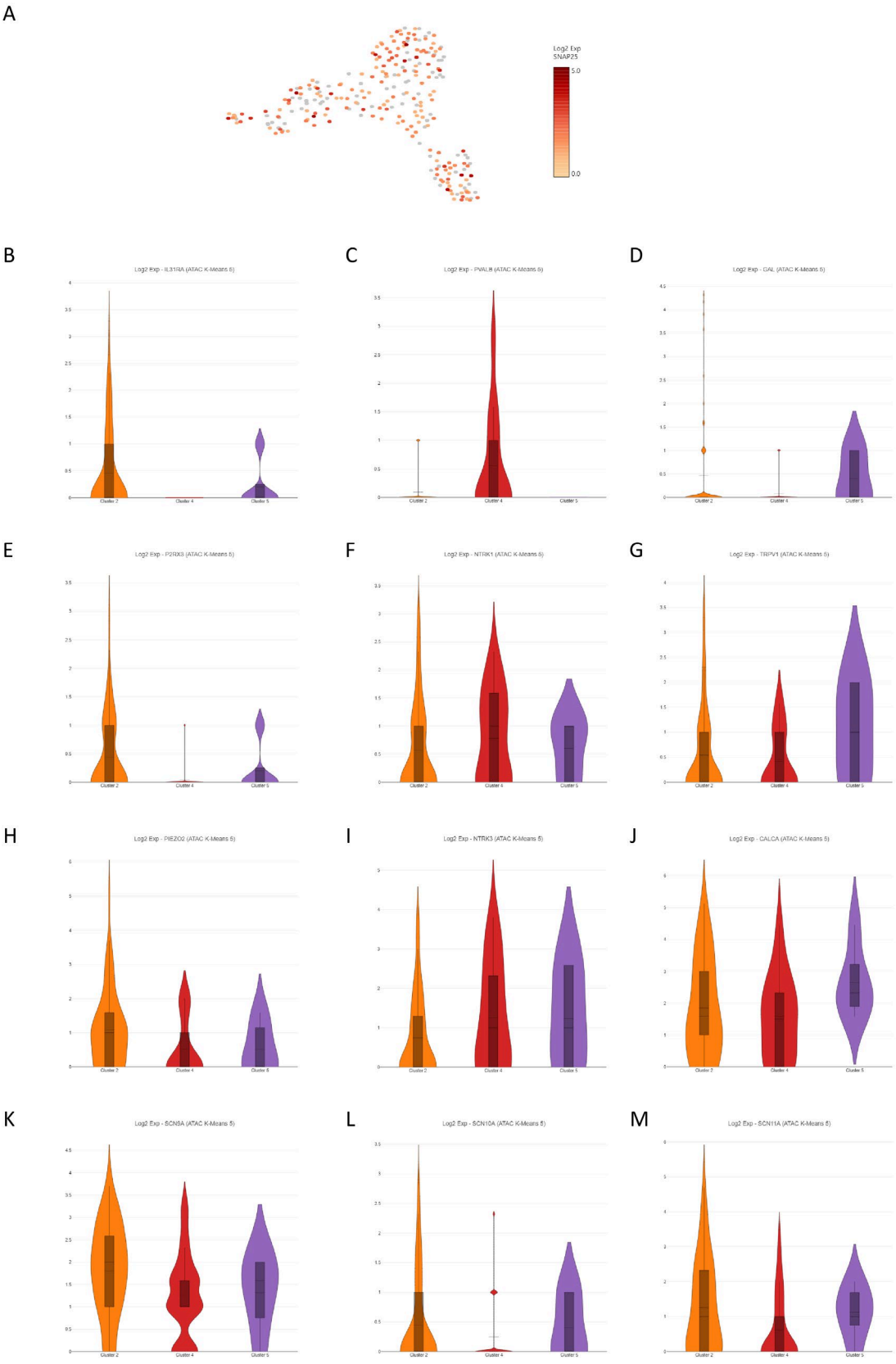

Supplementary figure 8- Combined gene expression and open chromatin information can result in more reliable clustering – feasibility stage (current sample size too small).

A) Expression levels of SNAP25 (a neuronal marker gene) in the 270 neurons detected based on gene expression clustering (Figure 3). Further clustering of these nuclei were performed based on their ATAC profiles (K=5).

B to M) Violin plots of selected biologically relevant gene expressions showing possible subclustering of neuronal nuclei.

Chapter 4:

General Discussion & Conclusion

In this chapter I will broadly discuss the general results (for both Chapters 2 and 3) with regards to arguments provided for the rationale of this dissertation - presented in the general introduction (Chapter 1). I will also introduce some of the limitations in sensory research (including mine), lay down some opinions regarding sensory coding theories (including concepts specific to itch and pain), and discuss some future directions for the field (and in continuation of my projects).

Detailed discussions regarding specific findings and results presented for specific objectives of the thesis are included within each data chapter.

Summary

As mentioned in the introduction, the first objective for this dissertation was set to be a proof of multimodality at the level of primary afferents. In Chapter 2, I showed that the MrgprA3-expressing primary afferents are sufficient for transmitting both pain and itch based on their activation mode. The results in this chapter also showed that these afferents contribute to both of these sensations transduction in naïve conditions, and that for itch signaling, but not pain, TRP channels are recruited by these neurons. While the importance of behavioral assay precisions is emphasized, technical limitations are brought forward as the probable cause of oversight in previous studies.

The second objective for this thesis was the construction of an atlas for documenting cellular heterogeneities in the primary sensory ganglia. To initiate this comprehensive resource, in Chapter 3 of the current dissertation, I provided a detailed report of how we are building a multi-modal database. Thorough quality control and meticulous optimization of methods detailed in this chapter ensure highly reliable data production. Combining transcriptomic and epigenomic information at the single-cell level, this one-of-a-kind resource is providing details about the molecular repertoire of neuronal and non-neuronal cells of human dorsal root ganglia.

Limitations

Sensory research is a unique field of study as the parameter under investigation can only be measured indirectly through secondary outcomes. Whether it be in humans or animal models, sensations are either measured through the subjective lens of the participant or through interpolation of behavioral reflexes. This has imposed limitations on the research, and knowledge derived from such research, that need to be carefully considered. Here I will mention some of these limitations that I believe have had direct impacts on sensory transduction theories. I will also discuss how in the research performed for this thesis I tried to address some of these limitations. Finally, I will describe some of the specific limitations that are required to be considered when interpreting the results presented here.

As mentioned above, sensory research is specifically prone to limitations of measurement tools. Some of these susceptibilities that concern the pain studies related to this work, can stem from low sensitivity (true positive rate) and high specificity (true negative rate) of the assays used for detection and measurement. Animal behavioral assays are generally developed by the following principals: Experimental stimulation (ε) produces signal (σ) which leads to response (ρ). As most of these assays are validated with the aim of investigating effectiveness of intervention/treatment (θ), in order to reduce ambiguity of the readouts, in many instances extreme reflexes ρ and intense stimuli ε are used. This results in highly specific assays. For example, we can claim with high confidence that rats bearing four constrictive stiches around their sciatic nerves (classic chronic constriction injury - CCI) are experiencing neuropathic pain (Gopalsamy et al., 2019; Wang et al., 2021), or that use of radiant heat on paw or tail of mice

until withdrawal is a measurement of pain (Hargreaves et al., 1988). Yet the sensitivity of such models to partial modification by interventions (θ) is low. In the previous examples this would translate into the CCI model of sever neuropathic pain not detecting the therapeutic value of mild treatments challenging the accuracy and clinical translatability of preclinical studies (Mogil, 2009; Sadler et al., 2021). Similarly, due to the high intensity of ε in the Hargreaves thermal assay, ablation of a small subpopulation of primary afferents as an intervention (θ) may be too subtle to reduce the response ρ and lead to declaring this population dispensable for pain (Han et al., 2013; Roberson et al., 2013). In results discussed in chapter 2, we showed that considering these limitations and choosing appropriately tuned assays can unravel effects previously declared absent.

Technical limitations specific to the utilized tools might be another cause for misinterpretations in previous research disputing multimodality. Novel genetic engineering technologies such as optogenetics or chemogenetics, and recombination-based transgenic approaches all have their limitations that need to be considered when experiments are designed and/or interpreted. For instance, the use of optogenetics as a way of activating neurons can give a unique opportunity for controlled action-potential (AP) generation studies which can prove the possibility of response generation. Nevertheless, as AP fidelity to light pulses is not flawless and cells are not necessarily excited in every aspect through optogenetics (e.g. possible differences in calcium responses and firing adaptation), the absence of certain responses post-optogenetic activation of a population cannot be interpreted as absence of involvement of the population for that response. Similarly, this can be true for chemogenetic approaches when metabotropic excitation of a population is just not sufficient for generation of some behavioral response

despite significantly contributing in facilitation or sensitization. To address such limitations, in our work described in Chapter 2 we took a wholesome approach that included specific controlled experiments for proofs of concept, combined with more general experiments for validation. For example, when controlled and specific activation of MrgprA3-expressing fibers in the cheek resulted in nociceptive behavior response, to rule out “unnatural” optogenetic excitation causing unusual paresthetic sensations, we followed the study by analgesic intervention in the hindpaw. Similarly, the chemogenetic activation of these fibers in cheek showed the possibility of pruriceptive behavior induction and we still followed this expected result with antipruriceptive interventions on the nape of the neck. In this approach, limitations of one technique or experiment are complemented by another orthogonal experiment pointing to similar results.

A similar mitigation approach ensuring complementary validation of experimental results can be taken in single-nucleus sequencing studies. In studies performed for Chapter 3, as capture efficiency of droplet-based single-cell techniques are not perfect and the complexity of libraries from such experiments is not on par with the complexities of cells such as neurons, we complemented these data with ATAC sequencing. This can enrich the data and mitigate some of the limitations in RNA representation at the level of individual nuclei. Furthermore, whole-tissue and whole-nuclei sample sequencings performed by long-read nanopore sequencers are also attempts to addressing such limitations.

Notwithstanding, the presented work still contain limitations that need to be considered when interpreting and more specifically generalizing the results. Although presented as examples with the expectation of generalizability, it is necessary to remember that the data in this

dissertation is limited to the experimental paradigms used: itch and pain were picked as model modalities, and mouse was used as model organism in chapter 2, while human lumbar DRGs was used as model primary sensory ganglia. Generalization of such results to other models should be considered with caution.

Prospects

In this section I will briefly propose some ideas that I believe can open new horizons in somatosensory research. I will introduce some frameworks borrowed from great works published in other fields of neuroscience and sensory biology about signal contents of activated neurons. Then I will discuss some evolutionary perspective on how itch and pain might be different in their transduction strategies and noise handling. I will then comment on how "sensory coding" may not be the best way for theorizing sensations. Finally, I will discuss some ideas about the flexibility and adaptation of the primary afferents and their signaling properties. I believe considering these points can bring novel ideas to the field of somatosensory biology, and pain research in particular.

Information content of neuronal signals and how other properties than firing rates, time of individual spikes may carry information were discussed in chapter 1. In fact, it is common belief now that digital all-or-nothing action potentials and their timing are the only information transferred through neuronal axons. Yet not long ago in the 2000s, there has been studies showing that neurons are capable of simultaneously transmitting analog signals through their axons while transferring action potentials (Alle and Geiger, 2006). The information embedded in subthreshold depolarizations carried through myelinated axons has been shown to modify the signals transmitted to post synaptic neurons by mechanisms such as facilitation of transmitter/modulator release (Shu et al., 2006). As these studies showed transmission of these analog signals hundreds of microns down the axons, in the case of primary somatosensory afferents, it is unlikely that soma-initiated presynaptic depolarizations would reach central axon

terminals but presynaptic axo-axonic connections may provide such facilitations (Ango et al., 2021; Cuello, 1983). Furthermore, it is suggested in the auditory cortex that the analog shape of action potentials can also be transmitted through primary sensory afferents, proposing another possible way to enrich the information content of afferents (Liu et al., 2021).

A key point about how pain and itch are differentially coded in vertebrates, could be found in their evolutionary value for survival. It is important to keep in mind that pain is the signal for damage or potential damage which generally leads to preventive or mitigating behaviors such as withdrawal, guarding, or rest. These behaviors can incur a toll on the organism energetically or in term of safety, so it is critically important that such decisions are not made by mistake. In other words, false positive detection of pain is costly and it is intuitive that the system evolves around lowering type I errors. In population coding schemes, this could be achieved by population voting, where activation of single or few primary afferents would be rejected as noise and only when a large enough population of afferents are activated (or smaller numbers are activated for long enough amount of time). Itch on the other hand, is the signal for irritants and insects that are supposed to be removed by a basic motor behavior, scratching. As this behavior is not as costly, and as the stimuli are generally small and hard to detect, it is intuitive that detection parameters for this sensation would be tuned for reduced type II errors. That is, false positives are more common for itch as paying the cost of falsely scratching an area is preferred to missing the removal of an infection-threatening insect. Hence, single, or relatively sparse, primary afferent activations might be sufficient for evoking itch sensation. Considering these differences in a noisy system like the peripheral nervous system can shine light on different aspects of these sensations and their coding conundrum.

When theorizing how sensations are perceived by the nervous system, as described in the introduction of this dissertation, “sensory coding” is the most commonly used term. “Coding” implies existence of “decoding” and also hints that decision making responsibilities are endowed to “decoders”. Furthermore, modeling the system in such hierarchical manner requires central processing loci that would at some level differentiate modalities and initiate responses. As there is no evidence of such modality specific loci throughout the somatosensory system and there are extensive arguments about decentralized processing in the nervous system (Kryklywy et al., 2020; Manrique et al., 2019; Zhang et al., 2016b), there are suggestions that instead of “encoding-decoding” frameworks, we could use “transformation” as a concept (Halpern, 2000). Such approach, to my belief, can change the way many questions are currently framed in the field of somatosensory biology and consolidate data from various schools of thought.

Finally, I would like to bring forward once more the wealth of studies that have shown for many years that the peripheral somatosensory system, like most other parts of the nervous system, is a dynamic and flexible system. The fact that neuronal activity can change the epigenomic and transcriptomic landscape of neurons (Lee and Fields, 2021; Su et al., 2017), added to the fact that changes in surface expression of transducing proteins can change the excitability and signaling properties of these cells (Geppetti et al., 2015; Senba and Kashiba, 1996; Waxman, 2000), shows that they cannot be understood by single snapshot “omics” experiments. Understanding their flexibility and the changes that the primary sensory afferents can go through can be critical in understanding their function in health and disease.

Complementary research

Among the future direction ideas that would complement what I have presented here, we will not forget the expansion of the approaches to disease conditions. In both results chapters of this dissertation (Chapter 2 and 3), our work was focused on healthy conditions yet studies can be performed in pathological states.

In continuation of Chapter 2, changes of sensory discrimination signaling in dysesthesia can be investigated. As described in Chapter 1 (section: Pain and itch), for both pain and itch, there are experimental conditions where the sensory modalities are misperceived. Targeting single populations of neurons using similar transgenic approaches used in Chapter 2, mechanisms of dysesthesia can be investigated. Moreover, in combination with microneurography, these approaches can provide the opportunity of recording the signals generated by these fibers after activation by optogenetic or chemogenetic actuators in health and diseased states.

In continuation of Chapter 3, changes in the transcriptomic and epigenomic repertoire of cells from the DRG in patients who were suffering from chronic pain conditions can be studied through similar single-nucleus experiments. The profile changes discovered in such studies can uncover pathological pathways that are recruited in chronic pain conditions, with the potential of identifying novel therapeutic targets.

Conclusion

In conclusion, I hope that this dissertation can provide some evidence that the primary sensory system is a complex and dynamic component of mammalian nervous system that serves as more than just a carrier of signals. Heterogeneous cell populations in the primary somatosensory system contribute in various ways to how the world is represented and integrated by the living organism. Playing multiple functional roles depending on what is presented to them from external or internal stimuli, these diverse cells can form how the nervous system perceives the constant flow of sensory information presented to it. Modulation of these roles or the way these stimuli are transformed in the nervous system can maintain health or cause disease. As some the most burdensome conditions that patients can experience, sensory complications such as chronic pain and itch require better understanding of somatosensation. Hence every step towards understanding the physiology of peripheral somatosensory neurons and their cellular environment, their diverse cellular functionalities, their heterogeneous nature, or their modulatory capacities, is a positive step towards improving the quality of life of millions of patients around the world. I hope that this dissertation is a valuable contribution.

References

Including references from Chapters 2 and 3.

10xGenomics (2019). Chromium' ' Next GEM Single Cell 3 ’ Reagent Kits v3.1 . Rev D.

10xGenomics (2021a). Nuclei Isolation from Complex Tissues for' ' Single Cell Multiome ATAC + Gene Expression Sequencing.

10xGenomics (2021b). Chromium Next GEM Single Cell Multiome ATAC + Gene Expression. CG000338.

Abraham, N.G., and Drummond, G. (2006). CD163-Mediated hemoglobin-heme uptake activates macrophage HO-1, providing an antiinflammatory function. Circ. Res. 99, 911–914.

Akiyama, T., Tominaga, M., Davoodi, A., Nagamine, M., Blansit, K., Horwitz, A., Carstens, M.I., and Carstens, E. (2012). Cross-sensitization of histamine-independent itch in mouse primary sensory neurons. Neuroscience 226, 305–312.

Akiyama, T., Nagamine, M., Carstens, M.I., and Carstens, E. (2014). Behavioral model of itch, alloknesis, pain and allodynia in the lower hindlimb and correlative responses of lumbar dorsal horn neurons in the mouse. Neuroscience 266, 38–46.

Albisetti, G.W., Pagani, M., Platonova, E., Hösli, L., Johannssen, H.C., Fritschy, J.-M., Wildner, H., and Zeilhofer, H.U. (2019). Dorsal Horn Gastrin-Releasing Peptide Expressing Neurons Transmit Spinal Itch But Not Pain Signals. J. Neurosci. 39, 2238–2250.

Alle, H., and Geiger, J.R.P. (2006). Combined analog and action potential coding in hippocampal mossy fibers. Science 311, 1290–1293.

Amir, R., and Devor, M. (1996). Chemically mediated cross-excitation in rat dorsal root ganglia. J. Neurosci. 16, 4733–4741.

Ango, F., Gallo, N.B., and Van Aelst, L. (2021). Molecular mechanisms of axo-axonic innervation. Curr. Opin. Neurobiol. 69, 105–112.

Azarfar, A., Calcini, N., Huang, C., Zeldenrust, F., and Celikel, T. (2018). Neural coding: A single neuron's perspective. Neurosci. Biobehav. Rev. 94, 238–247.

Baron, R., Schwarz, K., Kleinert, A., Schattschneider, J., and Wasner, G. (2001). Histamine-induced itch converts into pain in neuropathic hyperalgesia. Neuroreport 12, 3475–3478.

Bautista, D.M., Wilson, S.R., and Hoon, M.A. (2014). Why we scratch an itch: the molecules, cells and circuits of itch. Nat. Neurosci. 17, 175–182.

Beitel, R.E., and Dubner, R. (1976). Response of unmyelinated (C) polymodal nociceptors to thermal stimuli applied to monkey's face. J. Neurophysiol. 39, 1160–1175.

Bishop, G.H. (1959). The relation between nerve fiber size and sensory modality. J. Nerv. Ment. Dis. 128, 89–114.

Bland-Ward, P.A., and Humphrey, P.P. (1997). Acute nociception mediated by hindpaw P2X receptor activation in the rat. Br. J. Pharmacol. 122, 365–371.

Bourojeni, F.B. (2020). DEVELOPMENT AND INTERACTIVE CONTRIBUTION OFANTEROLATERAL SYSTEM NEURONS TO NOCICEPTION. Doctoral dissertation. McGill Neuroscience.

Brull, S.J., Atanassoff, P.G., Silverman, D.G., Zhang, J., and Lamotte, R.H. (1999). Attenuation of experimental pruritus and mechanically evoked dysesthesiae in an area of cutaneous allodynia. Somatosens Mot Res 16, 299–303.

Buenrostro, J.D., Giresi, P.G., Zaba, L.C., Chang, H.Y., and Greenleaf, W.J. (2013). Transposition of native chromatin for fast and sensitive epigenomic profiling of open chromatin, DNA-binding proteins and nucleosome position. Nat. Methods 10, 1213–1218.

Burgess, P.R., and Perl, E.R. (1967). Myelinated afferent fibres responding specifically to noxious stimulation of the skin. J. Physiol. (Lond.) 190, 541–562.

Campbell, B. (1946). Morphology and conduction of bipolar dorsal root ganglion cells of selachian fishes. J. Neurophysiol. 9, 173–179.

Carr, P.A., and Nagy, J.I. (1993). Emerging relationships between cytochemical properties and sensory modality transmission in primary sensory neurons. Brain Res. Bull. 30, 209–219.

Cevikbas, F., Wang, X., Akiyama, T., Kempkes, C., Savinko, T., Antal, A., Kukova, G., Buhl, T., Ikoma, A., Buddenkotte, J., et al. (2014). A sensory neuron-expressed IL-31 receptor mediates T helper cell-dependent itch: Involvement of TRPV1 and TRPA1. J. Allergy Clin. Immunol. 133, 448–460.

Chakraborty, R., Saddouk, F.Z., Carrao, A.C., Krause, D.S., Greif, D.M., and Martin, K.A. (2019). Promoters to study vascular smooth muscle. Arterioscler. Thromb. Vasc. Biol. 39, 603–612.

Chen, C.-Y.A., Ezzeddine, N., and Shyu, A.-B. (2008). Messenger RNA half-life measurements in mammalian cells. Meth. Enzymol. 448, 335–357.

Chisholm, K.I., Khovanov, N., Lopes, D.M., La Russa, F., and McMahon, S.B. (2018). Large Scale In Vivo Recording of Sensory Neuron Activity with GCaMP6. eNeuro 5.

Clark, S.L. (1926). NISSL granules of primary afferent neurones. J. Comp. Neurol. 41, 423–451.

Cobos, E.J., Nickerson, C.A., Gao, F., Chandran, V., Bravo-Caparrós, I., González-Cano, R., Riva, P., Andrews, N.A., Latremoliere, A., Seehus, C.R., et al. (2018). Mechanistic Differences in Neuropathic Pain Modalities Revealed by Correlating Behavior with Global Expression Profiling. Cell Rep. 22, 1301–1312.

Cuello, A.C. (1983). Nonclassical neuronal communications. Fed Proc 42, 2912–2922.

Dadwal, N., Mix, C., Reinhold, A., Witte, A., Freund, C., Schraven, B., and Kliche, S. (2021). The Multiple Roles of the Cytosolic Adapter Proteins ADAP, SKAP1 and SKAP2 for TCR/CD3 - Mediated Signaling Events. Front. Immunol. 12, 703534.

Daou, I., Tuttle, A.H., Longo, G., Wieskopf, J.S., Bonin, R.P., Ase, A.R., Wood, J.N., De Koninck, Y., Ribeiro-da-Silva, A., Mogil, J.S., et al. (2013). Remote optogenetic activation and sensitization of pain pathways in freely moving mice. J. Neurosci. 33, 18631–18640.

Davidson, S., and Giesler, G.J. (2010). The multiple pathways for itch and their interactions with pain. Trends Neurosci. 33, 550–558.

Dawson, G.D. (1956). The relative excitability and conduction velocity of sensory and motor nerve fibres in man. J. Physiol. (Lond.) 131, 436–451.

Devor, M. (1999). Unexplained peculiarities of the dorsal root ganglion. Pain Suppl 6, S27–S35.

Djouhri, L., and Lawson, S.N. (2004). Abeta-fiber nociceptive primary afferent neurons: a review of incidence and properties in relation to other afferent A-fiber neurons in mammals. Brain Res Brain Res Rev 46, 131–145.

Dong, X., and Dong, X. (2018). Peripheral and central mechanisms of itch. Neuron 98, 482–494.

Dong, X., Han, S., Zylka, M.J., Simon, M.I., and Anderson, D.J. (2001). A diverse family of GPCRs expressed in specific subsets of nociceptive sensory neurons. Cell 106, 619–632.

Drokhlyansky, E., Smillie, C.S., Van Wittenberghe, N., Ericsson, M., Griffin, G.K., Eraslan, G., Dionne, D., Cuoco, M.S., Goder-Reiser, M.N., Sharova, T., et al. (2020). The Human and Mouse Enteric Nervous System at Single-Cell Resolution. Cell 182, 1606–1622.e23.

Dymecki, S.M., Niederhuber, J.E., and Desiderio, S.V. (1990). Specific expression of a tyrosine kinase gene, blk, in B lymphoid cells. Science 247, 332–336.

Eccles, J.C. (1964). The controls of sensory communication to the brain. Australas Ann Med 13, 102–113.

Emery, E.C., Luiz, A.P., Sikandar, S., Magnúsdóttir, R., Dong, X., and Wood, J.N. (2016). In vivo characterization of distinct modality-specific subsets of somatosensory neurons using GCaMP. Sci. Adv. 2, e1600990.

Eraslan, G., Simon, L.M., Mircea, M., Mueller, N.S., and Theis, F.J. (2019). Single-cell RNA-seq denoising using a deep count autoencoder. Nat. Commun. 10, 390.

Esposito, M.F., Malayil, R., Hanes, M., and Deer, T. (2019). Unique characteristics of the dorsal root ganglion as a target for neuromodulation. Pain Med. 20, S23–S30.

Fardo, F., Beck, B., Allen, M., and Finnerup, N.B. (2020). Beyond labeled lines: A population coding account of the thermal grill illusion. Neurosci. Biobehav. Rev. 108, 472–479.

Feldman-Goriachnik, R., and Hanani, M. (2021). How do neurons in sensory ganglia communicate with satellite glial cells? Brain Res. 1760, 147384.

Feng, J., Yang, P., Mack, M.R., Dryn, D., Luo, J., Gong, X., Liu, S., Oetjen, L.K., Zholos, A.V., Mei, Z., et al. (2017). Sensory TRP channels contribute differentially to skin inflammation and persistent itch. Nat. Commun. 8, 980.

Fishman, S.M. (2007). Recognizing pain management as a human right: a first step. Anesth. Analg. 105, 8–9.

Foerster, O. (1933). The dermatomes in man. Brain 56, 1–39.

Follmann, R., Goldsmith, C.J., and Stein, W. (2018). Multimodal sensory information is represented by a combinatorial code in a sensorimotor system. PLoS Biol. 16, e2004527.

Forster, C., and Handwerker, H.O. (2014). Central nervous processing of itch and pain. In Itch: mechanisms and treatment, E. Carstens, and T. Akiyama, eds. (Boca Raton (FL): CRC Press/Taylor & Francis),.

Franzén, O., Gan, L.-M., and Björkegren, J.L.M. (2019). PanglaoDB: a web server for exploration of mouse and human single-cell RNA sequencing data. Database (Oxford) 2019.

Fukada, S., Uezumi, A., Ikemoto, M., Masuda, S., Segawa, M., Tanimura, N., Yamamoto, H., Miyagoe-Suzuki, Y., and Takeda, S. (2007). Molecular signature of quiescent satellite cells in adult skeletal muscle. Stem Cells 25, 2448–2459.

Gasser, H.S. (1950). Unmedullated fibers originating in dorsal root ganglia. J. Gen. Physiol. 33, 651–690.

Gasser, H.S., and Erlanger, J. (1927). The rôle played by the sizes of the constituent fibers of a nerve trunk in determining the form of its action potential wave. American Journal of Physiology-Legacy Content 80, 522–547.

Gatto, G., Smith, K.M., Ross, S.E., and Goulding, M. (2019). Neuronal diversity in the somatosensory system: bridging the gap between cell type and function. Curr. Opin. Neurobiol. 56, 167–174.

Georgopoulos, A.P., Kettner, R.E., and Schwartz, A.B. (1988). Primate motor cortex and free arm movements to visual targets in three-dimensional space. II. Coding of the direction of movement by a neuronal population. J. Neurosci. 8, 2928–2937.

Geppetti, P., Veldhuis, N.A., Lieu, T., and Bunnett, N.W. (2015). G Protein-Coupled Receptors: Dynamic Machines for Signaling Pain and Itch. Neuron 88, 635–649.

Gjorgjieva, J., Meister, M., and Sompolinsky, H. (2019). Functional diversity among sensory neurons from efficient coding principles. PLoS Comput. Biol. 15, e1007476.

Goldman, L., and Albus, J.S. (1968). Computation of impulse conduction in myelinated fibers; theoretical basis of the velocity-diameter relation. Biophys. J. 8, 596–607.

Gopalsamy, B., Sambasevam, Y., Zulazmi, N.A., Chia, J.S.M., Omar Farouk, A.A., Sulaiman, M.R., Tengku Mohamad, T.A.S., and Perimal, E.K. (2019). Experimental Characterization of the Chronic Constriction Injury-Induced Neuropathic Pain Model in Mice. Neurochem. Res. 44, 2123–2138.

Green, D., and Dong, X. (2016). The cell biology of acute itch. J. Cell Biol. 213, 155–161.

Green, A.D., Young, K.K., Lehto, S.G., Smith, S.B., and Mogil, J.S. (2006). Influence of genotype, dose and sex on pruritogen-induced scratching behavior in the mouse. Pain 124, 50–58.

Gregus, A.M., Levine, I.S., Eddinger, K.A., Yaksh, T.L., and Buczynski, M.W. (2021). Sex differences in neuroimmune and glial mechanisms of pain. Pain 162, 2186–2200.

Haberberger, R.V., Barry, C., Dominguez, N., and Matusica, D. (2019). Human dorsal root ganglia. Front. Cell Neurosci. 13, 271.

Halpern, B.P. (2000). Sensory coding, decoding, and representations. Unnecessary and troublesome constructs? Physiol. Behav. 69, 115–118.

Han, L., and Dong, X. (2014). Itch mechanisms and circuits. Annu. Rev. Biophys. 43, 331–355.

Han, S.-K., and Simon, M.I. (2011). Intracellular signaling and the origins of the sensations of itch and pain. Sci. Signal. 4, pe38.

Han, L., Ma, C., Liu, Q., Weng, H.-J., Cui, Y., Tang, Z., Kim, Y., Nie, H., Qu, L., Patel, K.N., et al. (2013). A subpopulation of nociceptors specifically linked to itch. Nat. Neurosci. 16, 174–182.

Hanani, M. (2005). Satellite glial cells in sensory ganglia: from form to function. Brain Res Brain Res Rev 48, 457–476.

Hanani, M., and Spray, D.C. (2020). Emerging importance of satellite glia in nervous system function and dysfunction. Nat. Rev. Neurosci. 21, 485–498.

Hao, Y., Hao, S., Andersen-Nissen, E., Mauck, W.M., Zheng, S., Butler, A., Lee, M.J., Wilk, A.J., Darby, C., Zager, M., et al. (2021). Integrated analysis of multimodal single-cell data. Cell 184, 3573–3587.e29.

Hargreaves, K., Dubner, R., Brown, F., Flores, C., and Joris, J. (1988). A new and sensitive method for measuring thermal nociception in cutaneous hyperalgesia. Pain 32, 77–88.

Harper, A.A., and Lawson, S.N. (1985a). Electrical properties of rat dorsal root ganglion neurones with different peripheral nerve conduction velocities. J. Physiol. (Lond.) 359, 47–63.

Harper, A.A., and Lawson, S.N. (1985b). Conduction velocity is related to morphological cell type in rat dorsal root ganglion neurones. J. Physiol. (Lond.) 359, 31–46.

Hatai, S. (1901). The finer structure of the spinal ganglion cells in the white rat. J. Comp. Neurol. 11, 1–24.

Heyer, G., Ulmer, F.J., Schmitz, J., and Handwerker, H.O. (1995). Histamine-induced itch and alloknesis (itchy skin) in atopic eczema patients and controls. Acta Derm. Venereol. 75, 348–352.

Hill, R.Z., Morita, T., Brem, R.B., and Bautista, D.M. (2018). S1PR3 Mediates Itch and Pain via Distinct TRP Channel-Dependent Pathways. J. Neurosci. 38, 7833–7843.

Hong, S., Ratté, S., Prescott, S.A., and De Schutter, E. (2012). Single neuron firing properties impact correlation-based population coding. J. Neurosci. 32, 1413–1428.

Hu, E., Liang, P., and Spiegelman, B.M. (1996). AdipoQ is a novel adipose-specific gene dysregulated in obesity. J. Biol. Chem. 271, 10697–10703.

Hursh, J.B. (1939). Conduction velocity and diameter of nerve fibers. American Journal of Physiology-Legacy Content 127, 131–139.

Ikoma, A., Fartasch, M., Heyer, G., Miyachi, Y., Handwerker, H., and Schmelz, M. (2004). Painful stimuli evoke itch in patients with chronic pruritus: central sensitization for itch. Neurology 62, 212–217.

Illa, I., Leon-Monzon, M., and Dalakas, M.C. (1992). Regenerating and denervated human muscle fibers and satellite cells express neural cell adhesion molecule recognized by monoclonal antibodies to natural killer cells. Ann. Neurol. 31, 46–52.

International Pain Summit Of The International Association For The Study Of Pain (2011). Declaration of Montréal: declaration that access to pain management is a fundamental human right. J. Pain Palliat. Care Pharmacother. 25, 29–31.

Iwai, H., Ataka, K., Suzuki, H., Dhar, A., Kuramoto, E., Yamanaka, A., and Goto, T. (2021). Tissue-resident M2 macrophages directly contact primary sensory neurons in the sensory ganglia after nerve injury. J. Neuroinflammation 18, 227.

Jakob, M.O., Kofoed-Branzk, M., Deshpande, D., Murugan, S., and Klose, C.S.N. (2021). An integrated view on neuronal subsets in the peripheral nervous system and their role in immunoregulation. Front. Immunol. 12, 679055.

Jessen, K.R., and Mirsky, R. (2019). Schwann cell precursors; multipotent glial cells in embryonic nerves. Front. Mol. Neurosci. 12, 69.

Johansson, R.S. (1976). Receptive field sensitivity profile of mechanosensitive units innervating the glabrous skin of the human hand. Brain Res. 104, 330–334.

Johansson, R.S., and Birznieks, I. (2004). First spikes in ensembles of human tactile afferents code complex spatial fingertip events. Nat. Neurosci. 7, 170–177.

Johansson, R.S., and Vallbo, A.B. (1980). Spatial properties of the population of mechanoreceptive units in the glabrous skin of the human hand. Brain Res. 184, 353–366.

Johansson, R.S., Trulsson, M., Olsson, K.A., and Westberg, K.G. (1988). Mechanoreceptor activity from the human face and oral mucosa. Exp. Brain Res. 72, 204–208.

Kakimoto, S., Nagakura, Y., Tamura, S., Watabiki, T., Shibasaki, K., Tanaka, S., Mori, M., Sasamata, M., and Okada, M. (2008). Minodronic acid, a third-generation bisphosphonate, antagonizes purinergic P2X(2/3) receptor function and exerts an analgesic effect in pain models. Eur. J. Pharmacol. 589, 98–101.

Kato, A., Ohkubo, T., and Kitamura, K. (2002). Algogen-specific pain processing in mouse spinal cord: differential involvement of voltage-dependent Ca(2+) channels in synaptic transmission. Br. J. Pharmacol. 135, 1336–1342.

Kim, Y.S., Anderson, M., Park, K., Zheng, Q., Agarwal, A., Gong, C., Saijilafu, Young, L., He, S., LaVinka, P.C., et al. (2016). Coupled activation of primary sensory neurons contributes to chronic pain. Neuron 91, 1085–1096.

Klein, A., Carstens, M.I., and Carstens, E. (2011). Facial injections of pruritogens or algogens elicit distinct behavior responses in rats and excite overlapping populations of primary sensory and trigeminal subnucleus caudalis neurons. J. Neurophysiol. 106, 1078–1088.

Koerber, H.R., and Mendell, L.M. (1988). Functional specialization of central projections from identified primary afferent fibers. J. Neurophysiol. 60, 1597–1614.

Koerber, H.R., Druzinsky, R.E., and Mendell, L.M. (1988). Properties of somata of spinal dorsal root ganglion cells differ according to peripheral receptor innervated. J. Neurophysiol. 60, 1584–1596.

Komohara, Y., Hirahara, J., Horikawa, T., Kawamura, K., Kiyota, E., Sakashita, N., Araki, N., and Takeya, M. (2006). AM-3K, an anti-macrophage antibody, recognizes CD163, a molecule associated with an anti-inflammatory macrophage phenotype. J. Histochem. Cytochem. 54, 763–771.

Koppert, W., Reeh, P.W., and Handwerker, H.O. (1993). Conditioning of histamine by bradykinin alters responses of rat nociceptor and human itch sensation. Neurosci. Lett. 152, 117–120.

Kryklywy, J.H., Ehlers, M.R., Anderson, A.K., and Todd, R.M. (2020). From architecture to evolution: multisensory evidence of decentralized emotion. Trends Cogn. Sci. (Regul. Ed.) 24, 916–929.

Kung, L.-H., Gong, K., Adedoyin, M., Ng, J., Bhargava, A., Ohara, P.T., and Jasmin, L. (2013). Evidence for glutamate as a neuroglial transmitter within sensory ganglia. PLoS One 8, e68312.

Kupari, J., Usoskin, D., Parisien, M., Lou, D., Hu, Y., Fatt, M., Lönnerberg, P., Spångberg, M., Eriksson, B., Barkas, N., et al. (2021). Single cell transcriptomics of primate sensory neurons identifies cell types associated with chronic pain. Nat. Commun. 12, 1510.

Lacy, S.E., Bönnemann, C.G., Buzney, E.A., and Kunkel, L.M. (1999). Identification of FLRT1, FLRT2, and FLRT3: a novel family of transmembrane leucine-rich repeat proteins. Genomics 62, 417–426.

Lähnemann, D., Köster, J., Szczurek, E., McCarthy, D.J., Hicks, S.C., Robinson, M.D., Vallejos, C.A., Campbell, K.R., Beerenwinkel, N., Mahfouz, A., et al. (2020). Eleven grand challenges in single-cell data science. Genome Biol. 21, 31.

Lallemend, F., and Ernfors, P. (2012). Molecular interactions underlying the specification of sensory neurons. Trends Neurosci. 35, 373–381.

LaMotte, R.H., Shimada, S.G., and Sikand, P. (2011). Mouse models of acute, chemical itch and pain in humans. Exp. Dermatol. 20, 778–782.

LaMotte, R.H., Dong, X., and Ringkamp, M. (2014). Sensory neurons and circuits mediating itch. Nat. Rev. Neurosci. 15, 19–31.

Lau, S.-F., Cao, H., Fu, A.K.Y., and Ip, N.Y. (2020). Single-nucleus transcriptome analysis reveals dysregulation of angiogenic endothelial cells and neuroprotective glia in Alzheimer's disease. Proc. Natl. Acad. Sci. USA 117, 25800–25809.

Lawson, S.N., and Waddell, P.J. (1991). Soma neurofilament immunoreactivity is related to cell size and fibre conduction velocity in rat primary sensory neurons. J. Physiol. (Lond.) 435, 41–63.

Lawson, S.N., Fang, X., and Djouhri, L. (2019). Nociceptor subtypes and their incidence in rat lumbar dorsal root ganglia (DRGs): focussing on C-polymodal nociceptors, Aβ-nociceptors,

moderate pressure receptors and their receptive field depths. Curr. Opin. Physiol. 11, 125–146.

Lee, P.R., and Fields, R.D. (2021). Activity-Dependent Gene Expression in Neurons. Neuroscientist 27, 355–366.

Lee, H., Kim, D.-W., Remedios, R., Anthony, T.E., Chang, A., Madisen, L., Zeng, H., and Anderson, D.J. (2014). Scalable control of mounting and attack by Esr1+ neurons in the ventromedial hypothalamus. Nature 509, 627–632.

Lee, M.K., Tuttle, J.B., Rebhun, L.I., Cleveland, D.W., and Frankfurter, A. (1990). The expression and posttranslational modification of a neuron-specific beta-tubulin isotype during chick embryogenesis. Cell Motil. Cytoskeleton 17, 118–132.

Lee, M.W.L., McPhee, R.W., and Stringer, M.D. (2008). An evidence-based approach to human dermatomes. Clin Anat 21, 363–373.

Lembo, P.M.C., Grazzini, E., Groblewski, T., O'Donnell, D., Roy, M.-O., Zhang, J., Hoffert, C., Cao, J., Schmidt, R., Pelletier, M., et al. (2002). Proenkephalin A gene products activate a new family of sensory neuron--specific GPCRs. Nat. Neurosci. 5, 201–209.

Levina, I.S., Kuznetsov, Y.V., Shchelkunova, T.A., and Zavarzin, I.V. (2021). Selective ligands of membrane progesterone receptors as a key to studying their biological functions in vitro and in vivo. J. Steroid Biochem. Mol. Biol. 207, 105827.

Li, H. (2018). Minimap2: pairwise alignment for nucleotide sequences. Bioinformatics 34, 3094–3100.

Liem, L., van Dongen, E., Huygen, F.J., Staats, P., and Kramer, J. (2016). The dorsal root ganglion as a therapeutic target for chronic pain. Reg. Anesth. Pain Med. 41, 511–519.

Liu, N.-J., von Gizycki, H., and Gintzler, A.R. (2007). Sexually dimorphic recruitment of spinal opioid analgesic pathways by the spinal application of morphine. J. Pharmacol. Exp. Ther. 322, 654–660.

Liu, Q., Tang, Z., Surdenikova, L., Kim, S., Patel, K.N., Kim, A., Ru, F., Guan, Y., Weng, H.-J., Geng, Y., et al. (2009). Sensory neuron-specific GPCR Mrgprs are itch receptors mediating chloroquine-induced pruritus. Cell 139, 1353–1365.

Liu, Q., Sikand, P., Ma, C., Tang, Z., Han, L., Li, Z., Sun, S., LaMotte, R.H., and Dong, X. (2012). Mechanisms of itch evoked by b-alanine. J. Neurosci. 32, 14532–14537.

Liu, W., Liu, Q., Crozier, R.A., and Davis, R.L. (2021). Analog transmission of action potential fine structure in spiral ganglion axons. J. Neurophysiol. 126, 888–905.

Liu, Y., Abdel Samad, O., Zhang, L., Duan, B., Tong, Q., Lopes, C., Ji, R.-R., Lowell, B.B., and Ma, Q. (2010). VGLUT2-dependent glutamate release from nociceptors is required to sense pain and suppress itch. Neuron 68, 543–556.

De Logu, F., Marini, M., Landini, L., Souza Monteiro de Araujo, D., Bartalucci, N., Trevisan, G., Bruno, G., Marangoni, M., Schmidt, B.L., Bunnett, N.W., et al. (2021). Peripheral Nerve Resident Macrophages and Schwann Cells Mediate Cancer-Induced Pain. Cancer Res. 81, 3387–3401.

Lomas, L.M., Barrett, A.C., Terner, J.M., Lysle, D.T., and Picker, M.J. (2007). Sex differences in the potency of kappa opioids and mixed-action opioids administered systemically and at the site of inflammation against capsaicin-induced hyperalgesia in rats. Psychopharmacology 191, 273–285.

Luo, J., Feng, J., Liu, S., Walters, E.T., and Hu, H. (2015). Molecular and cellular mechanisms that initiate pain and itch. Cell Mol. Life Sci. 72, 3201–3223.

Ma, Q. (2012). Population coding of somatic sensations. Neurosci. Bull. 28, 91–99.

Mack, M.R., and Kim, B.S. (2018). The Itch-Scratch Cycle: A Neuroimmune Perspective. Trends Immunol. 39, 980–991.

Manrique, P.D., Klein, M., Li, Y.S., Xu, C., Hui, P.M., and Johnson, N.F. (2019). Getting closer to the goal by being less capable. Sci. Adv. 5, eaau5902.

Marie-Cardine, A., Bruyns, E., Eckerskorn, C., Kirchgessner, H., Meuer, S.C., and Schraven, B. (1997). Molecular cloning of SKAP55, a novel protein that associates with the protein tyrosine kinase p59fyn in human T-lymphocytes. J. Biol. Chem. 272, 16077–16080.

Marmigère, F., and Ernfors, P. (2007). Specification and connectivity of neuronal subtypes in the sensory lineage. Nat. Rev. Neurosci. 8, 114–127.

Matsuda, S., Kobayashi, N., Terashita, T., Shimokawa, T., Shigemoto, K., Mominoki, K., Wakisaka, H., Saito, S., Miyawaki, K., Saito, K., et al. (2005). Phylogenetic investigation of Dogiel's pericellular nests and Cajal's initial glomeruli in the dorsal root ganglion. J. Comp. Neurol. 491, 234–245.

Matsuoka, R., Yoshida, M.C., Furutani, Y., Imamura, S., Kanda, N., Yanagisawa, M., Masaki, T., and Takao, A. (1993). Human smooth muscle myosin heavy chain gene mapped to chromosomal region 16q12. Am. J. Med. Genet. 46, 61–67.

Maze, I., Wenderski, W., Noh, K.-M., Bagot, R.C., Tzavaras, N., Purushothaman, I., Elsässer, S.J., Guo, Y., Ionete, C., Hurd, Y.L., et al. (2015). Critical role of histone turnover in neuronal transcription and plasticity. Neuron 87, 77–94.

McDonnell, M.D., and Abbott, D. (2009). What is stochastic resonance? Definitions, misconceptions, debates, and its relevance to biology. PLoS Comput. Biol. 5, e1000348.

McMahon, S.B., and Koltzenburg, M. (1992). Itching for an explanation. Trends Neurosci. 15, 497–501.

Meltzer, S., Santiago, C., Sharma, N., and Ginty, D.D. (2021). The cellular and molecular basis of somatosensory neuron development. Neuron 109, 3736–3757.

Mense, S. (1990). Structure-function relationships in identified afferent neurones. Anat. Embryol. (Berl.) 181, 1–17.

Merskey, H. (1979). Editorial The need of a taxonomy. Pain 6, 247–252.

Midavaine, É., Côté, J., Marchand, S., and Sarret, P. (2021). Glial and neuroimmune cell choreography in sexually dimorphic pain signaling. Neurosci. Biobehav. Rev. 125, 168–192.

Milev, P., Friedlander, D.R., Sakurai, T., Karthikeyan, L., Flad, M., Margolis, R.K., Grumet, M., and Margolis, R.U. (1994). Interactions of the chondroitin sulfate proteoglycan phosphacan, the extracellular domain of a receptor-type protein tyrosine phosphatase, with neurons, glia, and neural cell adhesion molecules. J. Cell Biol. 127, 1703–1715.

Miller, R.J., Jung, H., Bhangoo, S.K., and White, F.A. (2009). Cytokine and chemokine regulation of sensory neuron function. Handb Exp Pharmacol 417–449.

Mochizuki, H., Baumgärtner, U., Kamping, S., Ruttorf, M., Schad, L.R., Flor, H., Kakigi, R., and Treede, R.-D. (2013). Cortico-subcortical activation patterns for itch and pain imagery. Pain 154, 1989–1998.

Mogil, J.S. (2009). Animal models of pain: progress and challenges. Nat. Rev. Neurosci. 10, 283–294.

Momin, A., and McNaughton, P.A. (2009). Regulation of firing frequency in nociceptive neurons by pro-inflammatory mediators. Exp. Brain Res. 196, 45–52.

Montemurro, M.A., Rasch, M.J., Murayama, Y., Logothetis, N.K., and Panzeri, S. (2008). Phase-of-firing coding of natural visual stimuli in primary visual cortex. Curr. Biol. 18, 375–380.

Moore, C., Gupta, R., Jordt, S.-E., Chen, Y., and Liedtke, W.B. (2018). Regulation of pain and itch by TRP channels. Neurosci. Bull. 34, 120–142.

Namer, B., and Reeh, P. (2013). Scratching an itch. Nat. Neurosci. 16, 117–118.

Nascimento, A.I., Mar, F.M., and Sousa, M.M. (2018). The intriguing nature of dorsal root ganglion neurons: Linking structure with polarity and function. Prog. Neurobiol. 168, 86–103.

Nguyen, M.Q., Wu, Y., Bonilla, L.S., von Buchholtz, L.J., and Ryba, N.J.P. (2017). Diversity amongst trigeminal neurons revealed by high throughput single cell sequencing. PLoS One 12, e0185543.

Nguyen, M.Q., Le Pichon, C.E., and Ryba, N. (2019). Stereotyped transcriptomic transformation of somatosensory neurons in response to injury. Elife 8.

Nguyen, M.Q., von Buchholtz, L.J., Reker, A.N., Ryba, N.J., and Davidson, S. (2021). Single-nucleus transcriptomic analysis of human dorsal root ganglion neurons. Elife 10.

Nilsson, H.J., Levinsson, A., and Schouenborg, J. (1997). Cutaneous field stimulation (CFS): a new powerful method to combat itch. Pain 71, 49–55.

Oyler, G.A., Higgins, G.A., Hart, R.A., Battenberg, E., Billingsley, M., Bloom, F.E., and Wilson, M.C. (1989). The identification of a novel synaptosomal-associated protein, SNAP-25, differentially expressed by neuronal subpopulations. J. Cell Biol. 109, 3039–3052.

Pagani, M., Albisetti, G.W., Sivakumar, N., Wildner, H., Santello, M., Johannssen, H.C., and Zeilhofer, H.U. (2019). How Gastrin-Releasing Peptide Opens the Spinal Gate for Itch. Neuron 103, 102–117.e5.

Pannese, E. (1964). Number and structure of perisomatic satellite cells of spinal ganglia under normal conditions or during axon regeneration and neuronal hypertrophy. Z. Zellforsch. Mikrosk. Anat. 63, 568–592.

Pannese, E., Ledda, M., Cherkas, P.S., Huang, T.Y., and Hanani, M. (2003). Satellite cell reactions to axon injury of sensory ganglion neurons: increase in number of gap junctions and formation of bridges connecting previously separate perineuronal sheaths. Anat. Embryol. (Berl.) 206, 337–347.

Panzeri, S., Macke, J.H., Gross, J., and Kayser, C. (2015). Neural population coding: combining insights from microscopic and mass signals. Trends Cogn. Sci. (Regul. Ed.) 19, 162–172.

Panzeri, S., Harvey, C.D., Piasini, E., Latham, P.E., and Fellin, T. (2017). Cracking the neural code for sensory perception by combining statistics, intervention, and behavior. Neuron 93, 491–507.

Le Pichon, C.E., and Chesler, A.T. (2014). The functional and anatomical dissection of somatosensory subpopulations using mouse genetics. Front. Neuroanat. 8, 21.

Prescott, S.A., and Ratté, S. (2012). Pain processing by spinal microcircuits: afferent combinatorics. Curr. Opin. Neurobiol. 22, 631–639.

Prescott, S.A., Ma, Q., and De Koninck, Y. (2014). Normal and abnormal coding of somatosensory stimuli causing pain. Nat. Neurosci. 17, 183–191.

Ratté, S., Hong, S., De Schutter, E., and Prescott, S.A. (2013). Impact of neuronal properties on network coding: roles of spike initiation dynamics and robust synchrony transfer. Neuron 78, 758–772.

Ray, P., Torck, A., Quigley, L., Wangzhou, A., Neiman, M., Rao, C., Lam, T., Kim, J.-Y., Kim, T.H., Zhang, M.Q., et al. (2018). Comparative transcriptome profiling of the human and mouse dorsal root ganglia: an RNA-seq-based resource for pain and sensory neuroscience research. Pain 159, 1325–1345.

Rexed, B., and Sourander, P. (1949). The caliber of central and peripheral neuritis of spinal ganglion cells and variations in fiber size at different levels of dorsal spinal roots. J. Comp. Neurol. 91, 297–306.

Roberson, D.P., Gudes, S., Sprague, J.M., Patoski, H.A.W., Robson, V.K., Blasl, F., Duan, B., Oh, S.B., Bean, B.P., Ma, Q., et al. (2013). Activity-dependent silencing reveals functionally distinct itch-generating sensory neurons. Nat. Neurosci. 16, 910–918.

Rozanski, G.M., Kim, H., Li, Q., Wong, F.K., and Stanley, E.F. (2012). Slow chemical transmission between dorsal root ganglion neuron somata. Eur. J. Neurosci. 36, 3314–3321.

Ru, F., Sun, H., Jurcakova, D., Herbstsomer, R.A., Meixong, J., Dong, X., and Undem, B.J. (2017). Mechanisms of pruritogen-induced activation of itch nerves in isolated mouse skin. J. Physiol. (Lond.) 595, 3651–3666.

Sadler, K.E., Mogil, J.S., and Stucky, C.L. (2021). Innovations and advances in modelling and measuring pain in animals. Nat. Rev. Neurosci.

Sang, C.N., Gracely, R.H., Max, M.B., and Bennett, G.J. (1996). Capsaicin-evoked mechanical allodynia and hyperalgesia cross nerve territories. Evidence for a central mechanism. Anesthesiology 85, 491–496.

Satpathy, A.T., Granja, J.M., Yost, K.E., Qi, Y., Meschi, F., McDermott, G.P., Olsen, B.N., Mumbach, M.R., Pierce, S.E., Corces, M.R., et al. (2019). Massively parallel single-cell chromatin landscapes of human immune cell development and intratumoral T cell exhaustion. Nat. Biotechnol. 37, 925–936.

Scherrer, G., Imamachi, N., Cao, Y.-Q., Contet, C., Mennicken, F., O'Donnell, D., Kieffer, B.L., and Basbaum, A.I. (2009). Dissociation of the opioid receptor mechanisms that control mechanical and heat pain. Cell 137, 1148–1159.

Schmelz, M. (2015). Itch and pain differences and commonalities. Handb Exp Pharmacol 227, 285–301.

Senba, E., and Kashiba, H. (1996). Sensory afferent processing in multi-responsive DRG neurons. Prog. Brain Res. 113, 387–410.

Sharma, N., Flaherty, K., Lezgiyeva, K., Wagner, D.E., Klein, A.M., and Ginty, D.D. (2020). The emergence of transcriptional identity in somatosensory neurons. Nature 577, 392–398.

Shimada, S.G., and LaMotte, R.H. (2008). Behavioral differentiation between itch and pain in mouse. Pain 139, 681–687.

Shin, J.E., Ha, H., Kim, Y.K., Cho, Y., and DiAntonio, A. (2019). DLK regulates a distinctive transcriptional regeneration program after peripheral nerve injury. Neurobiol. Dis. 127, 178–192.

Shoemaker, J.K., Klassen, S.A., Badrov, M.B., and Fadel, P.J. (2018). Fifty years of microneurography: learning the language of the peripheral sympathetic nervous system in humans. J. Neurophysiol. 119, 1731–1744.

Shu, Y., Hasenstaub, A., Duque, A., Yu, Y., and McCormick, D.A. (2006). Modulation of intracortical synaptic potentials by presynaptic somatic membrane potential. Nature 441, 761–765.

Sikand, P., Shimada, S.G., Green, B.G., and LaMotte, R.H. (2009). Similar itch and nociceptive sensations evoked by punctate cutaneous application of capsaicin, histamine and cowhage. Pain 144, 66–75.

Sikand, P., Shimada, S.G., Green, B.G., and LaMotte, R.H. (2011). Sensory responses to injection and punctate application of capsaicin and histamine to the skin. Pain 152, 2485–2494.

Simone, D.A., Zhang, X., Li, J., Zhang, J.-M., Honda, C.N., LaMotte, R.H., and Giesler, G.J. (2004). Comparison of responses of primate spinothalamic tract neurons to pruritic and algogenic stimuli. J. Neurophysiol. 91, 213–222.

Sinha, S., Satpathy, A.T., Zhou, W., Ji, H., Stratton, J.A., Jaffer, A., Bahlis, N., Morrissy, S., and Biernaskie, J.A. (2021). Profiling Chromatin Accessibility at Single-cell Resolution. Genomics Proteomics Bioinformatics 19, 172–190.

Snyder, S.E., Li, J., Schauwecker, P.E., McNeill, T.H., and Salton, S.R. (1996). Comparison of RPTP zeta/beta, phosphacan, and trkB mRNA expression in the developing and adult rat nervous system and induction of RPTP zeta/beta and phosphacan mRNA following brain injury. Brain Res. Mol. Brain Res. 40, 79–96.

Solinski, H.J., Kriegbaum, M.C., Tseng, P.-Y., Earnest, T.W., Gu, X., Barik, A., Chesler, A.T., and Hoon, M.A. (2019). Nppb Neurons Are Sensors of Mast Cell-Induced Itch. Cell Rep. 26, 3561–3573.e4.

Solís-Cámara, P., and Negrete-Martínez, J. (1968). Transmission of more than one sensory modality-message along a single axon. Bol. Estud. Med. Biol. 25, 193–204.

Song, J., Xian, D., Yang, L., Xiong, X., Lai, R., and Zhong, J. (2018). Pruritus: Progress toward Pathogenesis and Treatment. Biomed Res. Int. 2018, 9625936.

St Sauver, J.L., Warner, D.O., Yawn, B.P., Jacobson, D.J., McGree, M.E., Pankratz, J.J., Melton, L.J., Roger, V.L., Ebbert, J.O., and Rocca, W.A. (2013). Why patients visit their doctors: assessing the most prevalent conditions in a defined American population. Mayo Clin. Proc. 88, 56–67.

Stantcheva, K.K., Iovino, L., Dhandapani, R., Martinez, C., Castaldi, L., Nocchi, L., Perlas, E., Portulano, C., Pesaresi, M., Shirlekar, K.S., et al. (2016). A subpopulation of itch-sensing neurons marked by Ret and somatostatin expression. EMBO Rep. 17, 585–600.

Stuart, T., Butler, A., Hoffman, P., Hafemeister, C., Papalexi, E., Mauck, W.M., Hao, Y., Stoeckius, M., Smibert, P., and Satija, R. (2019). Comprehensive Integration of Single-Cell Data. Cell 177, 1888–1902.e21.

Su, Y., Brooks, D.G., Li, L., Lepercq, J., Trofatter, J.A., Ravetch, J.V., and Lebo, R.V. (1993). Myelin protein zero gene mutated in Charcot-Marie-tooth type 1B patients. Proc. Natl. Acad. Sci. USA 90, 10856–10860.

Su, Y., Shin, J., Zhong, C., Wang, S., Roychowdhury, P., Lim, J., Kim, D., Ming, G.-L., and Song, H. (2017). Neuronal activity modifies the chromatin accessibility landscape in the adult brain. Nat. Neurosci. 20, 476–483.

Sun, Y.-G., and Chen, Z.-F. (2007). A gastrin-releasing peptide receptor mediates the itch sensation in the spinal cord. Nature 448, 700–703.

Sun, S., Xu, Q., Guo, C., Guan, Y., Liu, Q., and Dong, X. (2017). Leaky Gate Model: Intensity-Dependent Coding of Pain and Itch in the Spinal Cord. Neuron 93, 840–853.e5.

Sun, Y.-G., Zhao, Z.-Q., Meng, X.-L., Yin, J., Liu, X.-Y., and Chen, Z.-F. (2009). Cellular basis of itch sensation. Science 325, 1531–1534.

Tang, B.L. (2021). SNAREs and developmental disorders. J. Cell Physiol. 236, 2482–2504.

Tang, M., Wu, G., Wang, Z., Yang, N., Shi, H., He, Q., Zhu, C., Yang, Y., Yu, G., Wang, C., et al. (2016). Voltage-gated potassium channels involved in regulation of physiological function in MrgprA3-specific itch neurons. Brain Res. 1636, 161–171.

Than, J.Y.-X.L., Li, L., Hasan, R., and Zhang, X. (2013). Excitation and modulation of TRPA1, TRPV1, and TRPM8 channel-expressing sensory neurons by the pruritogen chloroquine. J. Biol. Chem. 288, 12818–12827.

Todd, A.J., and Koerber, H.R. (2006). Neuroanatomical substrates of spinal nociception. In Wall and melzack's textbook of pain, (Elsevier), pp. 73–90.

Torebjörk, H.E., and Ochoa, J.L. (1980). Specific sensations evoked by activity in single identified sensory units in man. Acta Physiol Scand 110, 445–447.

Tsuda, M., Shigemoto-Mogami, Y., Ueno, S., Koizumi, S., Ueda, H., Iwanaga, T., and Inoue, K. (2002). Downregulation of P2X3 receptor-dependent sensory functions in A/J inbred mouse strain. Eur. J. Neurosci. 15, 1444–1450.

Ueda, H., Amano, H., Shiomi, H., and Takagi, H. (1979). Comparison of the analgesic effects of various opioid peptides by a newly devised intracisternal injection technique in conscious mice. Eur. J. Pharmacol. 56, 265–268.

Urban, D.J., and Roth, B.L. (2015). DREADDs (designer receptors exclusively activated by designer drugs): chemogenetic tools with therapeutic utility. Annu. Rev. Pharmacol. Toxicol. 55, 399–417.

Usoskin, D., Furlan, A., Islam, S., Abdo, H., Lönnerberg, P., Lou, D., Hjerling-Leffler, J., Haeggström, J., Kharchenko, O., Kharchenko, P.V., et al. (2015). Unbiased classification of sensory neuron types by large-scale single-cell RNA sequencing. Nat. Neurosci. 18, 145–153.

Vallbo, A., Olausson, H., Wessberg, J., and Norrsell, U. (1993). A system of unmyelinated afferents for innocuous mechanoreception in the human skin. Brain Res. 628, 301–304.

Valtcheva, M.V., Copits, B.A., Davidson, S., Sheahan, T.D., Pullen, M.Y., McCall, J.G., Dikranian, K., and Gereau, R.W. (2016). Surgical extraction of human dorsal root ganglia from organ donors and preparation of primary sensory neuron cultures. Nat. Protoc. 11, 1877–1888.

Vos, T., Allen, C., and Arora, M. (2016). Global, regional, and national incidence, prevalence, and years lived with disability for 310 diseases and injuries, 1990-2015: a systematic analysis for the Global Burden of Disease Study 2015. Lancet 388, 1545–1602.

Wang, C., Chen, P., Lin, D., Chen, Y., Lv, B., Zheng, K., Lin, X., and Wu, Z. (2021). Effects of varying degrees of ligation in a neuropathic pain model induced by chronic constriction injury. Life Sci. 276, 119441.

Wang, F., Bélanger, E., Côté, S.L., Desrosiers, P., Prescott, S.A., Côté, D.C., and De Koninck, Y. (2018). Sensory afferents use different coding strategies for heat and cold. Cell Rep. 23, 2001–2013.

Wang, Y., Wu, Q., Hu, M., Liu, B., Chai, Z., Huang, R., Wang, Y., Xu, H., Zhou, L., Zheng, L., et al. (2017). Ligand- and voltage-gated Ca2+ channels differentially regulate the mode of vesicular neuropeptide release in mammalian sensory neurons. Sci. Signal. 10.

Wangzhou, Vivekan, Jeevakumar, Sankaranarayanan, I., Er, C., Copits, B., Dougherty, P., IV, R., Burton, M., Dussor, G., et al. Title: Spatial transcriptomics reveals unique molecular fingerprints of human nociceptors.

Wangzhou, A., McIlvried, L.A., Paige, C., Barragan-Iglesias, P., Shiers, S., Ahmad, A., Guzman, C.A., Dussor, G., Ray, P.R., Gereau, R.W., et al. (2020). Pharmacological target-focused transcriptomic analysis of native vs cultured human and mouse dorsal root ganglia. Pain 161, 1497–1517.

Warren, S., Yezierski, R.P., and Capra, N.F. (2018). The somatosensory system II. In Fundamental neuroscience for basic and clinical applications, (Elsevier), pp. 258–277.e1.

Warwick, R.A., and Hanani, M. (2013). The contribution of satellite glial cells to chemotherapy-induced neuropathic pain. Eur. J. Pain 17, 571–580.

Waxman, S.G. (2000). The neuron as a dynamic electrogenic machine: modulation of sodium-channel expression as a basis for functional plasticity in neurons. Philos. Trans. R. Soc. Lond. B, Biol. Sci. 355, 199–213.

Wilson, S., and Bautista, D. (2013). Itching for relief. Nat. Neurosci. 16, 775–777.

Wilson, S.R., Gerhold, K.A., Bifolck-Fisher, A., Liu, Q., Patel, K.N., Dong, X., and Bautista, D.M. (2011). TRPA1 is required for histamine-independent, Mas-related G protein-coupled receptor-mediated itch. Nat. Neurosci. 14, 595–602.

Xie, Z., and Hu, H. (2018). TRP channels as drug targets to relieve itch. Pharmaceuticals (Basel) 11.

Yoshida, S., and Matsuda, Y. (1979). Studies on sensory neurons of the mouse with intracellular-recording and horseradish peroxidase-injection techniques. J. Neurophysiol. 42, 1134–1145.

Yousefpour, N. (2021). Spinal Cord Structural Plasticity in Neuropathic Pain. Doctoral dissertation. McGill Pharmacology.

Yu, X., Liu, H., Hamel, K.A., Morvan, M.G., Yu, S., Leff, J., Guan, Z., Braz, J.M., and Basbaum, A.I. (2020). Dorsal root ganglion macrophages contribute to both the initiation and persistence of neuropathic pain. Nat. Commun. 11, 264.

Yuan, T., Li, J., Shen, L., Zhang, W., Wang, T., Xu, Y., Zhu, J., Huang, Y., and Ma, C. (2016). Assessment of itch and pain in animal models and human subjects. Adv. Exp. Med. Biol. 904, 1–22.

Zeisel, A., Hochgerner, H., Lönnerberg, P., Johnsson, A., Memic, F., van der Zwan, J., Häring, M., Braun, E., Borm, L.E., La Manno, G., et al. (2018). Molecular architecture of the mouse nervous system. Cell 174, 999–1014.e22.

Zeldenrust, F., Wadman, W.J., and Englitz, B. (2018). Neural Coding With Bursts-Current State and Future Perspectives. Front. Comput. Neurosci. 12, 48.

Zhang, H., Li, Y., de Carvalho-Barbosa, M., Kavelaars, A., Heijnen, C.J., Albrecht, P.J., and Dougherty, P.M. (2016a). Dorsal Root Ganglion Infiltration by Macrophages Contributes to Paclitaxel Chemotherapy-Induced Peripheral Neuropathy. J. Pain 17, 775–786.

Zhang, W.-H., Chen, A., Rasch, M.J., and Wu, S. (2016b). Decentralized multisensory information integration in neural systems. J. Neurosci. 36, 532–547.

Zylka, M.J., Dong, X., Southwell, A.L., and Anderson, D.J. (2003). Atypical expansion in mice of the sensory neuron-specific Mrg G protein-coupled receptor family. Proc. Natl. Acad. Sci. USA 100, 10043–10048.